INJECTABLE HYDROGEL-MICROGEL COMPOSITES FOR DRUG DELIVERY

INJECTABLE *IN SITU* GELLABLE HYDROGEL-MICROGEL COMPOSITES FOR DRUG DELIVERY

By

DARYL N. SIVAKUMARAN, B. Eng.

A Thesis

Submitted to the School of Graduate Studies

In Partial Fulfillment of Requirements

For the Degree

Master of Applied Science

McMaster University

MASTER OF APPLIED SCIENCE (2010) McMaster University

(Chemical Engineering) Hamilton, Ontario

TITLE: Injectable *In Situ* Gellable Hydrogel-Microgel Composites For Drug Delivery

AUTHOR: Daryl N. Sivakumaran, B. Eng. (McMaster University)

SUPERVISOR: Dr. Todd Hoare

NUMBER OF PAGES: xiv, 120

ABSTRACT

Hydrogels are water soluble polymer networks that are similar to the extra-cellular matrix of cells. Drug delivery systems based on hydrogels are of interest given their high biocompatibility. Obstacles with their use include their macroscopic dimensions (requiring surgical implantation) and quick elution of drugs from the swollen hydrogel matrix.

These challenges can be addressed through the use of microgels, hydrogel particles with nanoscale dimensions. Microgels made from poly(N-isopropylacrylamide) (PNIPAM)) are of particular interest given that the effective diameter and water content of these microgels decreases at ~32°C. The degree of deswelling and drug release rates can be tuned by controlling distributions of comonomers inside microgels. Microgels can be immobilized within an injectable hydrogel network which is a liquid outside the body but quickly gels upon injection inside the body.

The bulk, entrapping hydrogels were fabricated from carboxymethyl cellulose (CMC) and dextran modified with hydrazide (CMC A) and aldehyde (Dex B) functional groups. When mixed via co-injection through a needle at concentrations of 2 wt%, a hydrazone-crosslinked hydrogel network was formed. AA-NIPAM microgels were synthesized via mixed precipitation-emulsion free radical polymerization in a dilute (~1 wt% monomer) aqueous solution and were co-injected with the B polymer for encapsulation inside the hydrogel.

Current results show that the release of bupivacaine, a cationic local anesthetic, can be sustained over a period of up to 30 days using these composite hydrogel systems. Release rates scaled directly with the anionic functional group content of the microgel. Release rates from the composite microgels appear to be driven by ion exchange between the microgel and drug as opposed to simple diffusion.

The composite hydrogels, hydrogel pre-polymers, and microgels all showed no significant cytotoxicity to fibroblasts or myoblasts at concentrations up to 2mg/mL according to the MTT assay, suggesting their utility as effective *in vivo* drug delivery vehicles.

ACKNOWLEDGEMENTS

Firstly, I would like to thank God and my savior Jesus Christ for giving me the ability and desire to complete my studies. Secondly, I would like to thank my supervisor Dr. Todd Hoare. He was willing to take me on as his first graduate student and has allowed me to grow academically, learn independently and solve research problems on my own. At the same time, I appreciate his openness to discuss any research problems and lend his endless support. Thank you so much for everything you have given me.

Thank you for the support I have received in the Chemical Engineering department and at McMaster University. Thank you Dr. Robert Pelton and Dr. Heather Sheardown for allowing me to use your equipment in the fulfillment of my academic requirements. Thank you Marta Prinz and Laura Wells for being my lab mothers and helping me with almost everything. To my groups mates, thank you for all the stimulating discussions and research advances. I cannot wait for the next four years. Thanks to my only summer student Danielle Mailtland. Without her hard work, this research would not have been possible.

To my parents, without your love and support I would not be the man I am today. Dad, you push me to be a better man everyday and I can only hope that I can surpass what you have accomplished in your life. Mom, you are my rock and I owe you everything. My sister Diane, you are an awesome person and thank you for all your artistic skills. To my dear Michelle Molon, you are my best friend in the world and you make everything better. I am so glad that you are here for the next two years. And lastly, to all my lunch buddies, workout friends, and teammates, Lets do it all again!

TABLE OF CONTENTS

LIST OF FIGURES

LIST OF TABLES

NOMENCLATURE

AA	Acrylic Acid
AA-P(NIPAM)	Poly(NIPAM-co-Acrylic Acid)
ADH	Adipic acid dihydrazide
APS	Ammonium persulfate
CMC	Carboxymethylcellulose
CMC-A	Hydrazide-functionalized carboxymethylcellulose
CMC-B	Aldehyde-functionalized carboxymethylcellulose
C2C12	Mouse muscle myoblast cells
Dex-B	Aldehyde-functionalized dextran
DLS	Dynamic light scattering
DMEM	Dulbecco's Modified Eagle medium-high glucose
DMSO	Dimethyl sulfoxide
EDC	N'-ethyl-N-(3-dimethylaminopropyl)- carbodiimide
FBS	Fetal bovine serum
HA	Hyaluronic acid
HCl	Hydrochloric acid
HDAM	N-hexadecylacrylamide
HS	Horse serum
LCST	Lower critical solution temperature
log P	Hydrophobic partitioning coefficient
MAA	Methacrylic acid

MBA	N,N'-methylene bisacrylamide
MTT	Thiazolyl blue tetrazolium bromide
NaCl	Sodium chloride
NaOH	Sodium hydroxide
NHS	N-Hydroxysuccinimide
NIPAM	N-Isopropylacrylamide
PAA	Poly(acrylic acid)
PBS	Phosphate-buffered saline
PCS	Photon correlation spectroscopy
PEG	Polyethylene glycol
PEO	Poly(ethylene oxide)
PGLA	Poly(lactic-co-glycolic acid)
P(NIPAM)	Poly(NIPAM)
PPO	Poly(propylene oxide)
PS	Penicillin Streptomycin
RGD	Arg-Gly-Asp peptide sequence
TNBS	Trinitrobenzenesulfonic acid
VAA	Vinyl acetic acid
VPTT	Volume phase transition temperature
3T3	*Mus musculus* mouse cells

Chapter 1: Introduction

In recent years, there has been significant progress in the development of biotechnology tools for addressing human health challenges, including the development of artificial organs, tissue engineering strategies, and drug delivery vehicles. Polymeric materials have been key to many of these advances. In particular, the development of novel biomaterials has become essential in the administration of drugs to patients. Formulating drugs with biomaterials allows for long-term controlled release of drug, significantly improving patient quality of life by affording more control over drug administration. Of particular interest is the development of 'smart' materials that have the potential to dynamically gauge the dose of drug delivered as a function of a physical or biological stimulus (Hoare and McLean, 2006). Such materials would allow drug delivery to be directly correlated with the patient's need for that drug. However, there have been challenges in creating 'smart' materials that can alter the rate of drug release based on environmental stimuli. The aim of this work is to investigate the use of 'smart' hydrogels, microgels, and microgel-hydrogel composites as potential biomaterials for drug delivery.

The use of hydrogels as a drug delivery vehicle has been explored thoroughly. Hydrogels are water soluble polymer networks that swell in an aqueous environment. They are often physically and mechanically similar to the extra-cellular matrix of cells, making them particularly favourable for use in the body. They can be made of a variety of polymers such as dextran, hydroxyethylmethacrylate, and carboxymethycellulose

(Barbucci *et al.*, 2000). Hydrogel delivery systems are advantageous due to their biocompatibility as well as their tunable affinity for drugs. Obstacles with their use include the quick elution of drugs from the highly swollen hydrogel matrix and the inability for macroscopic hydrogels to be injected into the body.

Materials at the micro or nanoscale offer an even wider range of potential applications than traditional macro-scale biomaterials. In particular, microgels, hydrogel particles with nanoscale dimensions, have great potential for drug delivery. Microgels are formed by water-soluble polymers and have a porous gel microstructure consisting of a cross-linked polymer network. Spherical microgels made from poly(N-isopropylacrylamide) (P(NIPAM)) are materials of particular interest given that the effective diameter and water content of the microgels decrease dramatically at ~32°C (Pelton, 2000). When comonomers are polymerized into the gel network, the temperature range of the phase transition can be altered according to the hydrophilic or hydrophobic characteristics of the comonomer. This change in size due to temperature fluctuation can lead to the development of smart materials. From previous research, it was shown that the phase transition of acrylic acid functionalized PNIPAM microgels would occur at around 35-40°C (Hoare, and Pelton 2004). This allows drug loading to occur at room temperature under swollen gel conditions, thus optimizing drug entrapment by optimizing drug diffusion into the gel phase. Subsequently, when placed at body temperature, the microgels would collapse, reducing the effective diffusion coefficient of drug through the microgel phase and slowing drug release. However, the major disadvantage of microgels is the nanoscale size of the gels results in relatively rapid drug release and permits

consumption by the macrophages and rapid clearance from the injection site to the liver. Thus, long-term local drug delivery is not possible using microgels alone.

The aim of the research that follows is to optimize the features of both hydrogels and microgels to create an injectable *in situ* gellable long-term controlled release drug delivery system. Microgels will be immobilized within an injectable hydrogel network which is liquid outside the body but gels inside the body. By doing so, we can control drug release according to the cross-link density, degree of swelling, and the drug affinity of both the hydrogel and microgel phases. Furthermore, studies will be made to determine cytotoxicity as well as structural information regarding the hydrogels and microgels.

Chapter 2: Literature Review

2.1 Drug Delivery

Medication has become important in our daily lives. The effectiveness of any given drug depends on several factors. One important factor is the dosage of the drug. An effective drug would have maximum effects with a minimal amount of drug. However, even highly potent drugs are not effective if they cannot be delivered to the required site of action within the body. Thus, the main challenge of modern drug therapy is not finding more potent drugs but rather finding improved ways to deliver those drugs to the place required at the rate required inside the body.

There is a very important relationship between the chemical properties of the medication and its subsequent movement through the body, that drug delivery technique plays a vital role in the effective use of the drug (Saltzman). The method of drug administration plays a large role in the pharmacokinetics of the drug in the body. There are many routes and methods one can use in the administration of medication. The most well-known are oral medicines such as pills or syrups. However, absorption of the drug through the intestine may be hindered by the degradation of compounds in the gastrointestinal tract. Thus, other methods such as injections, lotions, and suppositories are popular (Saltzman). Injections are particularly effective, as they bypass many degradation mechanisms and are delivered directly to the target site via intravenous,

intramuscular or subcutaneous routes. Encapsulation of the drug allows for protected and timed release of the drug through the body.

Polymers have been primarily used in conjunction with drugs to alter the limitations and pharmacokinetics of the drugs on their own. Polymer-based drug delivery systems can allow for controlled and/or sustained release of the drug in the body which differs than that of the characteristics of the naked agents. A controlled release system would deliver drugs at a predetermined rate for a specified period of time, with little or no effects from environmental conditions (Langer). Polymers can be utilized in a variety of methods to effect controlled drug delivery. The first involves chemical modification of the drug for attachment to the polymer delivery vehicle. This can be done for several reasons, such as altering biodistribution or increasing agent solubility (Langer). With attachment to a polymer, there is an increase in the effective size of the active agent, changing its diffusion coefficient inside the body. Polymers like polyethylene glycol (PEG) can also be attached to alter the immunogenic response of the host, imparting "stealth" properties minimizing recognition of the drug by phagocytes or white blood cells (Bazile *et al.*,1995). Polymers can also be used to increase the solubility of poorly soluble drugs; for example, PEG has been used extensively in the distribution of proteins and other drugs (Hoare and Kohane, 2008). For polymer conjugates to be effective, the polymer-drug conjugate must be connected using a reliable linker than can be degraded in the body either via hydrolysis or specific enzymatic degradation at the target site. This is

important as in many cases the drug cannot be absorbed into cells with the delivery vehicle (Saltzman).

The creation of particles/vesicles made of polymer materials can also be used to improve drug delivery. Much like drug-macromolecule conjugates, factors such as biodistribution can be altered by encapsulating the drug relative to a naked drug agent alone (Saltzman). However, with particles, there is the added benefit of potentially having a significantly higher drug loading capacity. Vesicles can be composed of lipids, carbohydrates, or other types of natural block copolymers. By using these materials, one can help ensure maximum biocompatibility, since these materials are routinely found in the body.

Vesicles or particles can be designed to be targeted by cells for uptake by controlling their particle size, hydrophobic interactions, or ligand-receptor or antigen-antibody interactions (Mohanraj and Chen, 2006). This will increase the efficacy of the drug while minimizing side-effects. Particle size is important in the absorption of particles into cells. It has been found that 100nm nanoparticles had a 2.5 times greater uptake than that of their 1μm counterparts using certain cell lines (Desai *et al*,1996).

The surface chemistry of the particles can be used to enhance uptake of the drug particles by cells as well as protect the drugs from rapid degradation away from the target site. Enhanced or specific uptake can be achieved by altering the surface chemistry of the vesicle or particle. Direct cell communication can also be achieved with the addition of certain ligands or antibodies that will interact with cell receptors or antigens to promote

cell uptake. It has been seen that cell interactions can be enhanced with the incorporation of the peptide RGD (ARg-Gly-Asp). This peptide has been known to bind with integrin receptors on cell membranes, inducing cell uptake (Alsberg *et al*, 2001). The addition of hydrophilic polyethylene glycol (PEG) has been observed to prevent phagocytosis (Olivier, 2005).

Encapsulation or conjugation of drugs with polymers enables the engineering of the release rate of that drug from the polymer matrix depending on the physical properties of both the drug and the polymer. In general, the objective is to tune these properties to control the therapeutic concentration of the drug in the body. Each drug has a therapeutic concentration range above which it becomes toxic to the user and below which it is clinically ineffective (Langer). The drug concentration in the blood stream between these two extremes is known as the therapeutic window. This is represented graphically in Figure 2.1.

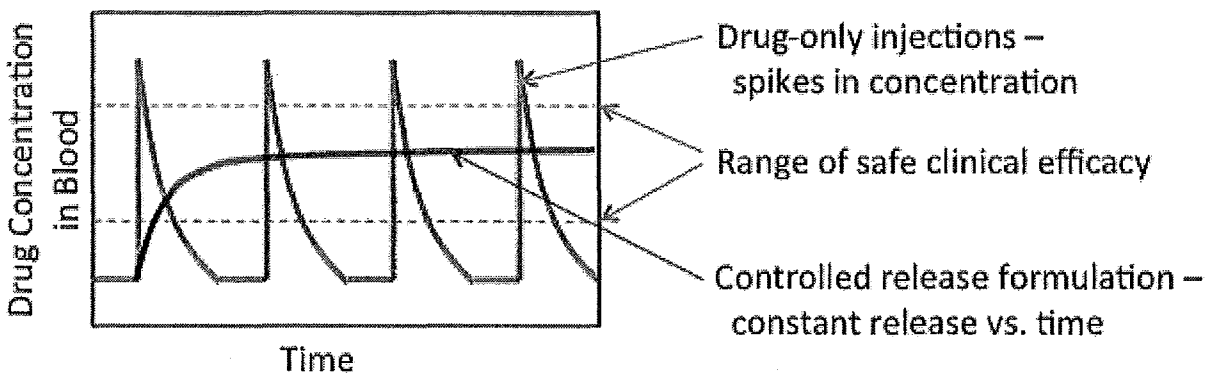

Figure 2.1: Clinical Window of Drug Delivery (Reproduced with Permission of Dr. Todd Hoare, McMaster University)

In standard dosage systems (such as injections), the drug concentration in the blood stream increases rapidly, peaks, and is followed by a decline out of the therapeutic window. Thus, constant re-administration is needed for the patient to receive adequate treatment. With constant or controlled release systems, the same increase and peak would occur at point of administration. However, the subsequent decrease would last longer within the therapeutic window, thus reducing the frequency of re-administration of the drug (Saltzman). Ideally, therapy could be achieved by a single administration of the drug delivery vehicle. Other advantages of a controlled delivery system include the ability to delivery drugs locally to specific body parts or organs, thus lowering the systematic drug concentration in the body. Local delivery could also lead to preservation of drug bioactivity, as drugs would no longer be subjected to defense mechanisms in the blood stream. Added benefits include the reduced need for follow-up care as well as improved comfort and compliance from patients (Langer).

2.2 Mechanisms for Release

Depending on the type of drug, polymer, or delivery site, there are many different mechanisms by which drug release can occur. Although many polymers can be used for drug delivery systems, hydrophobic, non-degradable polymers have been chosen most frequently. These polymers present the best features for retention of drug and biocompatibility. They have been used extensively in the creation of drug reservoirs, transdermal systems, and matrix delivery systems. The most common mode of drug release from drug reservoirs and other polymeric controlled release systems is via

molecular diffusion of the drug into the external media (Saltzman). In each of these systems, the diffusive release of the drug occurs over the course of three steps. The first involves the dissolution of the drug into the polymer matrix or slab prior to implantation in or on the body. Once implanted in the patient, diffusion across the polymer membrane, out the pores of the matrix, or through the matrix material itself occurs. Lastly, effective delivery occurs with the dissolution of the drug into the external phase (i.e. bodily fluids surrounding the drug delivery vehicle) (Saltzman).

Since diffusion is the main mechanism of release, the encapsulating polymer can be engineered to alter the effective diffusion coefficient of drug through the polymeric matrix to control drug release. Diffusion can be engineered in part by creating degradable polymer systems. Degradable polymers may degrade via a bulk erosion or surface erosion method. In bulk erosion, water infuses through the polymer matrix, uniformly attacking cross-links until mass degradation occurs (Edlund and Albertsson, 2002). This typically occurs when water penetration is faster than that of the erosion rate. It is important in drug release systems that the entire drug content is released prior to the device collapsing as to prevent a burst in concentration of the plasma drug concentration. Most currently available degradable drug delivery systems degrade via a bulk mechanism (e.g. PLGA). Surface erosion, however, is in many ways more favourable, as it results in the gradual release of polymers at the surface due to low water flow into the hydrogel and the slow and controlled release of drug. Ideal surface erosion would occur when the erosion rate is proportional to the external surface area of the device (Edlund and Albertsson, 2002). For

optimal sustained release, surface erosion should be faster than that of water penetration into the bulk phase. To achieve this, the polymer should be hydrophobic but have bonds that are easily hydrolysable. Additionally, for added biocompatibility, the products of hydrolysis should be easily processed by cells for removal from the body. For surface-eroding systems, the release would be a function of the polymer erosion rate as well as the diffusion coefficient of drug through the polymer matrix. (Saltzman).

Another factor influencing drug release from polymeric drug delivery vehicles is drug-polymer interactions. Electrostatics can play a large role in rate of release of the drug from the polymer system. For example, cationic polysaccharides such as cellulose ethers or guar gums can interact with anionic ibuprofen to regulate drug release (Rodriguez *et. al.*, 2003). Similarly, anionic carboxylic groups in hyaluronic acid can interact with cationic drugs such as lidocaine (Doherty *et al.*, 1995). In either case, the ionic binding of the drug to the polymer will slow the release of the drug from the drug-polymer system. Covalent bonding between the drug and polymer side groups may take place, leading to slower release times depending on the increase in the effective drug molecular weight and/or the degradation time of the drug-polymer bond. For example, chitosan and salicylic acid have been reported to react to create salicylate (Puttipipatkhachorn *et al., 2001*). This results in diffusion driven release initially, followed by controlled release as the salicylate reverts back to salicylic acid for release into the external environment.

Hydrophobic partitioning effects can also play a role in the rate of release of the drug from the polymer system. Hydrophobicity parameters can be used to predict how the interactions between drugs, polymers, and the solute play a role in the release of the drug from the system. This can be done with the use of the hydrophobic partitioning coefficient, log P, calculated using Equation (1):

$$\log P = \frac{[solute]_{octanol}}{[solute]_{un-ionized\ water}} \quad (1)$$

Experimentally, the solute (drug) is placed into a two phase system of water and octanol (Poole and Poole, 2003). Depending on the hydrophobicity of the solute, it will either partition primarily into the octanol or water phase. A positive log P value indicates that the solute is more hydrophobic and prefers the non-polar octanol. Likewise, a negative value indicates the solute is more hydrophilic and prefers to partition into an aqueous solution. Thus, the values of log P are an indicator of whether the hydrophobicity of a molecule will play a role in the interactions between it and another functional group on the polymer. In terms of drug release, a more hydrophilic drug would likely partition into a hydrophilic region of the polymer. This leads to easy release of the drug into the aqueous external environment via simple diffusion. Hydrophobic drugs would be more likely to stay within the hydrophobic domain and less likely to release into the aqueous

environment (Kang, *et al*, 2006). Initial release occurs due to diffusion, but some drug will stay within the hydrophobic domains. A secondary controlled release may occur at later stages in the lifetime of the release system via hydrolysis or other mechanisms of degradation of the release system. Degradation would occur within the core which would lead invariably to a lowering the number of end groups available for drug-polymer interaction. With this increase in free volume, more degradation would occur and more drugs would be released from the system. Thus, a two-stage release profile would ensue. This partitioning effect can be used as a means of secondary control in the drug release profile of polymeric drug release systems. (Jeong *et al.,* 2000)

2.3 Hydrogels

There has been substantial progress in the development of controlled release systems. Hydrogel systems have attracted particular interest. Hydrogels are three-dimensional, cross-linked networks made of water soluble polymers (Hoare and Kohane, 2008). These networks can swell and absorb water, but do not dissolve in water themselves (Saltzman). They can literally be made from any type of water-soluble polymer, so their creation can employ a large field of polymers depending on the specified application. The polymers are largely hydrophilic in nature and can absorb from 10-20% up to a thousand times their dry weight in water (Hoffman, 2002). Depending on the polymer chosen and the type of crosslinking used to prepare the gel, the hydrogels can be largely stable or designed to disintegrate or degrade as needed. They can be found in various morphologies and forms, such as slabs, microparticles, coatings, pressed power

matrices, and films (Hoffman and Hoare, 2008). Examples of everyday hydrogels include contact lenses, Jello, and diaper linings. Due to their versatility, they have been used in various medical applications, including diagnostics, cellular immobilization, and regenerative medicine (Hoare and Kohane, 2008).

The advantages of using hydrogels in drug delivery systems are numerous. The high water content allows the hydrogels to be physically, mechanically, and (as desired) chemically similar to the extracellular matrix of the host cells (Hoare and Kohane, 2008), leading to generally good biocompatibility. This has been demonstrated with their successful use in the peritoneum and other *in vivo* locations (Sutton, 2005). Their soft nature also allows the hydrogels to protect transported materials that otherwise may be fragile. The polymers themselves can easily be chemically modified for specific applications, thus allowing precise tuning of the swelling and interfacial properties of the hydrogels. Hydrogels can be prepared using both natural and synthetic polymers. Examples of natural polymers include chitosan, dextran, hyaluronic acid, and collagen (Sinha *et al*, 2003). Synthetic polymers that are commonly utilized include poly(hydroxy-ethyl methacrylate,), poly(vinyl alcohol) poly(propylene oxide)(PPO), or poly(n-Isopropylacylamide) (Dai *et al*, 2005).

Hydrogels have a highly porous structure that can be tuned by controlling cross-link density as well as tuning the polymer-environment interactions. The cross-links between polymer chains determine key hydrogel parameters such as pore size, pore size distribution, and tortuosity (Hoffman, 2002). In turn, these factors will all influence how

much the network will swell when the hydrogel is exposed to water. Swelling will vary the inter-chain separation, which regulates the average pore size of the hydrogel and thus the rate of drug diffusion through the hydrogel matrix. By controlling the cross-link extent, one can thus predict how fast the drug can escape the system (Saltzman).

Other factors besides crosslink density can also influence gel swelling equilibrium and thus the rate of drug release from hydrogel systems. Charged hydrogel networks can swell via Donnan counterion partitioning effects, increasing the average pore size and thus the rate of drug release (Hoare and Pelton, 2008). Other factors that govern diffusion include the drug size and charge interactions between the drug and hydrogel (Hoffman, 2002). Environmental effects can also change the degree of crosslinking and/or the equilibrium water content within the hydrogel depending on the type of polymers used, thus leading to tunable hydrogels. For example, for typical hydrogel systems, temperature increases lead to increases in the mobility of chains, resulting in a greater degree of swelling of the hydrogel (Bajpai and Mishra, 2004). Thus, the main benefit of using a hydrogel system is the ability to manage pharmokinetics within the body.

Despite these advantages, one must be mindful of some disadvantages of hydrogels. Hydrogel materials can be difficult to handle due to their low mechanical strength. Hydrogels are often difficult to sterilize, which is of great importance for *in vivo* applications (Hoffman, 2002). Hydrogels also typically exhibit low tensile strength, which limits their use where load bearing occurs and/or the hydrogel is exposed to high-shear flows. The use of hydrophobic drugs is also limited with hydrogels, as the high

water content prevents partitioning of the drug into the system during the loading phase. The macroscopic size of gels also generally requires that moderately invasive measures be used for implantation in patients, such as subcutaneous implantation operations (Hoare and Kohane, 2008). However, these limitations can be overcome depending on the nature of the cross-links used to form the hydrogel network.

Cross-linking of hydrogels can occur via several mechanisms. These cross-linking approaches are broadly separated into two distinct categories: physical cross-linking and covalent cross-linking. Physical cross-linking includes hydrophobic interactions, charge interactions, and hydrogen bonding.

Hydrophobic gelation occurs via the formation of aggregates of hydrophobic polymers. When this occurs, the hydrophobic domains minimize the hydrophobic surface area contacting the water, reducing the amount of structured water surrounding the domains and maximizing the entropy of the system (Hoare and Kohane, 2008). The formation of the gel is dependent on the polymer concentration, degree of hydrophobicity, and the chemical structure of the polymer. Examples of such hydrogels include PEO-PPO-PEO tri-block polymer hydrogels (Hoare and Kohane), 2008 and PEO-PPO-PAA (Cleary *et al,* 2003.). Charge interactions can allow for polymer-polymer or polymer-drug cross-linking to occur, in which different charge domains of polymers interact ionically. Release would then occur when competing ionic species would degrade the cross-links, resulting in drug release at the delivery site. Hydrogen bonding can occur between polymers such as gelatine-agar and starch-carboxymethyl cellulose to enhance the

rheological properties of the mixtures relative to the properties of the polymers alone. However, these types are hydrogels are typically short-lived *in vivo*, as influxes of water will lead to a breakdown of the hydrogen bonds. Indeed, via any physical gelation technique, the major limitation of physically cross-linked hydrogels is their penchant to breaking down in water. In addition, physically-cross-linked hydrogels have generally weaker mechanical strength and are difficult to characterize, given the dynamic nature of the crosslinking.

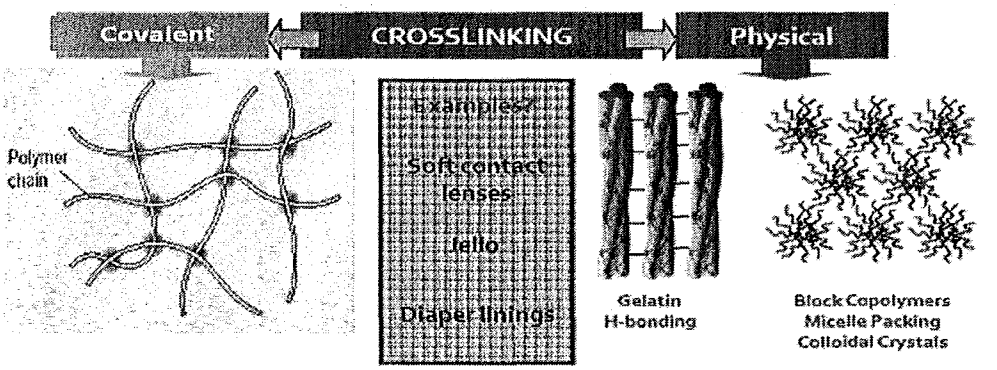

Figure 2.2: Cross-linking of Hydrogels (Reproduced with Permission of Dr. Todd Hoare, McMaster University)

The short half-lives of most physically-cross-linked hydrogels *in vivo* can be resolved with the creation of covalently cross-linked hydrogels. The benefit of covalently cross-linked hydrogels is the prevention of dilution of the hydrogel matrix and diffusion of the polymer away from the injection site (Hoare and Kohane, 2008). In addition, the design of covalently bonded hydrogels is much more flexible than that of their physically-cross-linked counterparts. This is due to the fact that the properties of physically cross-

linked hydrogels are directly related to the chemical properties of its gelators (Hoare and Kohane, 2008).

Hydrogels can be formed via covalent cross-linking using small-molecule crosslinkers or polymer-polymer cross-linking. In small-molecule cross-linking, reactive small molecule crosslinkers are added to covalently crosslink polymer chains. This has been demonstrated with molecules such as genipin (for amino-functionalized polymers) and glutaraldehyde (for carbohydrate-based polymers), both of which facilitate rapid gelation. The main problem with small molecule chemistry is that many of the small molecule additives can prove to be cytotoxic, resulting in a non-biocompatible hydrogel not amenable to *in vivo* use (Hoare and Kohane, 2008).

Polymer-polymer cross-linking occurs when reactive side chains are attached to the polymer backbone. An example of polymer-polymer cross-linking for hydrogel formation is the process of photopolymerization. Some examples of photopolymerizable macromers include PEG acrylate derivatives and polyvinyl alcohol derivatives (Nguyen and West, 2002). However, with photo-cross-linking can lead to a local increase in temperature when done in vivo, which may damage neighbouring tissues in the body (Jin *et al.*, 2007). The features of polymer-polymer cross-linking are especially favourable for injectable *in situ* gelling. Covalently *in situ* gellable hydrogels can overcome the toxicity, injectability, and degradation issues that may arise from standard hydrogels created outside the body or prepared *in situ* via the use of small molecules. Several non-toxic chemistries have been demonstrated. Schiff base cross-links can be formed via the

reaction of aldehydes and amines. Another example involves the reaction between aldehydes and hydrazides to create hydrazone bonds. This has been demonstrated with hyaluronic acid hydrazone cross-linked polymers for anaesthesia delivery (Ito *et al,* 2007). Michael addition between nucleophiles and vinyl groups is another common technique that has been used, typically resulting in rapid gelation in under 10 minutes (Hiemstra *et al*, 2007).

In most cases, cross-linking chemistries are designed such that the hydrogels will degrade over a desired time frame inside the body. Degradable hydrogels have many advantages for drug delivery. The major advantage is the added control of drug release kinetics as a function of polymer degradation. Furthermore, residual degradation products from the hydrogels could be absorbed by the body, thus eliminating the need for retrieval of the device once the drug has been fully released (Saltzman). In all, to create an effective device, the polymers that are used must degrade in a controllable fashion and degrade into naturally occurring or inert compounds (Saltzman). Degradation of the hydrogel occurs when cleavage of the main bonds occurs, resulting in the production of oligomers. This can be accomplished either chemically (hydrolysis, oxidation) or biologically (bacteria, enzymes) (Edlund and Albertsson, 2002).

2.4 Microgels

Microgels are micro/nanoscale polymeric materials that are spherical in nature and have a cross-linked gel microstructure. Dimensionally, they can be considered colloidal particles with average diameters ranging between 50nm and 5μm (Pelton, 2000).

However, microgels are not restricted to this size and have been reported with larger sizes. The structure of microgels can be typically described as porous gel particles that can be homogenous in nature or consist of different copolymers (Pelton, 2000). A schematic of the typical microgel structure is found on Figure 2.3.

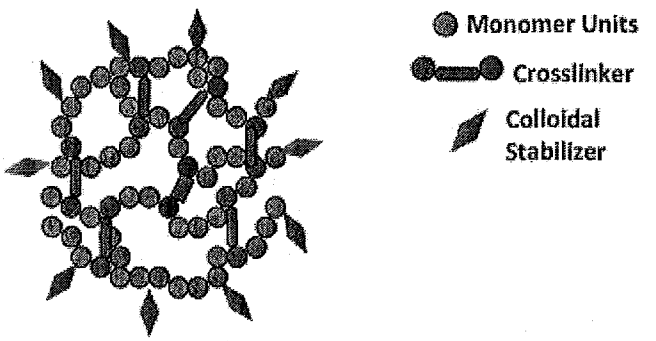

Figure 2.3: Microgel Particle (Reproduced with Permission of Dr. Todd Hoare, McMaster University)

On the macroscopic level, microgels behave much colloidal particles which are colloidally stable but can aggregate depending on salt concentration. On the microscale, microgels have the ability to swell in response to their solvent environment (Saunders and Vincent, 1999). Microgel swelling is dependent on balances in polymer/polymer interactions as well as polymer/environment interactions, with all the same factors contributing to hydrogel swelling also influencing microgel swelling (Pelton, 2000). Key microgel properties important for applications include the extent of swelling in response to a stimulus, the cross-link density, and the characteristic time constants of swelling and shrinking (Pelton, 2000). Typical analysis of microgels can be done with photon correlation spectroscopy (PCS), dynamic light scattering (DLS), or electrophoresis

(Saunders and Vincent, 1999). Applications involving microgels have included drug delivery, diagnostics (Hoare and Kohane, 2008), the surface coatings, printing, and other industrial processes (Saunders and Vincent, 1999).

Recently, much attention has been brought to the development of "smart" microgels. These microgels are able to respond to environmental stimuli, resulting in large changes in physical properties such as swelling characteristics, cross-link density, and time constants for swelling and shrinking as a function of a stimulus (Pelton, 2000). In addition, the physical changes observed should be reversible as to be able to regulate the swelling changes in both directions (Roy and Gupta, 2003). The degree of reversibility is dependent on the polymer structure, polymer functionality, and the microgel's ability to dynamically adjust its nanostructure depending on stimuli (Roy and Gupta, 2003). Various polymers have been developed to respond to various types of stimuli. Sensitivity to pH can be achieved with the used of poly(propyl acrylic acid) or poly(*N*,*N*9 -diethylaminoethyl meth acrylate), in which ionization occurs on the polymer backbone (Qiu and Park, 2001). Light sensitivity can be used as a stimulus when polyacrylamide is crosslinked with 4-(methacryloylamino)azobenzene (Roy and Gupta, 2003). Modifications to swelling can be dictated with the use of electric fields and electroporation with microgels that contain lipid bilayers (Kiser *et al,* 2000). Magnetic field sensitive polymers can be achieved by the incorporation of ferromagnetic nanoparticles within the soluble region of the microgel network (Roy and Gupta, 2003). Temperature sensitive microgels are also possible with the use of poly(N-

isopropylacrylamide) (P(NIPAM)) or other similar N-alkylacrylamide-based polymers (Pelton, 2000).

In all these cases, the swelling (or uptake of water) have similar mechanisms; specifically, the affinity of water for the polymer changes as a function of the applied stimulus. In the case of pH sensitive microgels, the ionization of basic or acidic functional groups (such as carboxylic acids) can lead to changes in the swelling characteristics due to Donnan equilibrium. In turn, more water would be allowed to either enter or exit the microgel structure. Temperature sensitivity can be achieved by allowing conformational changes to occur below and above a volume phase transition temperature (VPTT) (Shibayama).

2.4.1: N-isopropylacrylamide (NIPAM)

The thermosensitive class of "smart" polymeric microgels is among the most intriguing materials being researched today. In particular, much interest in the field has been focused on the development and use of poly(N-isopropylacrylamide) microgels (Pelton 1986). The main motivator to this interest is P(NIPAM)'s ability to demonstrate inverse solubility upon heating, which is the opposite behaviour to how most polymers react at standard temperature and pressure. The linear version of the polymer has a base structure as seen in Figure 2.4. P(NIPAM) contains two primary domains; the hydrophilic amide bonds and the hydrophobic isopropyl structure.

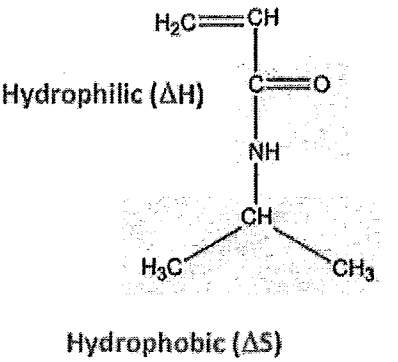

Figure 2.4: N-Isopropylacrylamide (NIPAM) (Reproduced with Permission of Dr. Todd Hoare, McMaster University)

The behaviour of the polymer in a solvent is determined by the interactions of the polymer with itself as well as with the solvent. In particular, aqueous solutions allow for hydrogen bonding to occur and are excellent at the partial structuring of polymers in solution. The ordering of P(NIPAM) is dictated by the specific orientation of water around the hydrophobic domain of the isopropyl group. It is best described by the Gibbs free energy of the system which is represented by equation 2 below:

$$\Delta G = \Delta H - T\Delta S \quad (2)$$

Here, G is the Gibbs free energy, H is enthalpy, T is temperature and S is the entropy of the system. The cage-like structuring of water around the hydrophobic isopropyl group in the polymer, known as the hydrophobic effect, results in decreased entropy (a negative ΔS) upon mixing (Schild and Tirrell, 1991). The cage structure also forbids polymer-polymer interactions from occurring. Upon heating, the temperature-entropy term (TΔS) is increased until a positive term is obtained. This results in the

entropy term dominating the hydrogen bonding interactions, thus cancelling the enthalpy interactions (ΔH) between water and the amide, in which dissolution occurs. Entropy primarily drives the ordering of the isopropyl group with other isopropyl groups and allows for hydrophobic interactions to occur at which point full polymer-polymer interactions transpire resulting in precipitation (cloud point) of the polymer (Pelton, 2000). This temperature point of phase separation is known as the lower critical solution temperature (LSCT); the polymer is soluble below the LCST and insoluble above the LCST. For P(NIPAM), the LCST can occur at temperatures between 15°C and 50°C, but typically occurs at 32°C. (Pelton, 2000).

The LCST of P(NIPAM) can be adjusted with the addition of additives, copolymers, or via the functionalization of the base polymer. Depending on the hydrophobic/hydrophilic nature of the additive, the LCST can be altered. For instance, the addition of a hydrophobic monomer/molecule, such as N-hexadecylacrylamide (HDAM), can lead to a lowering of the LCST (Schild and Tirrell, 1991). Likewise, an increase in hydrophilic domains, for example via copolymerization of vinyl acetic acid leads to an increase in the LCST (Hoare and Pelton, 2004). This ability to shift temperatures allows for the design of specifically "smart" materials depending on the application.

The first microgels of P(NIPAM) were discovered in 1978 and consisted of a highly monodisperse colloid dispersion. This microgel was found to have a LSCT in water of approximately 32°C. However, with gels, there is no distinct cloud point of precipitation. Gels and microgels exhibit volume change behaviour, (Shibayama and

Tanaka, 1993) over a range of temperatures at the VPTT. In most cases, the LSCT and VPTT of poly(NIPAM) (linear and gel) differs by ~1-3°C, with the gel exhibiting a higher temperature due to the presence of the cross-linker. This volume change is represented physically by the swelling and deswelling of microgels. Like linear polymers, P(NIPAM) microgels can have their VPTT altered based on copolymerization or functionalization. Copolymerization can lead to shifting of the VPTT due to changes in the relative hydrophilicity/hydrophobicity of the gel matrix. There has been much literature regarding the copolymerization of NIPAM, with extensive research being conducted with carboxylic acid containing monomers such as acrylic acid (AA), methacrylic acid (MAA), or vinyl acetic acid (VAA) (Hoare and Pelton, 2008) Carboxylic acids are ionisable, leading to an increase in VPTT upon ionization, and provide an electrophilic reaction site for polymer modification. Thus, carboxyl groups can allow for P(NIPAM) gels to be tunable as a function of both temperature and pH. Research has shown that the microstructure of such microgels would predominately be that of a random co-polymer with carboxylic acid groups dispersed throughout the P(NIPAM) regions. There is very little evidence of many block regions of carboxylic acid groups (Hoare and Mclean, 2006). However, with VAA, the microstructure would resemble that of a core-shell particle, with an internal NIPAM core and carboxyl groups on the outer shell. Aside from providing a tunable effect on the VPTT, comonomers or functionalized groups can also provide a basis for attachment of small molecules to the microgel via covalent bonding or further post-modification depending on the final application of the microgel.

P (NIPAM) microgels are typically synthesized via a mixed precipitation-emulsion polymerization reaction, as described by Pelton. Polymerization is conducted in water until the polymer reaches a critical molecular weight, at which point it undergoes a phase transition and deposits on to the growing microgel particles. The gels are electrostatically stabilized by a surfactant concentration below the critical micelle concentration. Initiation is achieved using a persulfate initiator.

Applications for P(NIPAM) microgels are numerous due to their ability to reversibly respond to temperature changes. Interesting applications include the use of P(NIPAM) microgels as a flocculants in oil reservoirs above the VPTT. Microgels can also be used as rheological modifiers, taking advantage of their dynamically-tunable water content as well as their ability to aggregate and create substantially larger particles that would slow the flow of the solution, leading to a higher viscosity (Bokias *et al,* 2000). The creation of colour-tunable colloidal crystals is another interesting application. With temperature changes, the Bragg diffraction of light through P(NIPAM) colloidal crystals can be changed. Thus, with changes to the structure and resulting size of the microgel, the Bragg peak and thus the colour can be tuned (Das *et al.*,2006). The use of microgels can be further extended to the use of micro-optical arrays. It has been shown that P(NIPAM) microgels have good affinity for certain substrates (such as gold) and thus can be attached to a variety of surfaces. By applying light to a lens shaped microgel, the focal length can be altered due to the radiation-induced heating, leading to better focusing

for the array. Given the relatively fast response time of microgels through the VPTT, the creation of dynamic tunable optical devices is very promising.

Another exciting application involves the use of P(NIPAM) microgels as a delivery vehicle for small molecules and macromolecules. Their small size allows for a greater surface area thus fast uptake and release of molecules (Sanders). Rates of delivery can be adjusted by the use of the VPTT, as this is a tunable feature depending on the application. In particular, the use of PNIPAM) as a delivery vehicle is realistic with applications for biotechnology and drug delivery. P (NIPAM)'s ability to react to changes in temperature allow for temperature-triggered drug release. It has been shown that rates of diffusion out of the gel will be higher below the VPTT since the increased water content and open pore space between polymer chains allow for low resistance to molecule movement. Above the VPTT, the microgel would collapse, providing higher resistance to molecules exiting the gel. This has been demonstrated with both fluorescein-labelled dextran and salicylamide, among other drugs (Snowden, 1992). Microgels can also be modified to have certain functional groups so that specific drug-polymer interactions can occur. This has been shown with hydrophobic/hydrophilic interactions as well as charge interactions (Hoare and Pelton, 2008). Likewise, controlled release can be obtained by "turning off" these interactions through a modification to environmental pH or temperature. Drug loading into the gels can also be enhanced because of the temperature sensitivity of the gels. Drug loading can be conducted in the swollen state, leading to facile drug diffusion into the microgel and optimal entrapment. When placed in the body,

as long as the VPTT is below physiological temperature, drug release can be slowed in the collapsed state of the gel (Pelton, 2000).

Cytotoxicity of P(NIPAM) has been observed as minimal at low concentrations over a range of temperatures. It is predicted that this will result in low *in vivo* toxicity. However, not much is known about bioaccumulation and physiological responses to degradation products in the body. Approaches in which known hydrolysable bonds can be used to fraction the polymer in known locations may be a suitable remedy for this issue.

2.5 Composite Hydrogels

The proven benefits of microgels and other particle-based drug delivery systems offer a potential solution to many of the limitations of bulk hydrogels. However, the high mobility of microgels *in vivo* and the fast release rates from microgels present challenges that are not problematic in bulk hydrogel systems. By combining microgels and hydrogels together to form soft nanocomposite hydrogels, also known as "plum pudding" hydrogels, the limitations of both microgels and hydrogels can both be mitigated (McGillicuddy *et al.*, 2006). In such systems, the drug-loaded microgels would be entrapped within the hydrogel matrix as seen in Figure 2.5.

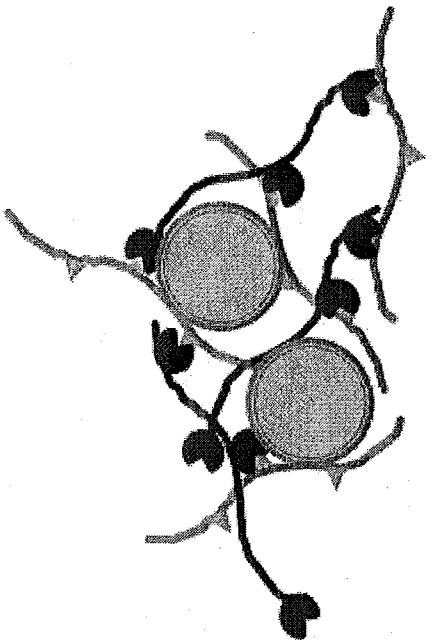

Figure 2.5: Microgels imbedded within Hydrogel Network (Reproduced with Permission of Dr. Todd Hoare, McMaster University)

Composite hydrogels offer several benefits from a biomedical engineering perspective. The hydrogel can mask any issues regarding particle biocompatibility, as the particles will be able to "hide" within the hydrogel system. The bulk hydrogel network prevents migration of the microgels from target sites (Hoare and Kohane, 2008). The hydrogel network also provides an additional diffusive barrier for drug release, offering potential for the generation of novel drug release profiles. As an example, the burst effect often seen in microgel-based drug release could be mitigated in a composite hydrogel system. Composite hydrogels also offer the unique potential to independently engineer both the hydrogel and microgel phase to optimize the drug release profile. This will allow for total control of how drug can be released and allow for tunable features to be used.

Microgels can also be functionalized to cross-link with the hydrogel to give added stability and prevent any migration of microgels out of the hydrogel matrix.

There are several examples of the use of composite hydrogels for drug delivery currently in literature. Liposomes have been entrapped within carbopol and hydroxyethylcellulose-based hydrogel and can control the release of calcein depending on the liposome membrane characteristic. Microparticles have been embedded within same polymer hydrogels to delivery drugs. Microgels made of N-isopropylacrylamide-N-tert-butylacrylamide-acrylic acid entrapped in dimethylacrylamide hydrogels can release rhodamineB at a controlled speed (Lynch *et al,* 2005). Hydrogel films made of N-isopropylacrylamide-N-tert-butylacrylamide and incorporated with the same polymer microspheres have been observed to release controlled rates of fluvastatin (McGillicuddy *et al.*, 2006). However, significant opportunities still exist for intelligently engineering the compositions, degradabilities, and swelling properties of each phase to achieve improved drug release profiles.

2.6 Materials Used

The materials chosen for use in designing soft composite hydrogels in this thesis were carboxymethylcellulose, dextran, acrylic acid functionalized (AA-P(NIPAM)), and bupivacaine. The materials chosen had to be easily modifiable, biocompatible, and allow for easy analysis of results. The materials chosen have all had previous literature regarding their use as hydrogels (carboxymethylcellulose, dextran), microgels (AA-

P(NIPAM)), and drug targets (bupivacaine), indicating that their use will be relevant for future drug delivery systems.

2.6.1 Carboxymethyl Cellulose

Carboxymethyl cellulose is a linear ionic ether derivative of traditional cellulose. It consists of β-linked glucopyranose residues (Li *et al*, 2007). It differs from cellulose with the addition of carboxymethyl groups on some of the cellulose hydroxyl groups. Substitution of the groups ranges in between 25-75% per disaccharide unit of cellulose (Barbucci *et al,* 2000). The structure is found below in Figure 2.6. Synthesis is commonly done by the alkali-catalyzed reaction of cellulose with chloroacetic acid. It can be purchased in several different molecular weight ranges, with common sizes ranging between 200 kDA and 700 kDa. Even at high molecular weight, it is a highly water soluble anionic compound that is chemically stable. Its most common form is that of a powered salt. This polysaccharide has been widely used as an emulsifying agent in pharmaceuticals, cosmetics, and in the food industries (Barbucci *et al,* 2000). In the biomedical field, it has been used to prevent epidermal scarring and tissue adherences (Barbucci *et al,* 2000). However, its potential for use as a hydrogel is promising in the realm of drug delivery.

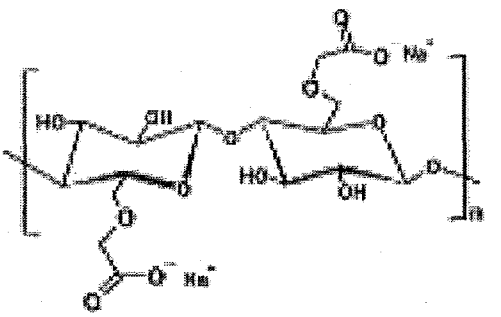

Figure 2.6: Carboxymethyl Cellulose

CMC is a viable candidate for an encapsulating hydrogel since it is non-toxic, environmentally friendly, biodegradable, and inexpensive (Li *et al,* 2007). It has unique swelling characteristics that can lead to "smart" release and excellent control of release kinetics (Kikuchi, and Okano, 2002). The "smart" swelling characteristic of CMC hydrogels is a function of its pH sensitivity, governed by the carboxylic groups on the polymer backbone. The ionization of these groups leads to weaker hydrogen bonding and increased charge-driven swelling, inducing swelling in the gel network (Bajpai and Mishra, 2004). This results in a controllable method to alter the network structure behaviour of the hydrogel.

Drug release has been observed from hydrogels made from CMC, with sustained release occurring *in vivo*. It has been used in conjunction with starch, polyethylene glycol, and polyacrylic acid for effective drug release. Drug release from CMC hydrogels is dependent on a couple of factors. First, the degree of cross-linking that occurs with itself and other potential co-monomers determines the amount of free space available for

drug diffusion as well as the amount the gel may swell. Cross-linking can occur with several agents such that modifications can be made on the hydroxyl or carboxyl groups of the polymer (Bajpai and Mishra, 2004). Another factor is the dosage amount placed in the polymer hydrogel. Various amounts will lead to differences in the release profile, with higher concentrations resulting in faster release from the system due to diffusion effects (Ikechukwu *et al,* 2000). Drug release has been observed from acrylamide-functionalized carboxymethyl cellulose hydrogels, with swelling behaviour determining the rate of drug release (Kulkarni and Sa, 2008).

2.6.2 Dextran

Dextran is a branched homopolysaccharide of glucose that contains mainly α-(1,6) linkages of D-glucopyranose residues (Zhang *et al*, 2005). These types of linkages constitute 50-97% of the total linkages (Naussens, *et al.* 2005). However, some chains will also contain branched α-(1,3) and α-(1,4) linkages depending on production. The structure of dextran is shown below in Figure 2.7. Molecular weights can vary but are typically in the range of 10-150 kDa (Naussens *et al,* 2005). Production of dextrans is routinely done via fermentation of sucrose by several different types of bacterial species. These species include *Leuconostoc, Streptococcus* and *Lactobacillis*. All of these species will synthesize dextran by excreting dextransucrase enzymes on sucrose media for conversion (Naussens *et al,* 2005). Dextran has many applications in the food industry, for photofilm manufacture, and as a soil conditioner (Shamala and Prasad, 1995). Its main

biomedical use is as a blood thinner since it is retained in the blood stream much better than crystalloids which penetrate into vascular membranes (Naussens *et al,* 2005).

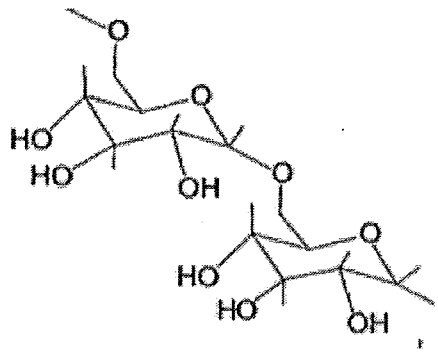

Figure 2.7: Dextran Molecule

As a potential hydrogel for a drug delivery device, dextran has great promise since it has already been well-established as a highly biocompatible material in medicine (Chiu, 1999). Dextran hydrogels show low protein absorption and water soluble versions can have molecular weights below 30kDa, which can allow for excretion through the kidneys (Hiemstra *et al,* 2007). Dextran exhibits low toxicity and high enzymatic degradability in the body, which could lead to the development of a biodegradable polymer (Chiu, 1999). Of great importance is the abundance of hydroxyl groups on the glucose resides, which means side chains can easily be modified to make dextran a tunable polymer.

There have been several reported examples of dextran-based hydrogels. Many of the developed hydrogels are homologous in nature with different crosslinking methods. Michael addition chemistry has been used with vinyl sulfone-functionalized dextrans to create degradable hydrogels (Heimstra *et al,* 2007). Carboxymethyl functionalized

dextran has been created with N'-ethyl-N-(3-dimethylaminopropyl)- carbodiimide/ N-Hydroxysuccinimide (EDC/NHS) chemistry to create "zero-length" ester cross-links between carboxylic acid and hydroxyl groups (Zhang *et al,* 2005). Other dextran hydrogels contain dextran in conjunction with other biocompatible materials to create copolymers blends. Examples of dextran-based copolymer hydrogels include dextran-HEMA, dextran-methacrylate copolymers (Van Dujk *et al,* 1997). In these cases, drug release from the hydrogels has been demonstrated and release rate has been controlled.

2.6.3 Gel Formation

Hydrogels will be made via cross-linking techniques involving the rapid formation of hydrazone bonds. These bonds are created via the reaction of aldehyde groups with hydrazide groups, as seen in Figure 2.8.

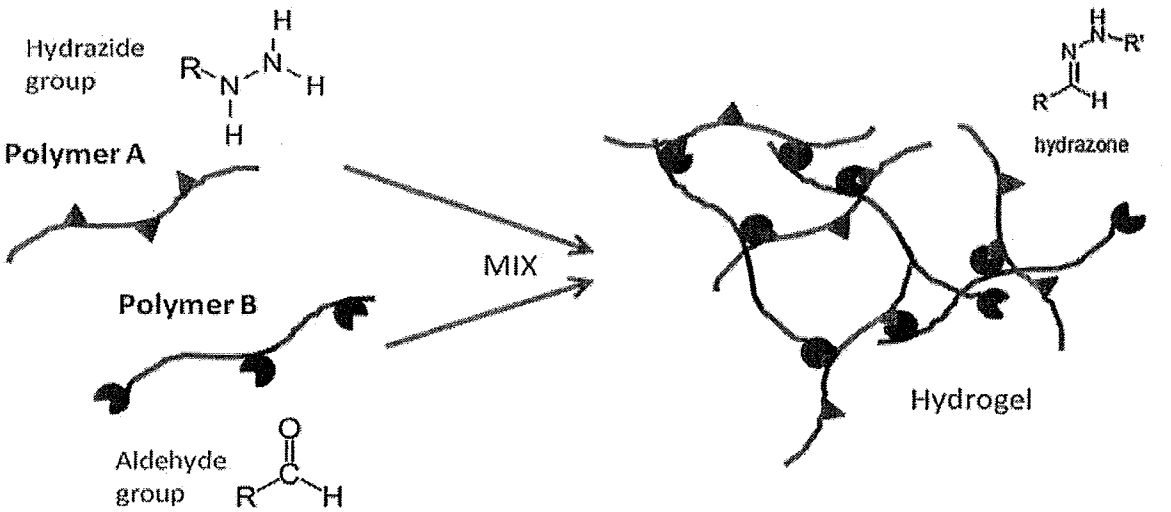

Figure 2.8: Hydrogel Formation via Hydrazone Formation (Reproduced with Permission of Dr. Todd Hoare, McMaster University)

Hydrazones are created via a rapid condensation reaction between the aldehyde and hydrazide groups, resulting in the release of water from the reaction. Carboxymethyl cellulose will be functionalized with hydrazide groups via NHS/EDC chemistry using adipic acid dihydrazide (pKa ~3.4 from potentiometric titration, see Appendix D). The associated aldehyde functionalized polymers will consist of either carboxymethyl cellulose or dextran, modified to contain aldehydes via sodium periodate oxidation (Figure 2.9). With either component, an injectable *in-situ* gelling hydrogel will be prepared upon mixing the two functionalized polymers. It must be noted that hydrazone bonds can undergo degradation.

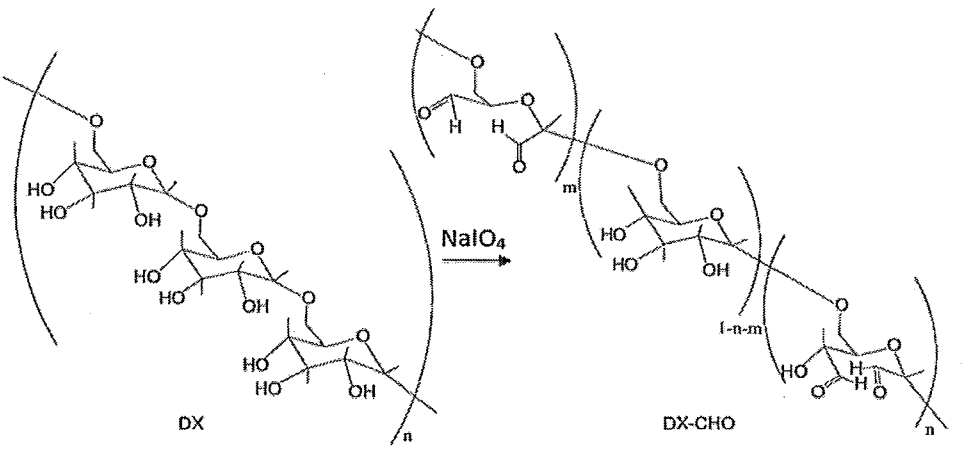

Figure 2.9: Oxidation of Dextran for Aldehyde formation

However, the erosion of the bonds is a slow acid-labile reaction that results in hydrolysis (Nathan *et al.*, 1996). Hydrazone degradation has been used as a controllable method to control the rate of degradation for hydrogels such as ones based on poly(aldehyde guluronate) (Lee *et al.*, 2000). Degradation is mediated by a bulk erosion process and is

dependent on the cross-link density of the hydrogel. Low cross-linked hydrogels tend to erode faster than that of hydrogels that are more cross-linked. In addition, during degradation, it is possible for the hydrazide bonds to re-cross-link with other aldehyde groups. The probability of this occurring increases for heavily cross-linked hydrazone hydrogels, which explains the slow degradation kinetics of highly cross-linked gels (Lee *et al.* 2000).

2.6.4 Poly(NIPAM-co-Acrylic Acid)

Poly(NIPAM-co-acrylic) microgels were used for several reasons in the development of the hydrogel-microgel composites. From previous research conducted by Hoare, AA-P(NIPAM) can be tuned for specific applications with modifications to functional monomer content, functional group distribution and changes in microgel size. Loading of drug has been proven to occur on the basis of the anionic microgels being able to bind onto cationic molecules. Furthermore, loading of drug into the microgel matrix can be differed based on temperature and functional group distributions. Lastly, AA-P(NIPAM) microgels can be further modified as to be able to cross-link with the hydrogel portion of the composite if necessary.

2.6.5 Bupivacaine Hydrochloride

The management of pain in a patient after surgery is important in the improvement of quality of life. Post-operative pain is found to be significant and is one of the primary concerns of patients admitted to the intensive care unit. Most analgesic

methods to alleviate pain center around intravenous injections that must be carried out by the patient or by the nurse every few hours (White *et al.*). Thus, developing strategies for reducing the frequency of drug administration and dosage for pain management via the development of controlled release vehicles is an important step toward improving patient care.

Bupivacaine is a cationic local anaesthetic that blocks the conduction of nerve impulses by decreasing nerve membrane permeability to sodium (Lexi-Comp). It is used mainly in pain management. In solution it behaves like a weak acid and has a pKa of 8.2. Its solubility is ~40mg/mL in acidic conditions, with solubility dropping 1000 times in basic conditions (Shah and Maniar, 1993). The structure is seen in Figure 2.10.

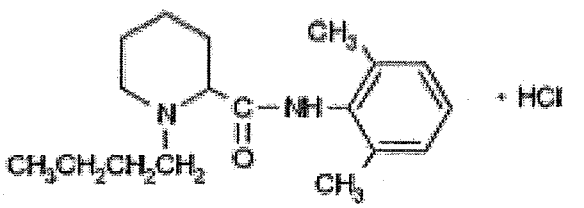

Figure 2.10: *Bupivacaine Hydrocholride*

Bupivacaine gives typically long-lasting anaesthesia effects, with recorded therapeutic times being four to nine hours when injected in solution. It is generally used to moderate post-surgical pain in both medicine and dentistry. It can be administered via central routes such as spinal or epidurals (Le Corre *et al,* 1994). It can also be administered via dextrose injection or in combination with epinephrine (Shah and Mania,

1993). Although considered long lasting, bupivacaine therapy only routinely uses concentrations that are low in nature varying from 0.5-0.75% due to the myotoxicity of bupivacaine at higher concentrations (Lexi-Comp). Thus repeated administration is needed. There has been much research to find ways to deliver fixed amounts of the drug for extended periods of time culminating in controlled release. Controlled release has been achieved in a few polymer systems such as polylactide and PLGA microspheres (Le Corre, *et al,* 1994). Very promising results have been found with the use of P(NIPAM) microgels, in which the microgels allow for a higher dose of bupivacaine to be administered without adverse effects (Hoare and Kohane, unpublished).

Bupivacaine was chosen to due the presence of anionic acrylic groups in the AA-P(NIPAM) microgels. Bupivacaine is cationic at physiological pH, allowing for electrostatic interactions to take place between the microgels and the drug, thus optimizing the load of drug into the hydrogel-microgel system. In addition, at physiological pH, there are hydrophobic partitioning driving forces that can act on the drug. The octanol-water partition coefficient (log P) of NIPAM residues and bupivacaine are similar. The log P of a NIPAM monomer sub-unit is approximately 0.06. For the cationic bupivacaine, the log P value is 0.18 (Sudoh *et al*, 2004). Since the log P values are similar, bupivacaine would prefer to partition into the hydrophobic domains of the microgel phase at physiological conditions rather than any bodily fluid (Hoare and Kohane, unpublished).

2.7 Objectives of Research

There has been recent progress in the development of composite hydrogel networks that contained entrapped microgel particles within the hydrogel matrix. These systems have great potential for drug delivery applications for controlled release of drugs (Yeo). These systems have several desirable features that utilize the benefits of both hydrogels and microgels. Hydrogel delivery systems are advantageous due to their biocompatibility as well as their tunable affinity for drugs. Obstacles with their use include the quick elution of drugs from the highly swollen hydrogel matrix and the inability for macroscopic hydrogels to be injected into the body. These hydrogels are routinely gelled and fabricated outside of the body and subsequently implanted. Microgels based on P(NIPAM) have great tunable responses that can maximize drug loading and control release and are readily injectable. However, there is typically rapid sequestering of the microgels into the liver or spleen. We can combat these problems by creating microgels that can be immobilized within an injectable hydrogel network which is liquid outside the body but gels inside the body. The goal of this work is to use acrylic acid-functionalized PNIPAM microgels combined with *in situ*-gelling hydrogel materials to make an injectable long-term drug delivery system for the delivery of local anaesthetics, aiming to address clinical needs in long-term pain management . The hydrogels were made of carboxymethyl cellulose (CMC) and dextran (Dex) modified with hydrazide (CMC-A) and aldehyde (Dex-B, CMC-B) functional groups. When mixed via co-injection through a needle, these two polymers rapidly form a hydrogel. By

co-injecting microgels together with one of the reactive polymers, composite, *in situ* gellable hydrogel-microgel networks are formed. The impact of the crosslink density, degree of swelling, and the ionic drug affinity of both the hydrogel and microgel phases on the release kinetics of bupivacaine were investigated to determine how to engineer the microgel-hydrogel composites to achieve optimized drug release profiles. The effect of changes to the functional group content of either the microgel or the hydrogel was also be investigated to determine the impact of phase functionalization on drug release. Cross-linking of the microgels to the hydrogel matrix was also explored to see the effects of mechanically restricting the microgel phase transition on drug release. Rheological analysis was conducted to find the mechanical strength of these network polymers. Cell viability tests were also conducted to ensure that these polymer networks and the reactive gel precursors are not cytotoxic.

Chapter 3: Materials and Methods

3.1: Reagents

Acrylic Acid Functionalized P(NIPAM) Microgels

N-isopropylacylamide (NIPAM), acrylic acid (AA), ammonium persulfate (APS), N,N'-methylene bisacrylamide (MBA), and bupivacaine hydrochloride were all purchased directly from Sigma Aldrich (Oakville, ON). Sodium Dodecylsulfate (SDS) was obtained from Bioshop Canada (Burlington, ON).

Hydrazide Functionalized Carboxymethyl Cellulose

Sodium carboxymethyl cellulose (CMC) [MW 250,000] was purchased from Sigma Aldrich (Oakville, ON). Adipic acid dihydrazide (ADH), N-Hydroxysuccinimide (NHS), and N'-ethyl-N-(3-dimethylaminopropyl)- carbodiimide (EDC) were purchased from Sigma Aldrich (Oakville, ON). Dimethyl sulphoxide (DMSO) was purchased from Caledon Laboratory Chemicals (Georgetown, ON).

Aldehyde Functionalized Carboxymethyl Cellulose and Dextran

Sodium carboxymethyl cellulose (CMC) [MW 700,000], dextran from *Leuconstroc spp* [M_r – 500,000], ethylene glycol, and sodium periodate were all purchased from Sigma Aldrich (Oakville, ON).

Cell Culture

3T3 *Mus musculus* mouse cells and C2C12 mouse muscle myoblast cells were acquired from ATCC: Cederlane Laboratories Ltd. (Burlington, ON). Media contents included Dulbecco's Modified Eagle Medium-high glucose (DMEM), fetal bovine serum (FBS), horse serum (HS), and Penicillin Streptomycin (PS), which were obtained from Invitrogen Canada (Burlington, ON). Recovery cell culture freezing and trypsin-EDTA were purchased from Invitrogen Canada (Burlington, ON). Thiazolyl Blue Tetrazolium Bromide (MTT) was purchased from Sigma Aldrich (Oakville, ON).

Additional information regarding reagents is found in Appendix A.

3.1 Double Barrel Syringe Apparatus

Double barrel syringe supplies were purchased from Medmix Systems (Switzerland). The double barrel syringes are comprised of four components as seen in Figure 3.1. The first component is the double barrels (1) which have the capability to house two separate solutions that are to be mixed. The mixer (2) is affixed to the ejection side of the barrel and is screwed in. The mixer is responsible for the mixing of the two solutions within the barrels. The mixer can also be affixed with a needle (20 gauge) to provide further control of the resultant mixed solution/gel. Injection is facilitated by the double plunger (3) and the o-rings (4).

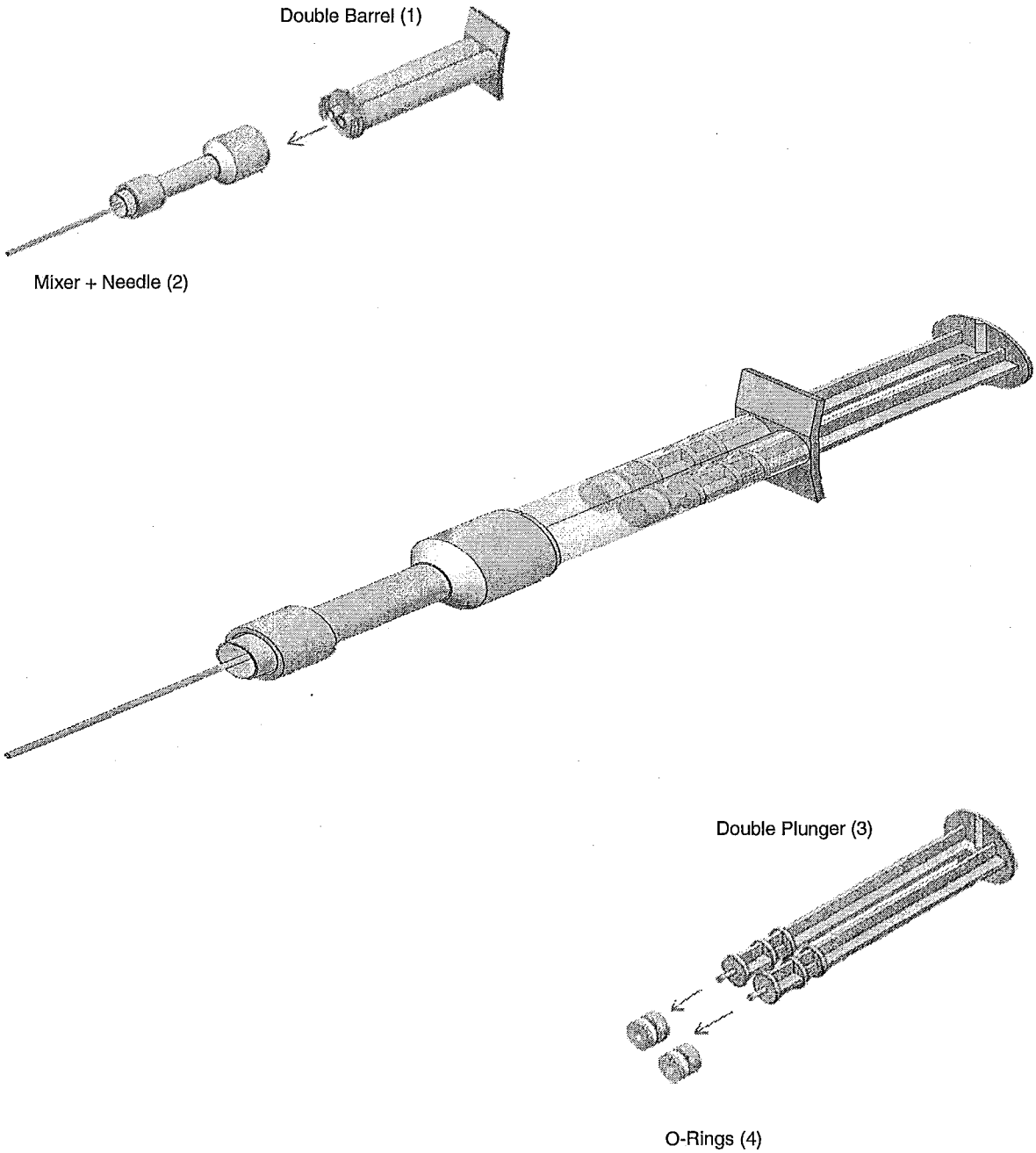

Figure 3.1: Double Barrel Syringe for Hydrogel-Microgel Composite Formation

3. 3 Acrylic Acid Functionalized Poly(NIPAM) Preparation

N-Isopropylacrylamide monomer was purified with a 60:40 toluene: hexane mixture. The amount of NIPAM added was equivalent in 1:1 w/v % ratio with toluene. The mixture was placed in an oil bath and heated to 60°C. Once dissolved, the solution was placed in ice bath for 2 hours until recrystallization occurred. The solution was then filtered to isolate the NIPAM crystals and the recrystallized product was dried under nitrogen for 12 hours prior to storage.

3.4 Acrylic Acid Functionalized Poly(NIPAM) Polymerization

Formulations for various degrees of microgel functionalization are found in Table 3.1. Microgels were synthesized based on methods described by Hoare and Pelton. Polymerizations were done in a three necked flask with magnetic stir bar and attached condenser. Appropriate amounts of NIPAM monomer, acrylic acid, MBA, and SDS were dissolved in 150mL Milli-Q water. Polymerization was done at a temperature of 70°C under nitrogen purge at a mixing rate of 200rpm. After 30 minutes of heating, APS was dissolved in 10mL of Milli-Q water and added to the mixture to initiate polymerization. Polymerization was allowed to continue for 12 hours followed by dialysis for purification. Dialysis was performed against MilliQ water with membrane tubing from Spectrum Labs (132680) with a molecular weight cut-off of 12,000 – 14,000 Da. A minimum of 6 dialysis cycles were conducted prior to the solutions being lyophilized and stored dry for future use.

Table 3.1: Formulations of AA-P(NIPAM) Microgels

Code	NIPAM (g)	Acrylic Acid (g)	MBA (g)	SDS (g)	APS (g) + 10mL H_2O	H_2O (mL)
AA1 (6mol % AA)	1.4	0.058	0.1	0.2	0.1	150
AA2 (11mol% AA)	1.4	0.116	0.1	0.2	0.1	150
AA4 (20mol% AA)	1.4	0.232	0.1	0.2	0.1	150
AA8 (33mol% AA)	1.4	0.464	0.1	0.2	0.1	150

3.5 Hydrazide Functionalized Carboxymethyl Cellulose Modification (A Polymer)

Formulations for various degrees of hydrazide attachment are found in Table 3.2. Hydrazide attachment was conducted following methods described by Hudson. Carboxymethyl cellulose (250kDa) was dissolved in a 200mL Milli-Q water in a 250mL round bottom flask. A magnetic stir bar at 200rpm was used. Adipic acid dihydrazide was added, resulting in a solution with a pH of ~ 7. N-hydroxysuccinimide was dissolved in 4mL DMSO:H_20 (1:1) and added dropwise to the CMC solution. N'-ethyl-N-(3-dimethylaminopropyl)- carbodiimide was dissolved in 1mL of 1:1 DMSO:H20 and added dropwise to CMC solution. The pH of the resulting mixture was continuously adjusted to

a pH of 6.8 with 0.1M NaOH. The reaction was permitted to react until the pH became constant, which took approximately 1 hour. The resulting polymer was dialyzed with membrane tubing from Spectrum Labs (S632724) with a molecular weight cut-off of 3,500 Da. A minimum of 6 dialysis cycles were conducted prior to the solutions being lyophilized and stored dry for future use.

Table 3.2: Formaulations for Hydrazide Functionalized Carboxymethylcellulose

Code	CMC (g)	ADH (g)	NHS (g)	EDC (g)	H_20 (mL)
CMC-A0.5	1	3	0.035	0.3	200
CMC-A1	1	3	0.07	0.3	200
CMC-A1.5	1	3	0.10	0.3	200
CMC-A2	1	3	0.13	0.3	200

3.6 Hydrazide Functionalized AA-P(NIPAM) Microgels

Recipes and methods are identical to hydrazide-functionalization of CMC. However, 1g of AA-P(NIPAM) was used instead of 1g of CMC per recipe.

3.7 Aldehyde Functionalized Dextran/Carboxymethyl Cellulose (B Polymer)

Dextran or carboxymethyl cellulose (1.5g, 250kDa) was slowly dissolved in 150mL Mill-Q water in a 250mL round bottom flask. A magnetic stir bar was rotated at 200rpm. Sodium periodate (0.8g) was dissolved in 10mL water, added dropwise to

polymer solution, and allowed to stir for 2hours. Ethylene glycol (0.4mL) was then injected into the solution and allowed to react for 1 hour. The resulting polymer was dialyzed with membrane tubing from Spectrum Labs (S632724) with a molecular weight cut-off of 3,500 Da. A minimum of 6 dialysis cycles were conducted prior to the solutions being lyophilized and stored dry for future use.

3.8 Hydrogel-Microgel Composite

Polymer solutions to be used for hydrogel fabrication were prepared in 2mL micro-centrifuge tubes. In the first tube, CMC-A polymer (40mg) was dissolved in 2mL of 0.15M saline at a concentration of 2w/v%. In the second tube, 2w/v% of CMC-B or Dex-B polymer (40mg), 20mg of total solution bupivacaine (5mg/mL), and 4w/v% of AA-poly(NIPAM) microgels (80mg) were dissolved in 2mL of 0.15M saline.

The microgel-hydrogel composites were created using double barrel syringes purchased from Medmix Systems (Switzerland). Each individual barrel contained the contents of one of the premade solutions from the micro-centrifuge tubes described above. A 20-gauge needle was affixed to the mixer end of the double barrel syringe to allow for ease of injection. Upon mixing within the mixer and needle, the resulting composite was injected into cylindrical moulds prepared from silicone rubber obtained from McMaster Carr (Illinois, USA). The moulds had a diameter of 0.95cm and height of 0.32cm, resulting in a disk shaped hydrogel-microgel composite.

Control hydrogels were made in identical fashion to the procedure described above. However, bupivacaine was not included in the formulation. Special hydrogel controls were also made that consisted of just the hydrogel components and contained no microgel fraction.

3.9 Hydrogel Characterization

3.9.1 Potentiometric and Conductometric Titration of Hydrazide-Functionalized CMC

Hydrazide attachment to the CMC backbone was primarily determined via potentiometric titration, as described by Hoare and Pelton (Langmuir, 2004). Titrations were performed using a Burivar-I2 automatic buret (ManTech associates) with PC-Titrate software (Version 2.0.0.79) for control. Samples of 50mg CMC-A polymers were dissolved in 50mL of 10^{-3}M NaCl for titration. Titrations were run in clean 100mL beaker and temperature controlled at 25°C. The beaker was fitted with overhead mixer, thermometer, pH electrode and conductivity electrode from ManTech associates. Nitrogen was purged into the system for 30 minutes to remove dissolved carbon dioxide from the solution. The pH of the solution was controlled by 0.1M HCl and 0.1M NaOH from Acculute standards. Prior to titration, the solution pH was lowered to 3.5. With a gentle nitrogen purge onto the sample to keep an inert atmosphere, data was obtained with a base into acid titration, using an end pH value of 11.5. Injections of NaOH were performed at a rate of 10min/unit pH over the course of the titrations. Since the pKa of hydrazide groups (~3.4) is approximately 2 units lower than the pKa of carboxylic acid groups (~5.3), independent characterization of hydrazide and carboxylic acid groups is

possible in this system. Indeed, >80% of hydrazide groups will be ionized before the ionization of CMC-bound –COOH groups begins (see Appendix D).

3.9.2 Aldehyde Detection Test

The quantity of aldehyde functional groups derived from the oxidation of dextran and CMC was determined by using a tert-butyl carbazate assay. Approximately 5mg of aldehyde functionalized polysaccharide was dissolved in 1mL sodium acetate buffer (10mM, pH 5.2, 0.2M NaCl) which contained tert-butyl carbazate (0.04g). This solution was mixed with the polysaccharide for 24 hours at room temperature. 0.005 mL of the reacted solution was extracted and added to 1.98mL borate buffer (50mM, pH 8). A further 50uL of 5 w/v% 2,4,6-tri-nitrobenesulfonic acid solution (TNBS) was added and reacted with the borate-buffered solution at room temperature. The resulting red solution was diluted 1:1 with 0.5M hydrochloric acid. This resulted in a yellow solution, of which 50µL was extracted and added to 1.95mL of 0.5 M hydrochloric acid. The absorbance of the solution was measured taken on a DU 800 UV/Visible Spectrophotometer (Beckman Coulter) with associated Beckman Coulter DU 800 software (version 3.0) at a wavelength of 334nm. Blanks were measured on the UV spectrophotometer to account for background noise generated by the solvent. The same dilutions with solvent were conducted above without reactive species (aldehyde, carbazate, or TNBS). The absorbance was then subtracted from the measured absorbencies of the carbazate-TNBS complex.

3.9.3 Rheology Measurements of Hydrogels and Microgel-Hydrogel Composites

Measurements on the hydrogel composite and hydrogel-microgel composite were done by following procedures set by Motlagh *et. al* (2007). Complex viscosity(η^*) as well as storage (G') and loss moduli (G") were measured using an ARES rheometer (TA Instruments) using parallel-plate geometry. The parallel plates had diameters of 7mm with a gel thickness adjusted to 1mm. A strain sweep test was conducted with strains between 0.1 – 100% and constant frequency of 1Hz to identify the linear viscoelastic range. This was done by finding the linear region of G' and η^* as a function of strain. A constant strain was then chosen within the linear viscoelastic region and a frequency sweep test was performed using the characteristic strain as a control variable. A frequency sweep range of 0.1-100 rad/s was determine the complex viscosity, G', and G" of the composite. All rheological measurements were conducted at 21°C.

3.10 Microgel Characterization

3.10.1 Dynamic Light Scattering

Particle sizing of the microgels was conducted with dynamic light scattering using a Melles Griot HeNe laser with a 632.8 nm light source. Detection was done at a 90° angle with a Brookhaven Instruments Corporation (BIC) detector model BI-APD. Correlation data was analysed with a BIC TurboCorr digital correlator and corresponding software (Version 3.34). Dried microgels were suspended in a 10mM PBS solution at a concentration of 4mg/mL, producing an intensity count between 100-250 kilocounts per second. Duration times for measurement were 5 minutes per sample. Readings were

conducted at 25°C and 37°C. At least five replicates were conducted for each sample; the experimental uncertainties represent the standard deviation of the replicate measurements. Drug solutions with 10mM PBS were mixed with microgels to determine drug-microgel interactions. Drug solutions were varied by weight percent with relation to the microgel content that was in solution (4mg/mL). The same measuring procedures as above were followed.

310.2 Electrophoretic Mobility

Electrophoretic mobility was measured using a ZetaPlus zeta potential analyser from Brookhaven Instrument Corporation operating in PALS (phase analysis light scattering) mode with polystyrene cuvettes. Samples were prepared in 10mM PBS and done in triplicates, with each run consisting of 15 cycles; the experimental uncertainties represent the standard deviation of the replicate measurements.

3.10.3 Potentiometric and Conductometric Titration of AA-P(NIPAM) microgels

Methods were similar to hydrogel titration in Section 3.8.1. For microgel titrations, solutions contained 50mg of AA-P (NIPAM) dissolved in 50mL of 10^{-3}M NaCl.

3.11 Drug Release Studies

Drug release studies for the AA-P(NIPAM) microgels were conducted in 1mL 100kDa float-a-lyzer cellulose membranes. Drug release for the hydrogels and

composites were conducted in 12 well plates from Falcon. Six hydrogel-microgel composites were used for each test sequence and were placed cell culture inserts (2.5cm diameter, 8μm pore size), which were subsequently placed in the 12 well plates. Prior to testing, the cell inserts were perforated 20 times using a 20 gauge needle to ensure facile release medium flow in and out of the insert. A total of 2mL of 10mM PBS was injected into each well for bupivacaine elution to occur. Incubation was allowed to occur in an incubating orbital shaker (VWR) at 37°C at a stir rate of 100 rpm. Gels were switched into fresh media every 30 minutes for the first 2 hours, then every hour for the next five hours. This was followed by subsequent measurements over the course of the gel lifetime. At all times, the drug concentration measured was less than 10% of the drug solubility in the PBS buffer, ensuring infinite sink conditions at all points during the release experiment.

Measurements of eluted drug content were performed using a DU 800 UV/Visible Spectrophotometer (Beckman Coulter) with associated Beckman Coulter DU 800 software (version 3.0). The drug-PBS solution was placed in a freshly cleaned quartz cuvette from VWR. Cuvettes were cleaned with Milli-Q water as well as acetone followed by an air purge to ensure excess reside was removed before each measurement. A wavelength scan was used with a UV light scale from 190nm to 400nm. A known peak at 262nm was observed from bupivacaine in measurements. A calibration curve was created with various known amounts of bupivacine with 10mM PBS buffer to quantify the amount of drug being released from the gels.

Blanks of the composites were created using the same hydrogel and microgel precursors of those used in drug release. The blank composites were exposed to 2mL of 10mm PBS for the same time periods as their drug-loaded composite counterparts. This was followed with UV measurements being made on the release media using the same wavelength range as used for the bupivacaine release studies. This was done to account for the dissolution of polymers into the release medium from the degradation of the hydrogel, which gave a small concentration-dependent signal at the UV wavelength use to quantify bupivacaine. The absorbance measured from the blank sample was subtracted from the absorbance measured using bupivacaine release samples collected at the same time with the same composite hydrogel to calculate the final release curves. At least six replicates were conducted for each sample; the experimental uncertainties represent the standard deviation of the replicate measurements.

3.12 Gel Swelling

Swelling of the microgel-hydrogel composite was determined by comparing the room temperature mass of the gel with its mass as a function of time at physiological temperature. Percentage mass changes were then calculated according to the equation:

$$\frac{Mass_{37^{\circ}C} - Mass_{20^{\circ}C}}{Mass_{20^{\circ}C}} \quad (3)$$

The mass of the cell insert and the gel was measured every time the 10mM PBS media was changed (i.e. at each time point for the release study), allowing continuous tracking

of hydrogel swelling/ deswelling/degradation over the lifetime of the gel composite. At least six replicates were conducted for each sample; the experimental uncertainties represent the standard deviation of the replicate measurements.

3.13 Cell Viability Testing

Cell viability was tested with the use of 3T3 *Mus musculus* mouse cells and C2C12 mouse muscle myoblast cells. Proliferation media consisted of 500mL DMEM, 50mL FBS, and 5mL PS. Differentiation media for the C2C12 cells (to facilitate differentiation of myoblasts to myotubes) used 10mL HS instead of FBS. A detailed procedure for cell splitting and culturing is available in Appendix A. Tests were conducted in polystyrene 24 well plates ($2cm^2$) containing either 10,000 3T3 cells or 50,000 C2C12 cells and containing 1mL HS containing media. A blank well containing no cells and wells containing cells but no polymer solutions were used as controls. Cells were exposed to various solutions of A polymer, B polymer, and poly(NIPAM-co-AA) microgels at concentrations ranging from 100μg/mL to 10,000 μg/mL. In addition, cells were exposed to the hydrogel-microgel composite using two different approaches: (1) placing the composite hydrogel on top of a cell layer and (2) casting the hydrogel in the 24 well plate and plating cells on top of the hydrogel layer. Each experiment was replicated 4 times each to ensure consistent behaviour among the cell response, with the error bars representing the standard deviation of the measurements.

3.13.1 Sterilization

Polymer precursors were sterilized using UV radiation. Polymer precursors were exposed to 2 hours of UV radiation per side of polymer. The polymer was then rotated and exposed for 2 hours again for a total of 4 hours of UV radiation to ensure sterilization. Hydrogel solvent (0.15M saline) was filtered though 0.2mμm pre-sterilized filters and exposed to UV light for 2 hours. Hydrogel composites were fabricated in a biohood to minimize bacterial contamination.

3.13.2 MTT Assay

Cell viability was assessed via the thiazolyl blue tetrazolium bromide (MTT) assay, modified from manufacturer's protocols as described by Pawlikowska (2006). The MTT stock solution (3mL) was reconstituted in PBS and sterile filtered. The concentration of the stock solution was 40mg/mL, prepared in 10mM PBS. When applied to cells, the solution was diluted to 0.4mg/mL with appropriate HS containing medium. After 24 hour exposure to polymers, cells were exposed to 150μm of MTT solution and incubated for 4 hours. After the incubation, 250μL DMSO was added to each well to solubilise the formazan precipitate. Plates were shaken for 10-20 minutes or until formazan was dissolved. The resulting solution was transferred to a 96 well plate (200μL per plate) and read in a microplate reader (Biorad, Model 550) at 540nm, with absorbance due to the plate and medium itself used as a control. Viability was measured as a function of formazan absorption at 540nm. Absorption was compared to a blank well, in which no

polymer was exposed to cells. Resultant cell viability was calculated using the following equation:

$$Cell\ Viability(\%) = \frac{Absorbance_{Polymer\ Solution}}{Absorbance_{Blank}} \quad (4)$$

Chapter 4: Material Characteristics

4.1 Hydrazide Functionalized Carboxymethyl Cellulose

Production of the hydrazide-functionalized CMC (CMC-A) was conducted at room temperature, with the extent of reaction indicated by increasing solution viscosity over time. After purification and lyophilisation, the solubility of the polymer varied depending on the degree of functionalization. The polymers functionalized with fewer hydrazide groups (CMC-A0.5) dissolved readily in 0.15M saline solution while the polymer with the highest degree of hydrazide functionalization (CMC-A1.5) required three days of constant shaking to fully dissolve. For all polymer solutions, the viscosity of the solution was much higher than that of water.

4.1.1 Degree of Functionalization

To assess the success of hydrazide functionalization onto the carboxymethyl cellulose backbone via NHS/EDC chemistry, base-into-acid potentiometric and conductometric titration was conducted with 0.1M NaOH. Reaction of adipic acid dihydrazide with CMC via EDC/NHS chemistry consumes one titratable –COOH group per hydrazide group conjugated to the polymer. Thus, the change in the number of titratable functional groups before and after hydrazide functionalization permits characterization of the hydrazide content of the CMC-A polymers. Figure 4.1.1 confirms that increased hydrazide functionalization of CMC results in fewer titratable carboxylic acid functional groups.

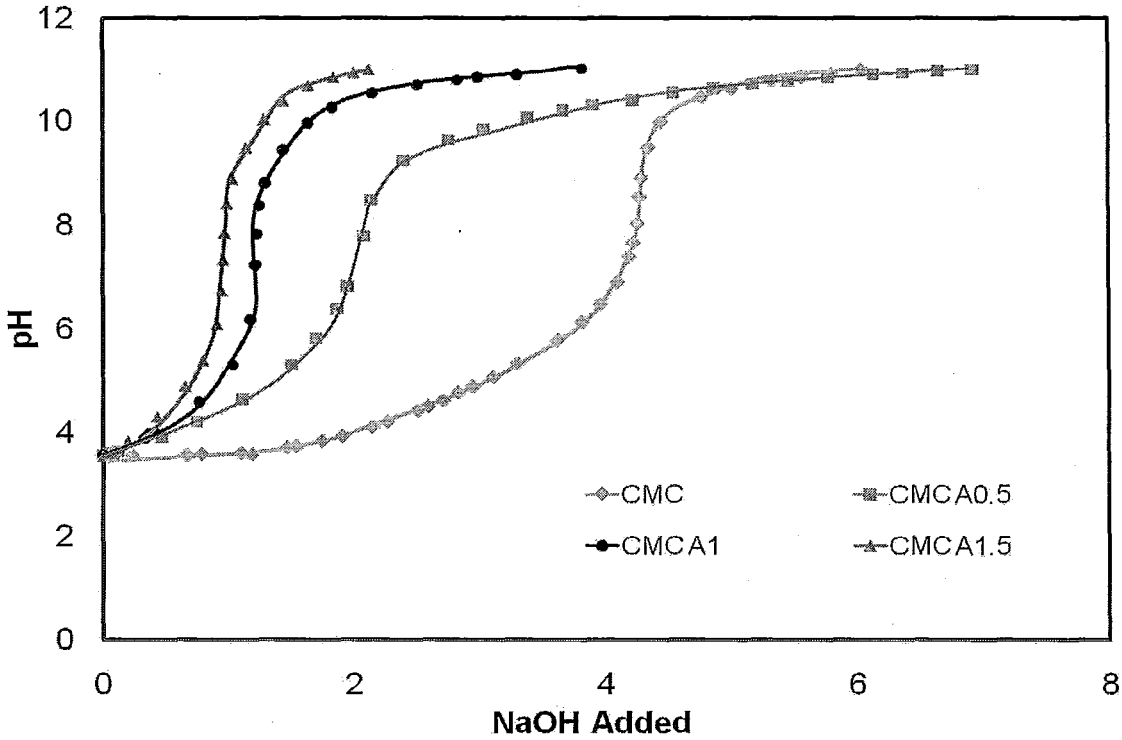

Figure 4.1.1: Potentiometric Titration of Hydrazide-Functionalized CMC (50mg) with 0.1 NaOH

Using the conductometric data, we can calculate how many of the carboxyl groups were converted using unmodified CMC as a reference point. Results are shown in Table 4.1.1.

Table 4.1.1: Percent Hydrazide Functionalization on CMC Backbone

Polymer	Percent of Carboxyl Groups Converted
CMC A0.5	30.4%
CMC A1.0	43.9 %
CMC A1.5	49.4%

The polymer with the highest degree of functionalization (CMC-A1.5) has ~ 50% conversion of carboxylic acids to hydrazides (average of ~700 hydrazide groups per single CMC chain), while the polymer with the lowest degree of functionalization (CMC-A0.5) has ~30% hydrazide functionalization (average of ~400 hydrazide groups per single CMC chain). Higher degrees of functionalization led to issues with polymer solubility, while lower degrees of functionalization led to issues with slow gelation times. The 20% range in hydrazide functionalization achieved offers potential control over the cross-linking density of the resulting hydrogel, which we will assess later.

4.2 Aldehyde Functionalized Dextran/CMC

Production of the aldehyde-functionalized dextran and CMC was conducted at room temperature and was followed by dialysis and lyophilisation. Solubility of the aldehyde polymers was very high in 0.15M saline solution.

4.2.1 Degree of Functionalization

The percentage oxidation of hydroxyl groups into aldehydes on the CMC and dextran backbones was determined using tert-butyl carbazate assay. Carbazates are well-known to react to form stable carbazones via a mechanism that is similar to the formation of hydrazones (Bouhadir *et al*, 1999). The carbazates will react with aldehydes to form carbazones in a 1:1 reaction. The amount of unreacted carbazate can then be determined with the addition of trinitrobenzenesulfonic acid (TNBS). This results in a coloured solution which can be assayed using UV/VIS spectrophotometery. After the

determination of residual carbazate, we can subtract that value from the total added carbazate to determine the number of aldehydes in the original solution. Table 4.2.1 shows the results of this analysis. Overall, 30-40% of hydroxyl groups along the carbohydrate backbones are converted to aldehydes via the oxidation reaction performed, with dextran exhibiting a slightly higher degree of aldehyde functionalization.

Table 4.2.1: Percent Aldehyde Functionalization on CMC or Dextran Backbone

Polymer	**Hydroxyl Groups Converted**
Dextran	37.0%
Carboxymethyl Cellulose	31.6%

4.3 Acrylic Acid-P(NIPAM) Microgel Characteristics

Production of the microgels occurred rapidly after injection of the initiator into the monomer solution. The colour of the solution changed from transparent to a blue-white colour while the microgel was formed. The turbidity of the suspension increased with the degree of acrylic acid functionalization, with the most functionalized microgels appearing completely opaque. Once lyophilized, the microgels were easily re-suspended in saline. To prepare the composite hydrogels, the microgels were mixed with the aldehyde polymer solution since the viscosity of that solution was much lower, offsetting the moderate viscosity of the microgel suspension at the concentrations used to prepare the

hydrogels (4wt%). Degree of functionalization was verified via conductometric titration and can be seen in Table D1.

4.3.1 Particle Size - Dynamic Light Scattering

Microgel sizing was conducted using dynamic light scattering. The particle sizes were measured at room temperature (25°C), at which the microgels are in their swollen state, and at physiological temperature (37 °C), in which the microgels have at least partially undergone a phase transition. Particle sizes for each microgel were tested in 10mM PBS, are displayed below in Table 4.3.1.

Table 4.3.1: Hydrodynamic Diameter of AA-P(NIPAM) Microgels

Microgel Type	**Particle Size at 25°C (nm)**	**Particle Size at 37°C (nm)**
6mol% AA	133.2 ±8.3	89.1 ± 0.4
11mol% AA	170.2 ± 6.4	161.8 ± 3.8
20mol % AA	270.8 ± 19.0	206.3 ± 4.6
34mol% AA	324. 5 ± 8.5	282.2 + 7.2

The data suggests that with an increase in acrylic acid groups per microgel, there is an associated increase in particle diameter. The least functionalized microgel had an average diameter of 133nm at room temperature, while a five-fold increase in acrylic acid groups results in an average diameter of 324nm. This can be attributed to charge-driven swelling

in microgels, in which microgels with more acrylic acid groups have a higher overall charge density and thus swell more due to Donnan equilibrium effects. The same trends are observed at elevated temperatures. The particles shrink in diameter at physiological temperatures but still increase in size with increased acrylic functionalization. It should be noted that AA-6% experiences a significantly higher volume change upon heating to 37 °C (-70%) than the AA-34% microgel (-34%), again owing to the increased hydrophilicity of AA residues that shift the volume phase transition temperature of more highly AA-functionalized microgels to higher temperatures.

4.3.2 Drug Loading Effects on Microgel Size

Drug-microgel interactions were studied to determine if the addition of bupivacaine would play a role in the swelling characteristics of the microgel. Microgel condensation has previously been observed when cationic drugs are loaded into anionic microgels, inducing large size changes and significantly inhibiting drug release at high loading levels (Hoare and Pelton, 2008). Correspondingly, if the microgel size increases as drug is exchanged out of the microgel phase, the effective diffusion coefficient of drug inside the microgel phase will increase over time. This may in part compensate for the lower concentration gradient present at longer release times as the drug delivery vehicle is depleted of drug, resulting in a more constant release over an extended duration.

The microgel containing 6 mol% and 20 mol% acrylic acid was used in the study, with measurements taken at both room temperature and physiological temperature. Drug loading was conducted at bupivacaine concentrations ranging from 0% to 12.5% on a

weight basis to the total microgel added (i.e. mass of drug:dry mass of microgel). In the standard hydrogel-microgel composite release studies, the microgels were loaded using bupivacaine solutions at 5mg/mL, which corresponds to a wt:wt ratio of approximately 12.5 wt%. The results of the drug-microgel interactions are displayed below in Figure 4.3.1 and Figure 4.3.2.

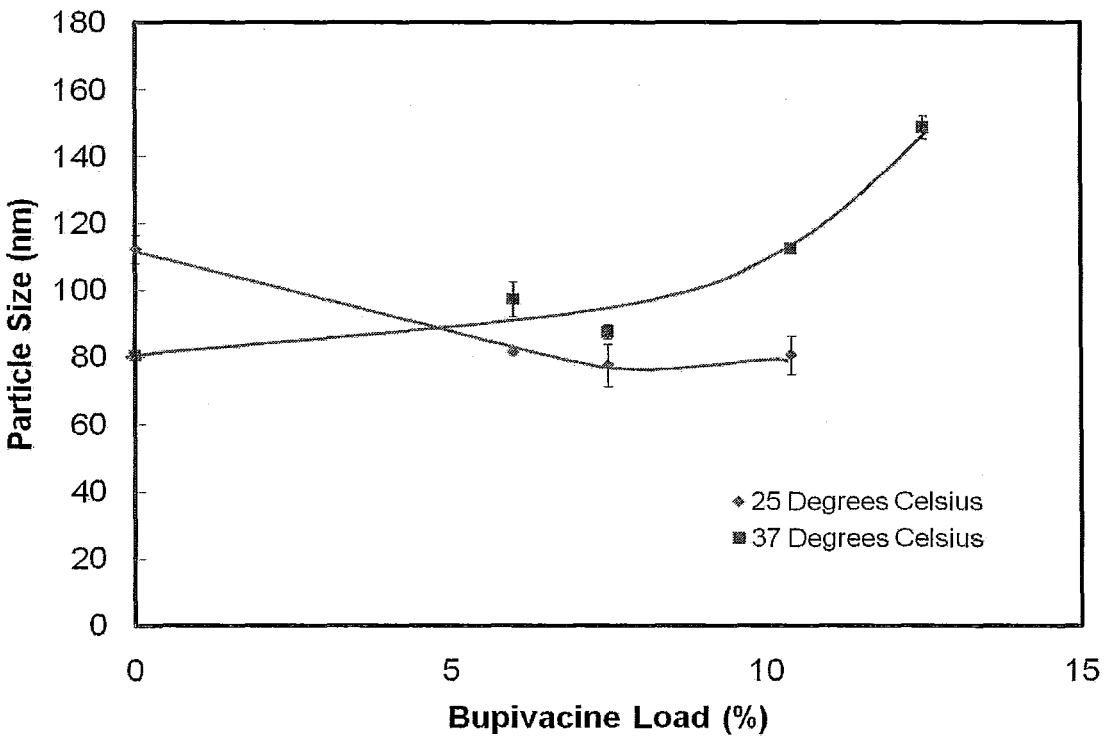

Figure 4.3.1: Particle Size of Bupivacaine-Loaded (w/w%) 6mol% AA-P(NIPAM) Microgels

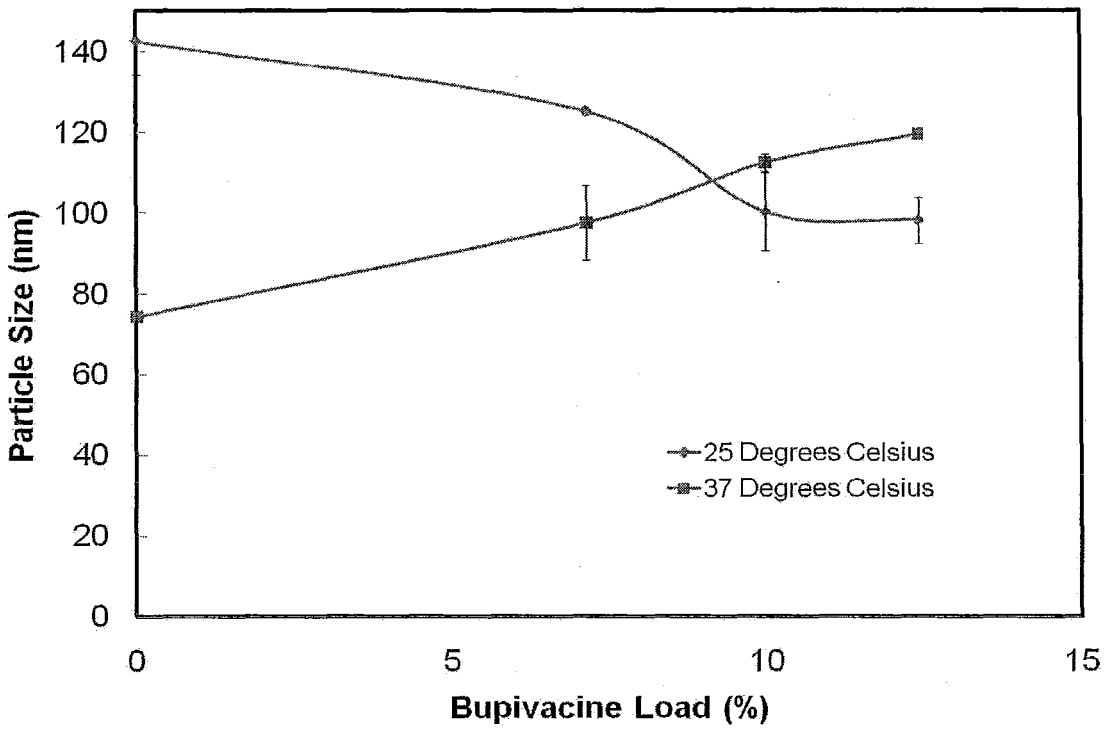

Figure 4.3.2: Particle Size of Bupivacaine-Loaded (w/w%) 20mol% AA-P(NIPAM) Microgels

When the drug is loaded at room temperature, the microgel diameter decreases with the amount of drug loaded into the microgel. The direct opposite effect is seen at physiological temperatures. There is a rapid increase in size in relation to drug content.

The reduction in particle size as a function of bupivacaine binding at low temperature is a result of the reduced charge density of the microgel network as the cationic bupivacaine is introduced, which neutralizes the acidic microgel sites, which in turn reduces swelling. Additionally, increased hydrophobicity caused by bupivacaine partitioning into the microgel can lead to the removal of water from the system (Hoare

and Pelton, 2008). Microgels reach their collapsed state at different drug concentrations depending on acrylic acid functionalization. The 6mol% AA microgel collapses fully at about 6wt% drug concentration where as the 20% AA microgel collapses fully at concentrations about 10 wt% drug. This suggests that the higher concentrations of acrylic groups allow for more drug binding before the charge density of the microgel is completely neutralized and the microgel reaches an equilibrium swelling.

At physiological temperatures (above the VPTT of the microgel), the microgel is already partially or completely collapsed at the high-salt conditions used in the test (and *in vivo*). However, with drug present, NIPAM-NIPAM interactions driving the microgel deswelling may be disrupted by the presence of adsorbed bupivacaine, either through direct blocking of isopropyl groups or steric restrictions on local chain mobility imposed by the bound bupivacaine molecule. As a result, deswelling is not as efficient as in the absence of drug in the collapsed state and the average diameter increases as a function of the bupivacaine loading. Microgel aggregation may also account for the increased particle size, particularly at high concentrations of bupivacaine. Bupivacaine binding to anionic functional groups on microgels consume the charges that are predominantly responsible for stabilizing the microgel above the VPTT, at which point the hair-like surface chains on the microgel which provide steric stabilization become insoluble. Thus, although no evidence is observed for the formation of large aggregates, small microgel clusters may form that increase the measured average diameter.

4.3.3 Electrophoretic Mobility

Electrophoretic mobilities for each of the AA-P(NIPAM) microgels tested, as measured in $m^2/V \cdot s$, are shown in Table 4.3.2.

Table 4.3.2: Electrophoretic Mobilities of AA-P(NIPAM) Microgels at 25°C

Microgel Type	**Electrophoretic Mobility ($x10^{-8}$ m^2/Vs)**
6mol% AA	-0.51 ± 0.09
11mol% AA	-1.07 ± 0.14
20mol % AA	-1.87 ± 0.18
34mol% AA	-1.80 ± 0.18

As anticipated, an increase in acrylic acid incorporation into the microgel leads to a higher mobility (i.e. surface charge). This data confirms that each type of microgel was synthesized with different fractions of acrylic acid incorporation into the microgel. The only exception to this trend occurs at higher degrees of functionalization; the 20mol % and 34mol% AA-NIPAM microgels have statistically identical electrophoretic mobilites. This may be attributable to changes in microgel aggregation kinetics as the AA:NIPAM ratio increases. Alternately, charge-driven swelling due to the presence of high charge densities in AA-34% may reduce the effective volumetric charge density, thereby reducing the measured mobility value. Approximate values for the charge density of the microgel and hydrogel phases used can be seen in Appendix D.

4.4 Hydrogel Characteristics

The polymer solutions were loaded into the dual-barrel syringe and injected into cylindrical moulds to create the hydrogel-microgel composites. The polymer solutions were easy to extrude and flowed from the syringe at a consistent rate. Gelling times for the hydrogel structure varied between 5-15 seconds, depending on the degree of hydrazide functionalization on the CMC-A polymer used. Less hydrazide-functionalized CMC polymers require longer gelation times. The hydrogels were optically clear. The gels were elastic to the touch and were easily handled without inducing any mechanical degradation.

4.5: Rheological Measurements

The mechanical properties of the hydrogel and hydrogel-microgel composite were studied with the use of parallel-plate rheometry. Using the parallel-plate rheometer, the G' (storage modulus), G" (loss modulus), and complex viscosity (η^*) of the composites were determined. Tests were conducted on gels prepared with aldehyde-functionalized dextran (Dex-B) with hydrazide-functionalized CMC containing different fractions of hydrazide functional groups, permitting detection of the differences in mechanical properties of the hydrogels as a function of hydrogel cross-linking. Gels prepared using CMC-A0.5 and/or CMC B polymers were extremely weak and did not possess sufficient friction with the rotating rheometer plate to record accurate results.

4.5.1 Degree of Cross-Linking In Hydrazide Functionalized CMC

Rheological tests were done to determine the impact of cross-linking on the mechanical strength of the hydrogels. It was hypothesized that with higher amounts of hydrazide, the gels would contain more cross-linking. From Figure 4.5.1, hydrogels prepared with CMC A1.5 (49% hydrazide functionalization) exhibited a ~60% higher storage modulus and a 40% lower loss modulus than hydrogels prepared with CMC A1 (43% hydrazide functionalization) across all frequency values studied. From the much higher G' values (with G'> G"), we can assume that the hydrogels have flow properties that are predominately elastic (Hoare, 2010, JBMR A, part I). This suggests that gels will be mechanically robust post-injection, even if injected in areas in the body exposed to shear forces.

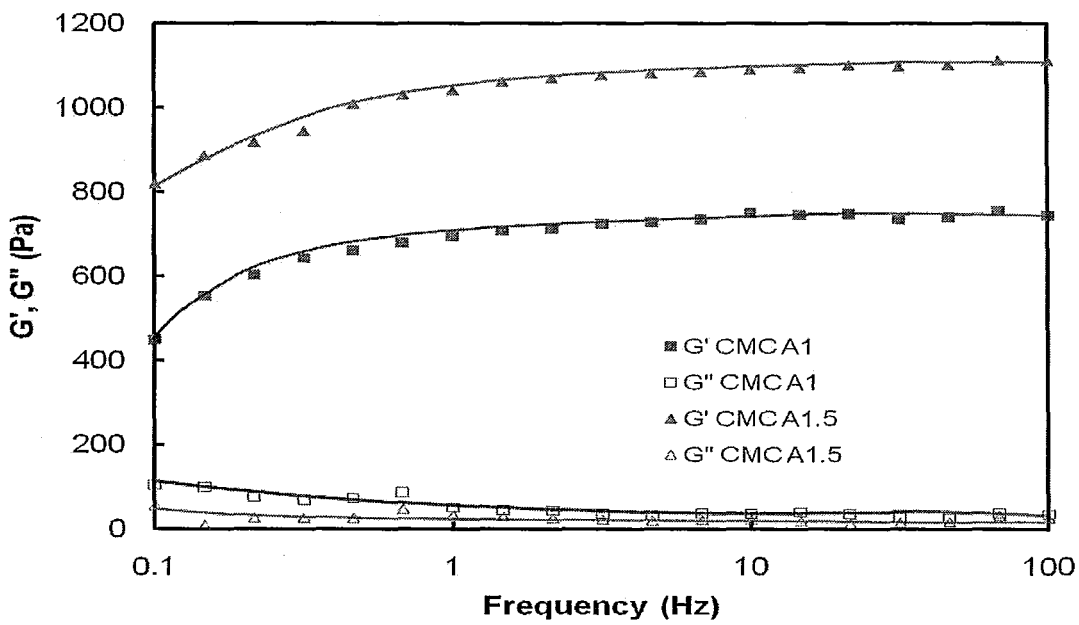

Figure 4.5.1: G' and G" values for different hydrazide functionalized CMC

Figure 4.5.2 shows the complex viscosity of the hydrogels as a function of applied frequency.

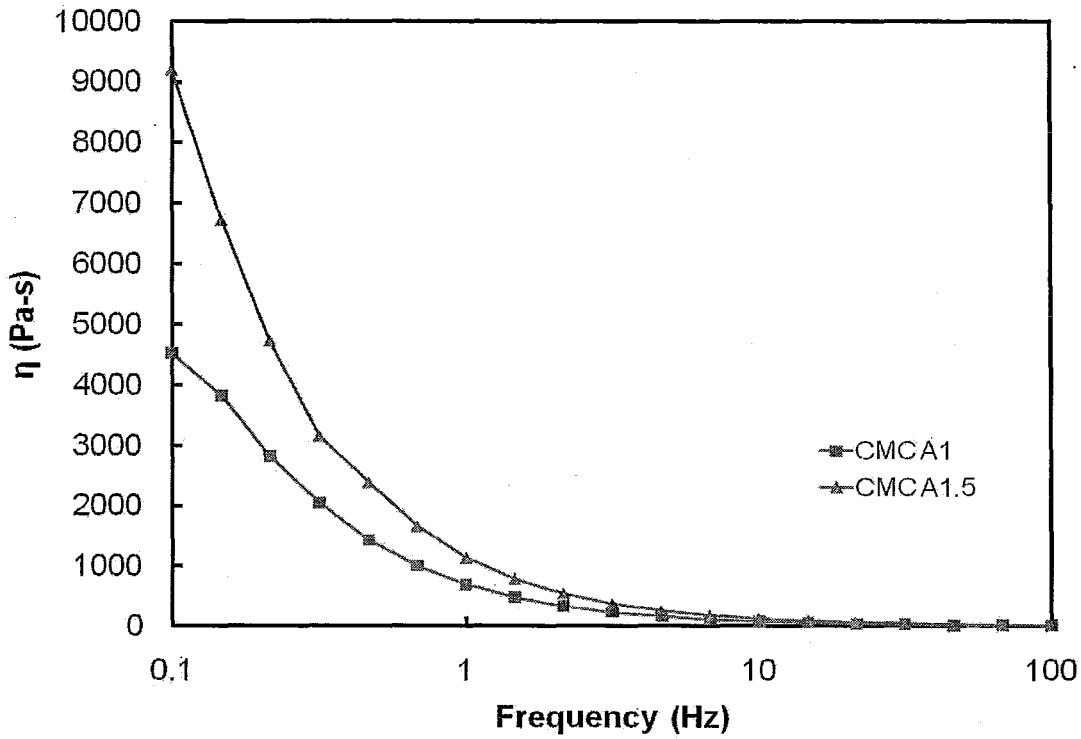

Figure 4.5.2: Complex Viscosity of Hydrogels

At low frequencies, there is a large difference in viscosities, with the higher functionalized CMC having a viscosity nearly twice that of its lower functionalized counterpart. As the oscillation frequencies are increased, there is an associated decrease in viscosity as the polymer chains of the hydrogel between cross-linking points are aligned in the shear field. The reduction in complex viscosity with increased oscillation frequencies indicates that the hydrogels exhibit shear thinning capabilities. Shear thinning occurs in polymers due to the alignment and de-entanglement of polymer chains induced

by an applied shear field (Lapasin, 1995). In this case, for an *in situ* injectable hydrogel, this kind of behaviour is desirable. This allows for maximum elasticity at low shear (ie. in the body), while promoting flow at higher shears (during injection), enabling the injection of high concentrations of polymer solutions and thus the formation of dense hydrogels *in vivo.* (Hoare, 2010, JBMR A, part I).

4.5.2 Impact of Imbedded Microgels on Hydrogel Rheology

Within the composite, the bulk hydrogel component is responsible for the majority of the mechanical strength in the system. The physical entrapment of microgels within this hydrogel phase may significantly alter the mechanical properties of the hydrogel. Specifically, the lack of cross-linking between the embedded microgel phase and the bulk hydrogel has the potential to significantly weaken the hydrogel composite, reducing its potential applicability in the body. The rheology of a CMC-A1/Dex-B hydrogel, with and without a 50wt% (dry basis) fraction of embedded AA-6% microgel, is presented in Figure 4.5.3.

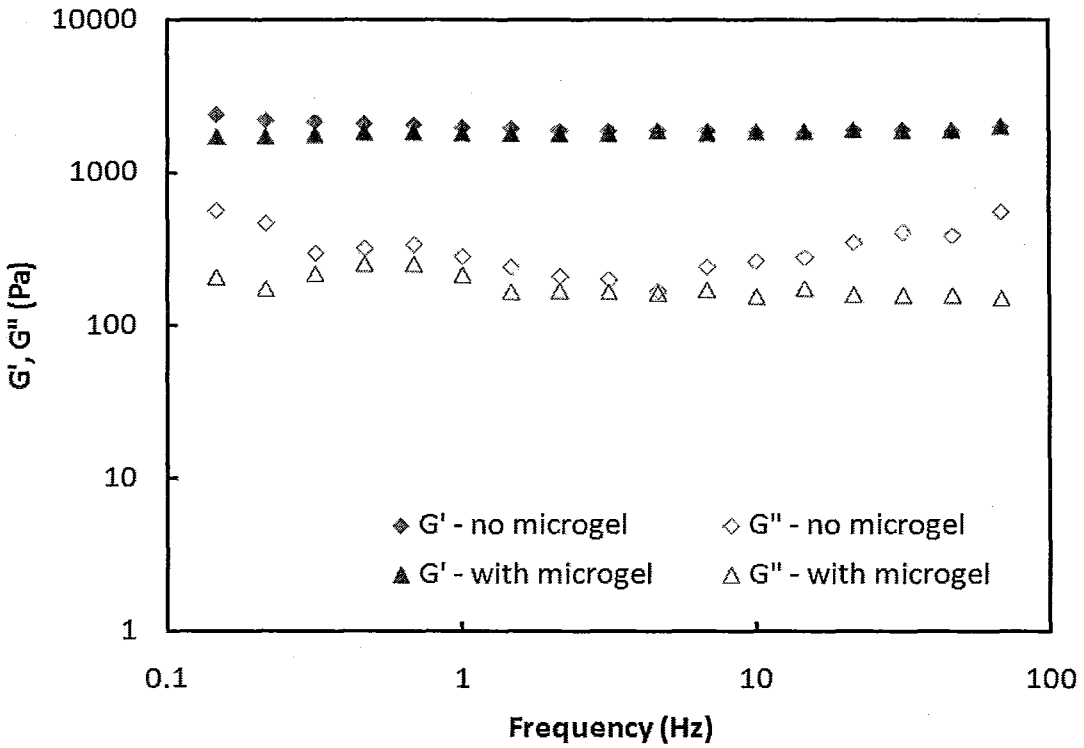

Figure 4.5.3: G',G" Characteristics of Hydrogels and Hydrogel-Microgel Composites

The moduli G' and G" are not significantly impacted by the presence of the microgel phase. This is likely attributable to the balance of mechanical contributions made by the lack of covalent connectivity between the hydrogel and microgel phases (reduced elasticity) and the significantly higher polymer fraction within of the microgel phase (~10wt%) relative to the hydrogel phase (~2wt%) (increased elasticity). Indeed, at higher frequencies, Figure 4.5.4 suggests that the presence of the denser microgel phases actually increases the G'/G" ratio relative to the bare hydrogel, indicating that the composite exhibits higher elasticity at higher shear than the bulk gel alone.

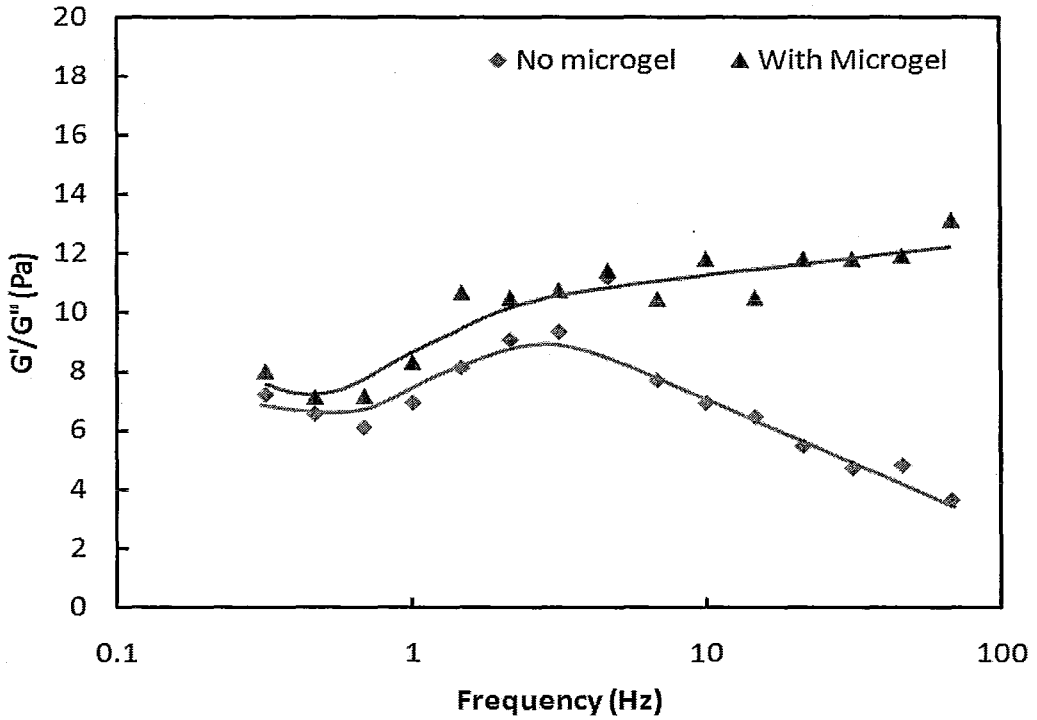

Figure 4.5.4: G'/G" Characteristics of Hydrogels and Hydrogel-Microgel Composites

Thus, physically embedding microgels into the hydrogel does not significantly reduce the mechanical strength of the hydrogel and, at high shear, somewhat improves the mechanical performance of the hydrogel.

Chapter 5: Cell Cytotoxicity

5.1: Raw Materials

For practical use *in vivo*, both the composite hydrogels as well as each of their constituent components (A polymer, B polymer, and microgels) must not induce significant cytotoxicity around the site of the injection. To determine the effects of the polymers, microgels, and hydrogels on cellular bodies, an *in vitro* thiazolyl blue tetrazolium bromide (MTT) assay was used. This assay is a metabolic process in which the concentration of the purple metabolite of the MTT dye can be correlated with the overall level of cell metabolism and thus the total number of viable cells. For these assays, tests were conducted with the raw materials as well as the hydrogel and hydrogel-microgel composites. Two cell types were used: 3T3 *Mus musculus* mouse cells and C2C12 mouse muscle myoblast cells. These cells were chosen since they are characteristic of the local cells the composite hydrogel would encounter when injected intramuscularly. Figure 5.1.1 shows the cell viability (measured as a percentage relative to a cell-only control) for the composite hydrogel precursors on 3T3 cells. No significant cytotoxicity is noted for CMC-A1, Dex-B, CMC-B, or AA-6% microgels at concentrations up to 1mg/mL, typically considered a threshold for cytotoxicity assessment. Indeed, at low concentrations, the presence of CMC-A1 and CMC-B slightly up-regulate cell metabolism. Minor decreases in cell viability were observed at concentrations >1mg/mL, decreasing to ~80% cell viability at concentrations of 2mg/mL

Dex-B, CMC-A1, and AA-6%. These results are consistent with many other studies involving P(NIPAM) microgels as biomaterials (McGillicuddy *et al*, 2006).

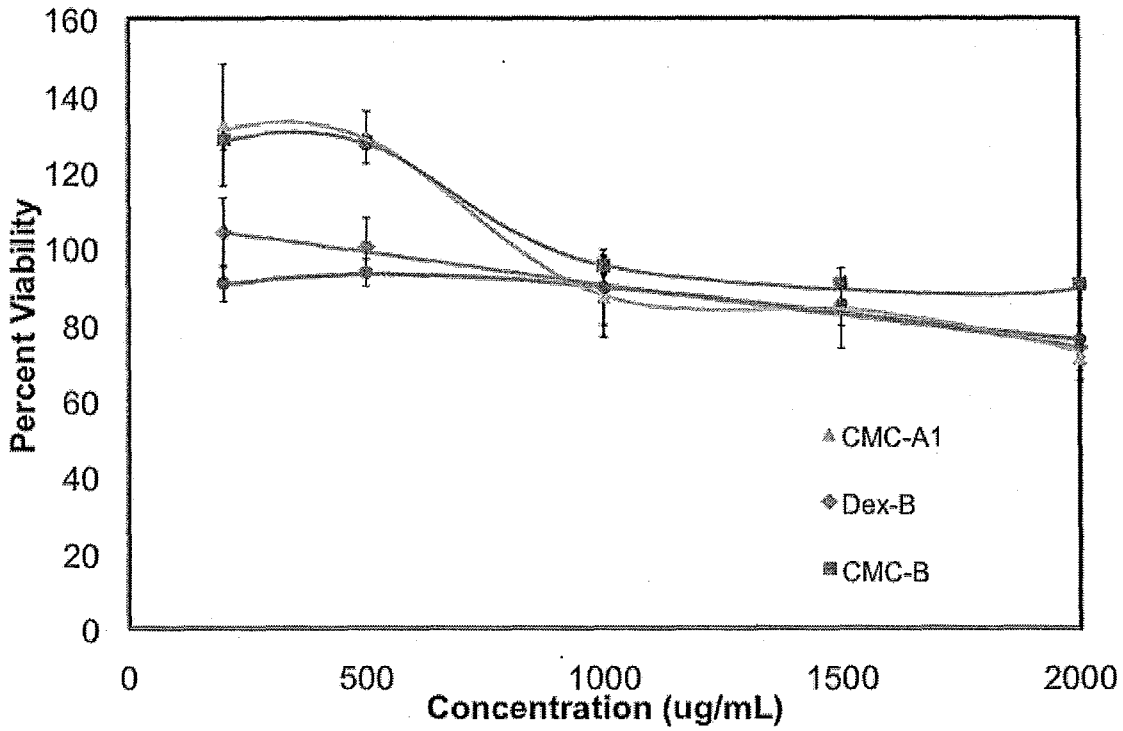

Figure 5.1.1: 3T3 Cell Viability versus Hydrogel/Microgel Precursors using MTT Assay

Similar results were obtained for C2C12 cells when exposed to the raw polymeric materials, as shown in Figure 5.1.2. Cell metabolism is slightly up-regulated at low concentrations of Dex-B and CMC-B and cells remain viable to concentrations up to 2mg/mL, although CMC-B exhibits slight cytotoxicity at concentrations >0.5mg/mL.

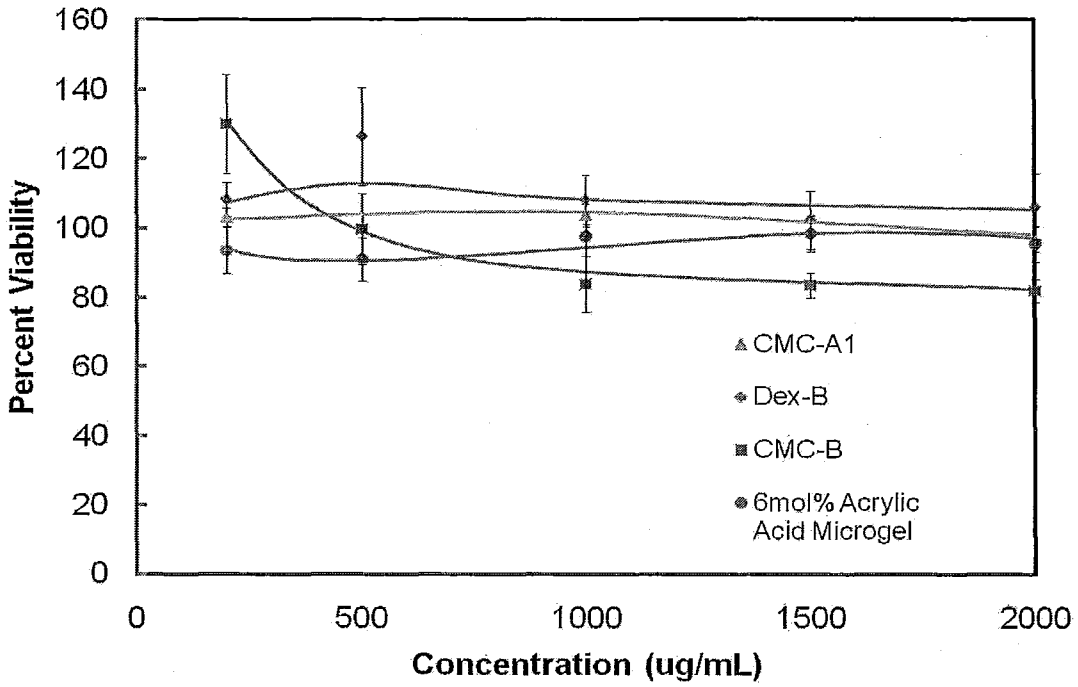

Figure 5.1.2: C2C12 Cell Viability versus Hydrogel/Microgel Precursors using MTT Assay

Many aldehyde-containing polymers have previously been shown to exhibit cytotoxicity to cells, predominantly through their high reactivity to nucleophilic sites on proteins (e.g. amines and thiols) (Deneer, 1988). Such reactions can result in protein denaturation and subsequent problems with cell growth and development, specifically via modification of membrane proteins and enzymatic systems. However, Figures 5.1.1 and 5.1.2 indicate that the aldehyde polymers used in this study maintain high cell viability at concentrations up to 2mg/mL. To assess the cell toxicity threshold of CMC-B and Dex-B, cytotoxicity to 3T3 cells (Figure 5.1.3) and C2C12 cells (Figure 5.1.4) was assessed up to concentrations of 10mg/mL. From previous experiments, dextran has been seen to be cell friendly and does not result in cell death (Cadee *et al*, 2000). With aldehyde

functionalized dextran, cell viability drops to ~50% at a concentration of 10,000 μg/mL for both 3T3 and C2C12 cells. Aldehyde-functionalized CMC, however, maintains at least ~80% cell viability even when added at a concentration of 10mg/mL. Thus, CMC-B and Dex-B both induce only minimal to moderate cytotoxicity even at concentrations far in excess of what would be present *in vivo* due to the presence of unreacted polymers and/or the degradation of the composite hydrogel. This is similar to the results found by previously, in which up to 100μg/mL of hydrogels (carboxymethyldextran) were found to have promising cell viabilities. In addition, the same hydrogels were found to have low toxicity in the peritoneum, which is one of the most demanding regions of the body (Ito *et al*, 2007). This result suggests that the composite hydrogels we have developed may have practical applications *in vivo*.

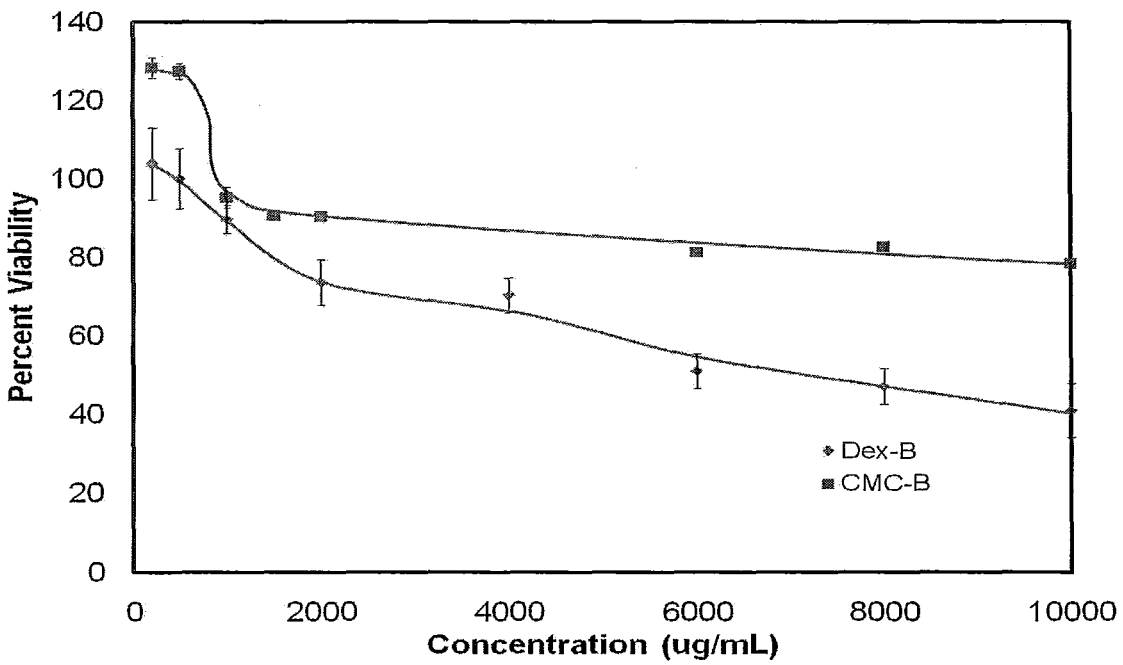

Figure 5.1.3: 3T3 Cell Viability for B-type Polymers using MTT Assay

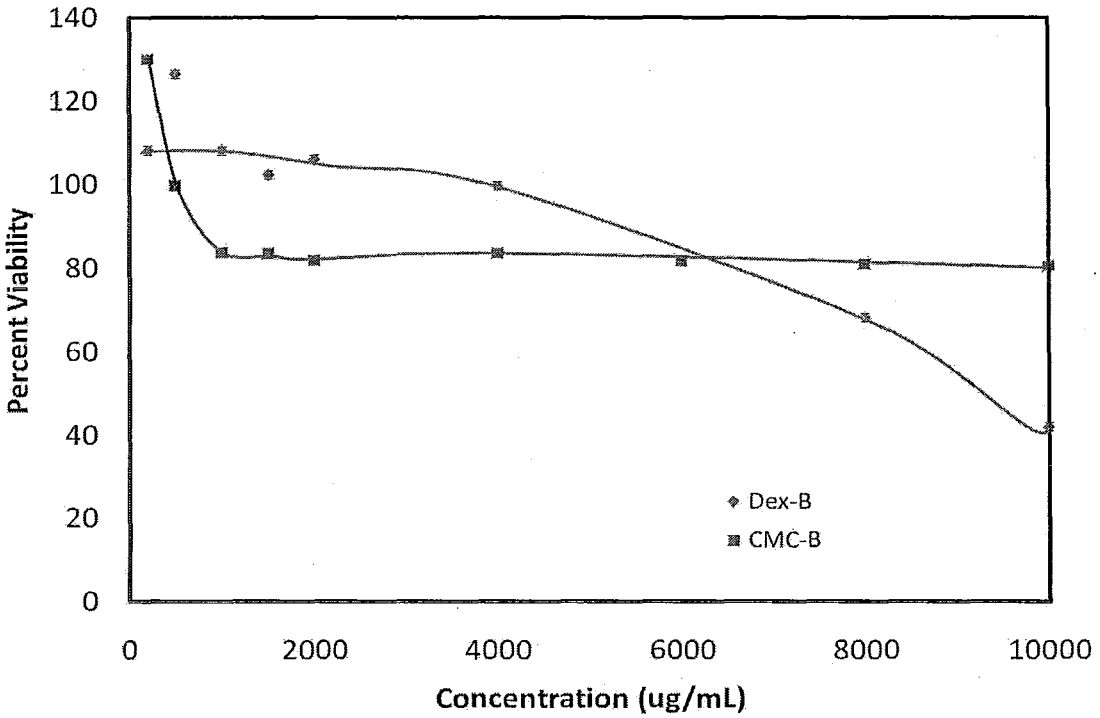

Figure 5.1.4: C2C12 Cell Viability for B-type Polymers using MTT Assay

5.2 Hydrogel-Microgel Composite

The cell viability of 3T3 and C2C12 cells in the presence of a CMC-A1/Dex-B hydrogel and a composite CMC-A1/Dex-B/AA-6% hydrogel was also assessed using the MTT assay. Two geometries were tested: (1) plating cells in the polystyrene well and placing a hydrogel disk on top of the cells and (2) extruding the hydrogel to fill the polystyrene well and plating cells on top of the hydrogel. These two geometries were selected to mitigate potential complications in terms of nutrient accessibility (hydrogel on top), cell-hydrogel contact (hydrogel on top) and cell adhesion (hydrogel on bottom) that

may skew the results of any cell viability study. The cell viability results, again expressed as a percentage relative to a cell-only control, are shown in Table 5.2.1.

Table 5.2.1: Cell Viability With Hydrogel and Hydrogel-Microgel Composite using MTT Assay

	3T3	**C2C12**
Hydrogel (CMC-A1-Dex B) on Top of Cells	84.3% ± 17.1%	97.4 % ± 5.4%
Cell Growth on Hydrogel (CMC-A1-Dex B)	94.1% ± 4.0%	107% ± 4.8%
Hydrogel-Microgel (CMC-A1-Dex B-6% AA-NIPAM) on Top of Cells	80.5% ± 3.2%	85.1% ± 4.2%
Cell Growth on Hydrogel-Microgel (CMC-A1-Dex B-6% AA-NIPAM)	75.0% ± 12.3%	86.5% ± 1.2%

When the cells were exposed to the hydrogel and hydrogel-microgel composite, exposure proved to be minimally cytotoxic. This was true for when the cells were grown on the composites as well as when the cells were exposed to contact with the composites, but grown on the well plates. Slightly higher cytotoxicity was noted with 3T3 fibroblast cells (on average resulting in ~10% lower cell viability than observed with C2C12 cells) and when cells were grown on top of the composite hydrogel, although this latter cytotoxicty

may be in part attributable to the highly hydrophilic nature of these composite hydrogels that may inhibit adhesion of the cells and thus normal metabolic function. The hydrogel-microgel composite appeared to be slightly more cytotoxic to the cells than the hydrogel on its own, particularly toward C2C12 cells. This could be due to the cumulative nature of exposing another component with a minor cytotoxic response (microgels) to the cells. Indeed, the cell response to the hydrogels seem to mimic cumulatively what would happen if all precursors (CMC, dextran, hydrazide, aldehyde) were combined. Overall, however, the high apparent cytocompatibility of the hydrogels observed here is consistent with other "plum-pudding" matrices reported in the literature (McGillicuddy *et al*, 2006). It should also be noted that any toxicities observed through *in vitro* experiments are typically significantly lower in the infinitely diluting *in vivo* environment, in which fluids around the hydrogel are rapidly exchanged (Hoare, 2010, JBMR A, part II).

Chapter 6: Drug Release Profiles

Drug release of bupivacaine was observed from the hydrogel-microgel composites into the external media, which consisted of 10mM PBS. In all cases, a large burst effect was observed at the beginning of the composite exposure to external media. This is consistent with many polymer type systems in which diffusion mechanisms play a role in delivery of medication (Edlund and Albertsson, 2002). This was followed by varying release profiles that were dependent on the type of cross-linking, polymer-drug interactions, and other factors. In most cases, the burst effect follows a first-order release profile. This is followed by the reduction of bupivacaine release until slow, near zero-order release is obtained.

When media was changed, the hydrogel-microgel composites retained their shape and degree of swelling during the testing protocol. It can be stated that over the duration of drug release the hydrogel-microgel composites displayed excellent structural strength, which in turn resulted in controlled release of bupivacaine. Over the course of time, the hydrogel-microgel composites experienced bulk erosion. Any degradation of the hydrogel matrix can most likely be attributed to the slow hydrolysis of the hydrazone groups (Hiemstra *et al*, 2007).

6.1 Composite Release Versus Raw Hydrogel and Microgel Release

Prior to the discussion of tunable features of the hydrogel-microgel composite, the benefits of the composite were compared to that of the hydrogel and microgel on its own.

Each type of microgel was loaded with 5mg/mL bupivacaine to study the release behaviour of the microgel. The same experiment was done for the hydrogel without embedded microgels. The results of release from the CMC-dextran hydrogel and a 20% AA-NIPAM microgel are displayed in Figure 6.1.1. These results are then compared to the release observed from a *composite* hydrogel containing a 50:50 mass ratio of the CMC-dextran hydrogel and the 20% AA-NIPAM microgel. The drug content had the same mass to mass ratio of microgel:composite. Over the first two days of release, each of the bulk hydrogel, the microgel, and the microgel-hydrogel composite exhibits a burst release profile followed by nearly first-order release characteristic of a diffusion-based process. However, the amounts of drug released from the microgel and hydrogel are significantly higher than that of the composite hydrogel, with release from both phases between 50-70% faster than from the composite hydrogel. The small size of the microgel (small diffusional path length) and the minimal affinity binding expected between bupivacaine and the bulk hydrogel promotes rapid diffusion-based release from both the microgel and the hydrogel alone. In comparison, drug loaded into the high-affinity microgel phase inside the composite hydrogel is not released to a great extent over this time period. Instead, after the burst release (diffusion of drug contained in bulk hydrogel phase out of the gel composite), slow and near zero-order release is observed from the hydrogel-microgel composite. We expect this slow, near-constant release is attributable to partitioning of drug from the microgel to the hydrogel phase and finally into the release medium, facilitating slow release of drug over time. Thus, it appears that microgel-hydrogel composites have the potential to facilitate long-lasting controlled release.

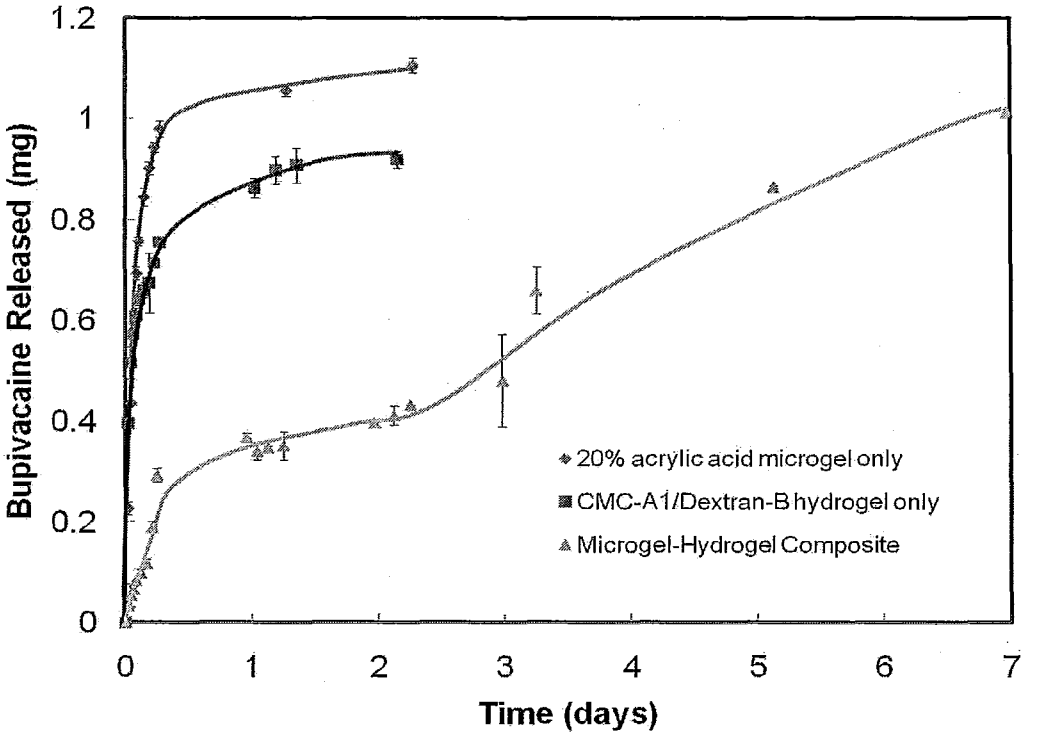

Figure 6.1.1: Comparison of Release Profiles from Microgel and Hydrogel and that of the Hydrogel-Microgel Composite

6.2 Effect of Microgel Functionalization on Drug Release

Figure 6.2.1 shows the effect of increasing the number of acrylic acid functional groups in the microgel on the drug release kinetics of the hydrogel-microgel composite. As the number of acrylic acid groups in the microgel is increased, the amount of drug released and the rate of that release both decreased. This result is attributable to charge-charge interactions between bupivacaine (cationic) and acrylic acid residues in the microgel (anionic), leading to tighter binding of the drug in the microgel phase and a lower driving force for partitioning of drug into the bulk phase for release. Indeed, for

microgels with higher degrees of functionalization, controlled release of bupivacaine from the hydrogel-microgel matrix could be achieved over the course of up to 60 days. It should also be noted that 20mol% acrylic acid-functionalized microgel, in which the most drug is bound within the microgel phase, exhibits by far the least burst release of drug early in the process, suggesting another advantage of a composite hydrogel system.

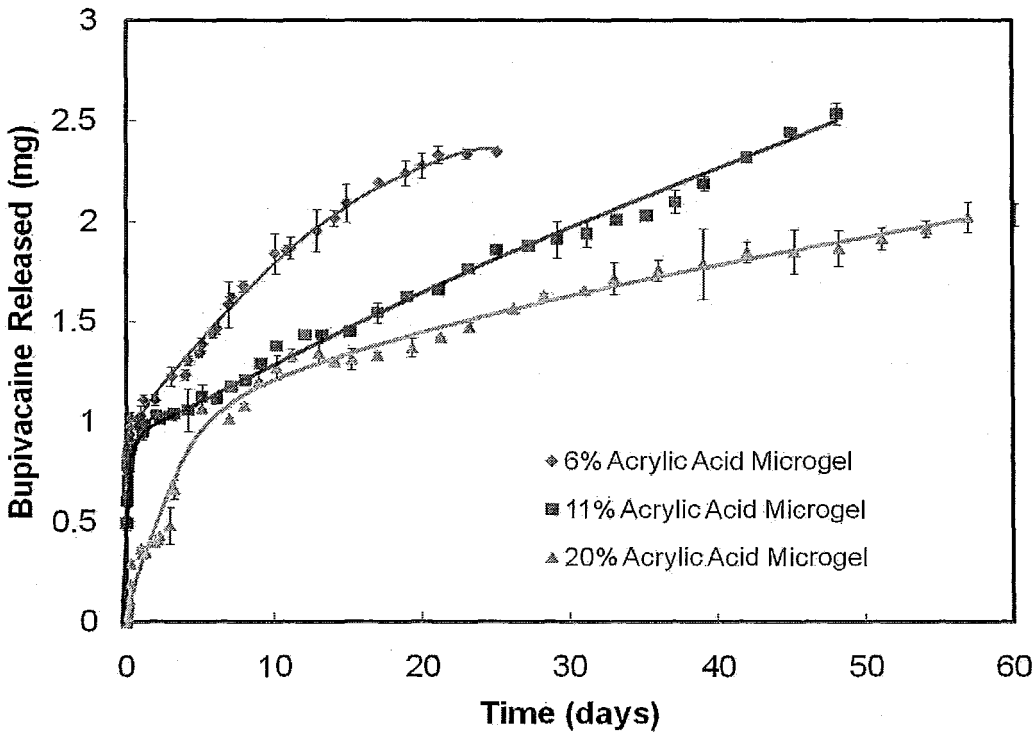

Figure 6.2.1: Varying Microgel Effects on Drug Release

When mixed ratios of microgels with different degrees of functionalization were entrapped within the hydrogel matrix, drug release kinetics could be achieved that were intermediate to those achieved using the two microgels individually. This is seen in Figure 6.2.2. In this case, microgels with acrylic acid fractions of 6mol% and 20mol%

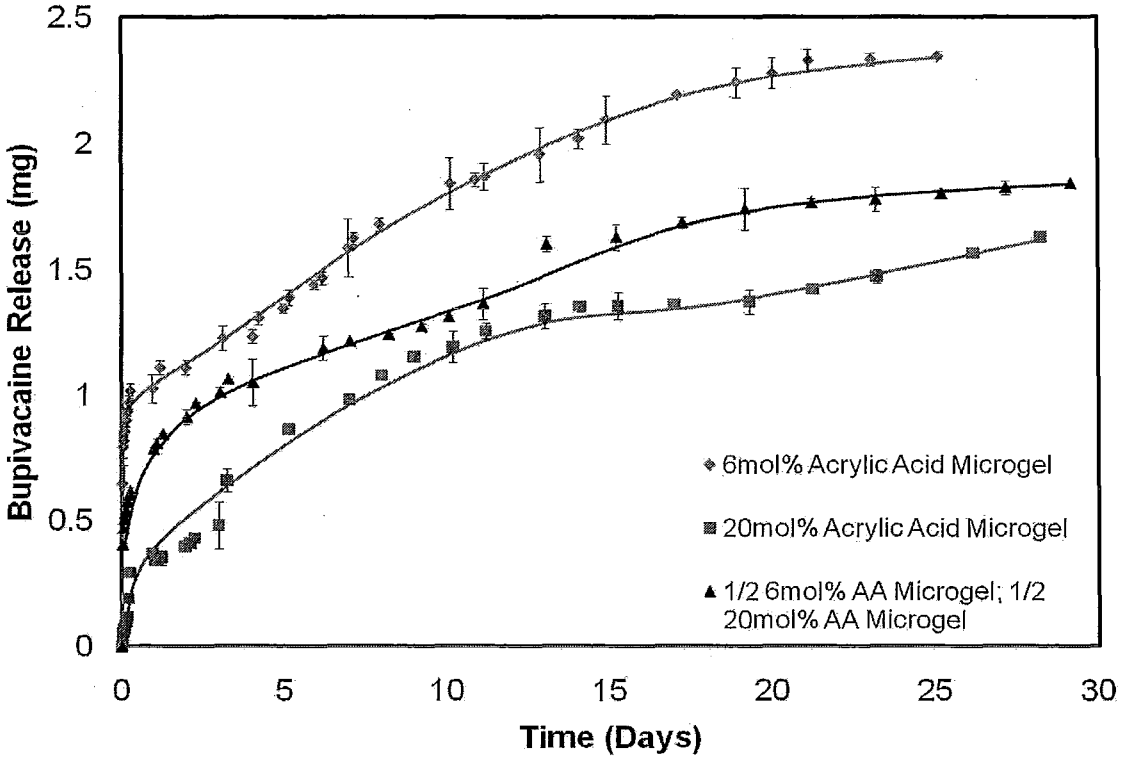

Figure 6.2.2: Mixed Microgel Composite Drug Release

were mixed in a 1:1 ratio and entrapped in a CMC-A1/Dextran B hydrogel. The release profile achieved fit directly between the release profiles achieved using the two microgels individually in the same bulk hydrogel. Thus, any kinetic profile can be achieved using a composite hydrogel simply by mixing nanophases with different affinities for the drug to be delivered.

Together, Figures 6.1.1 and 6.2.1 suggest that the primary factor controlling drug release from microgel-hydrogel composites is the degree of microgel functionalization and, specifically, the electrostatic interactions present between the microgel phase and the drug. Bupivacaine is a cationic drug which binds ionically with the acrylic acid groups

within the microgel, which are anionic at physiological pH. This electrostatic attraction can explain why bupivacaine is loaded at higher fractions in microgels that contain higher acrylic acid fractions (Hoare and Pelton, 2008). This also explains the additive behaviour of mixing microgel fractions, as the degree of drug-microgel interaction achieved is dependent on the total number of acrylic groups present in the microgel mixture.

6.3 Effect of Cross-Linking Degree due to Hydrazide Functionalized Polymers

The effect of degree of cross-linking in the bulk hydrogel phase on composite hydrogel drug release was studied by varying the degree hydrazide attachment to the CMC backbone of the A-type polymers. Increased hydrazide functionalization is associated with an increased degree of cross-linking, as the presence of more hydrazide groups results in a greater probability for reaction with aldehyde groups during the cross-linking process and thus a higher cross-linking density. Differences in cross-link density between hydrogels prepared using polymers with different degrees of hydrazide functionalization were previously confirmed based on rheological measurements on these hydrogels in the absence of an embedded microgel phase (Figure 4.5.1). Figure 6.3.1 indicates that higher degrees of cross-linking in the bulk hydrogel phase resulted in slower drug release. This is due to the increased cross-link density effectively reducing the diffusion of the drug through the matrix. Thus, these hydrogels most effectively reduced the rate of diffusion of drug out of the matrix and water into the hydrogel phase.

This result suggests that tuning the cross-link density of the bulk gel offers additional control over the drug release kinetics that can be achieved with composite systems.

The observed release behaviour of the low cross-linked composite (CMC-A0.5) can be explained by considering the swelling characteristics as a function of time of the various hydrogels tested, shown in Figure 6.3.2. In general, by increasing the cross-link density, the potential for the hydrogel to swell or shrink is restricted (Huang *et al*, 2004). The CMC-A/Dextran B polymers all deswelled over time, due to unfavourable polymer-solvent interactions generated upon cross-linking in this system due to consumption of the hydrophilic functional groups upon cross-linking. As a result, increasing the cross-link density reduced the degree of deswelling that could be achieved, resulting in higher pore sizes in the more highly cross-linked bulk hydrogels (CMC A1 and CMC A1.5).

It should be noted from Figure 6.3.2 that increasing the degree of hydrazide functionalization in the A polymer is effective at changing hydrogel swelling and thus drug diffusion only to a limit. Hydrogels prepared with CMC-A0.5 (30% hydrazide functionalization) released drug significantly more slowly than hydrogels prepared with CMC-A1 (44% hydrazide) due to deswelling of the matrix. However, when the degree of hydrazide functionalization was increased to 49% (CMC-A1.5), Figure 6.3.1 indicates that no significant change in drug release was observed and Figure 6.3.2 indicates that there is no statistically significant

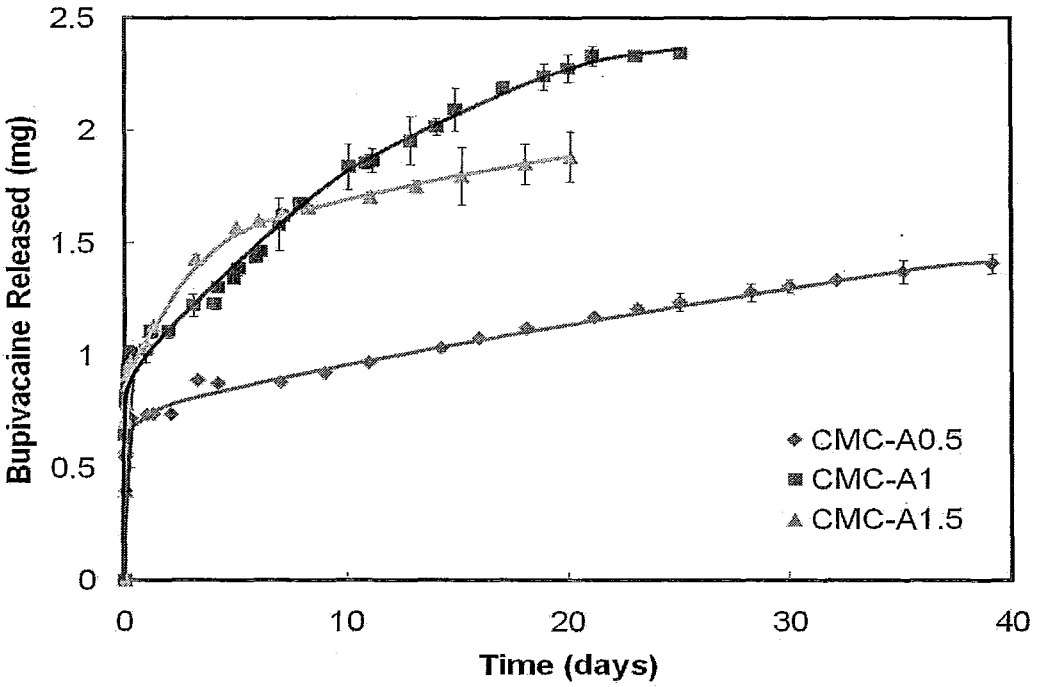

Figure 6.3.1: Varying Degree of Hydrazide-Functionalized CMC Effects on Drug Release

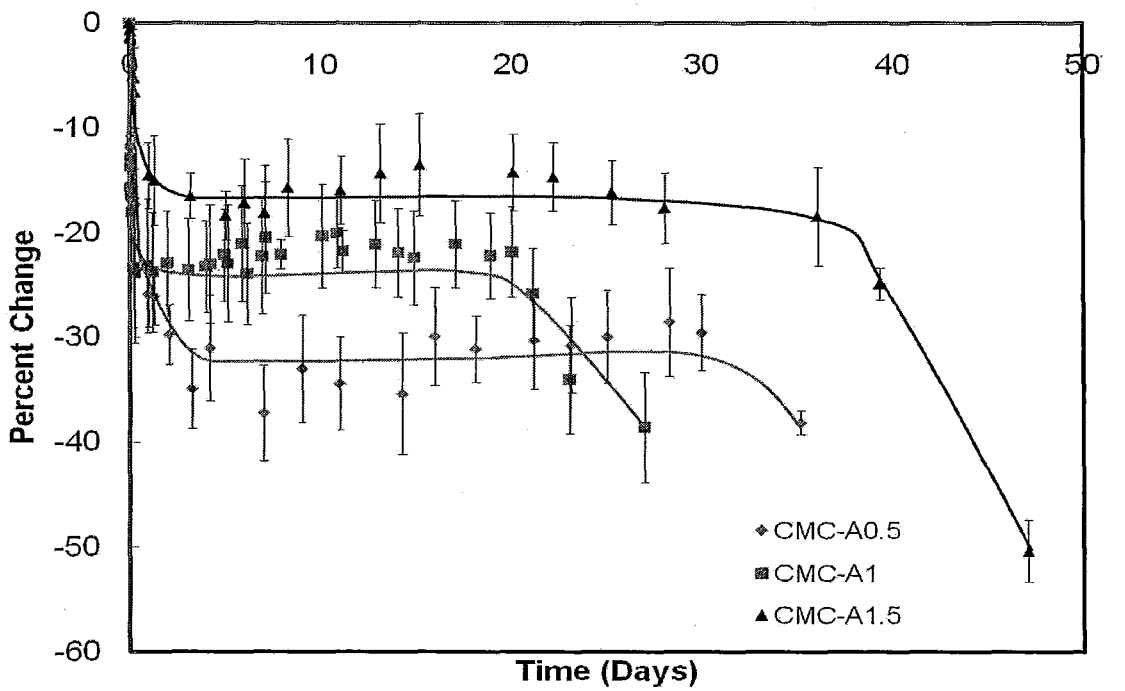

Figure 6.3.2: Swelling Characteristics of Hydrazide-Functionalized CMC with Dextran

difference in the deswelling response of two composite hydrogels. This observation is likely attributable to steric limitations introduced during the cross-linking process. Increasing the degree of cross-linking decreases the mobility of the polymer chains present between the cross-linking points, thus restricting the capacity of additional hydrazide groups to cross-link with excess aldehyde groups present in the system.

The degradation rates of the hydrogels varied significantly with the degree of cross-linking. From Figure 6.3.2, it can be determined that degradation occurred within thirteen days via hydrolytic cleavage of the hydrazone bonds between the CMC and dextran polymers comprising the hydrogel for the low functionalized CMC backbone (Hiemstra *et al*, 2007). Rapid degradation occurred since fewer hydrazone bonds need to hydrolyze before the hydrogel loses structural integrity and becomes a viscous polymer solution. While the higher cross-linked hydrogels also degraded over time, degradation occurred 4-5 weeks after immersion into the 10mM PBS solution. In this case, more hydrazone bonds must be hydrolyzed before the elastic nature of the hydrogel is compromised, resulting in slower overall degradation.

6.4 Effect of B polymer modification on Drug Release

The composition of the aldehyde-containing polymer used to prepare the bulk hydrogel was also varied to assess the impact of the composition of the bulk gel phase on drug release from hydrogel-microgel composites. Figure 6.4.1 indicates that drug release is not significantly changed with CMC-B is substituted for Dextran-B in preparing the bulk hydrogels.

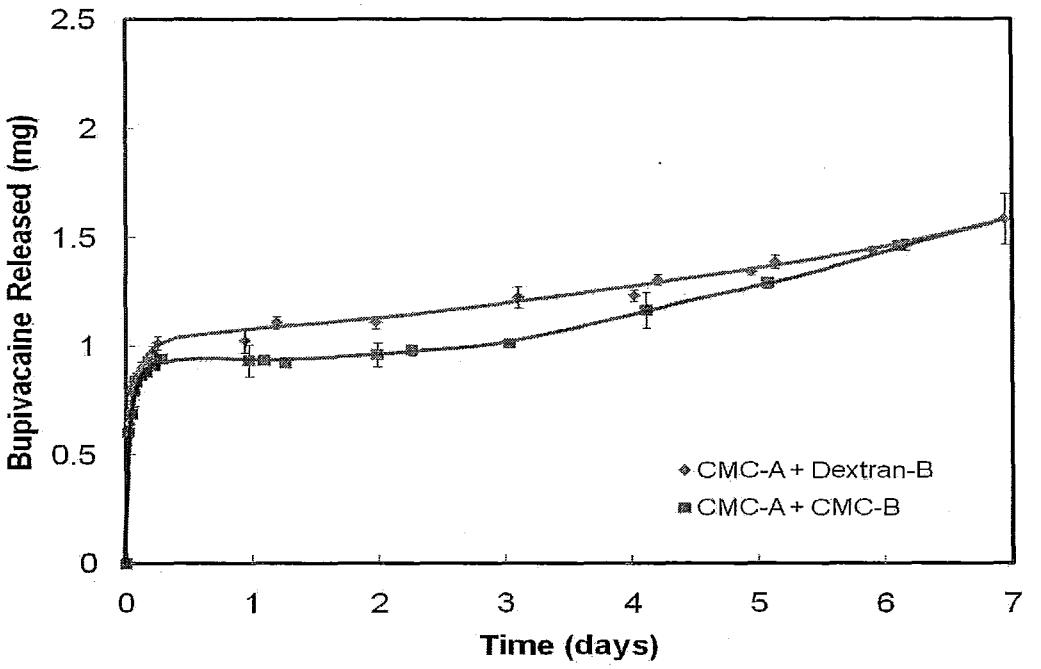

Figure 6.4.1: Varying Aldehyde Functionalized Polymer Effects on Drug Release

Bulk hydrogels prepared with CMC-B facilitate slightly slower drug release than bulk hydrogels prepared using Dextran-B, although the release profiles converge over time. However, despite the observed similarities in drug release profiles, Figure 6.4.2 indicates that extremely large differences exist in the swelling responses of these two hydrogels as a function of time in the PBS release medium.

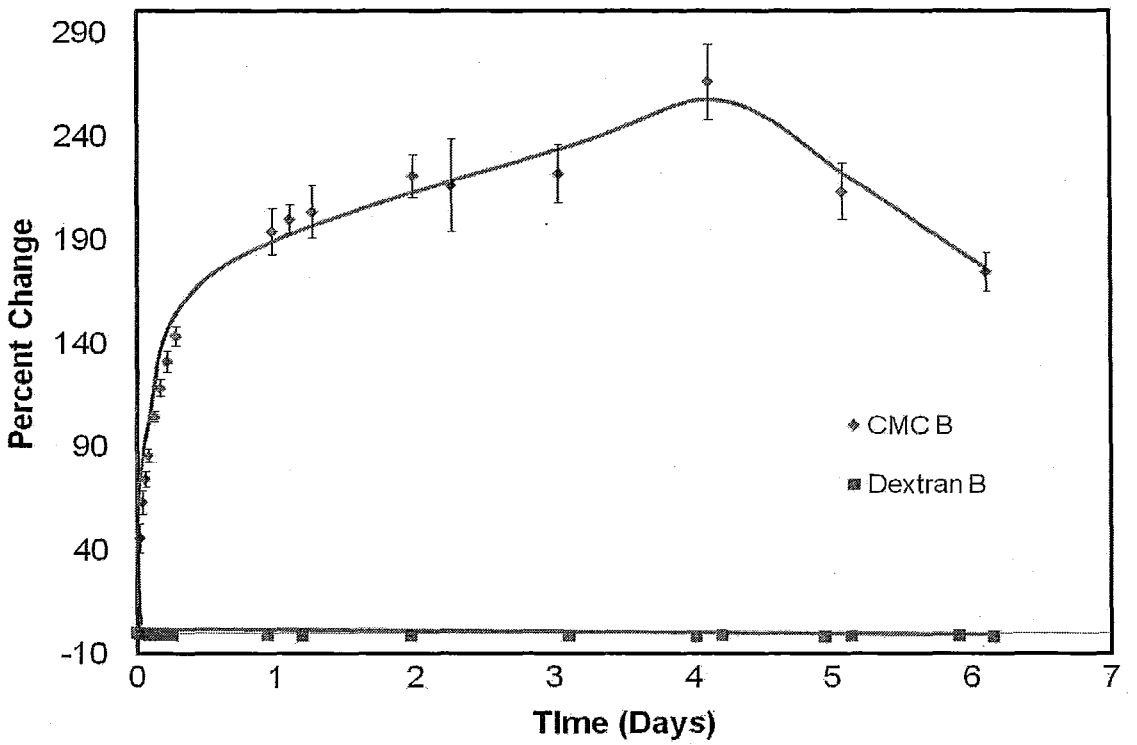

Figure 6.4.2: Swelling Differences in Aldehyde-Functionalized Polymer Type

While CMC-A1/Dextran-B hydrogels show little or no swelling as a function of time, hydrogel-microgels composites made of CMC-A1 and CMC B swell by a factor of up to 2.5 times of their initial weight (at formation) after just one day of exposure to the PBS release solution. Water uptake in CMC hydrogels is governed by the carboxylic groups on the CMC. The ionization of the carboxylic acid groups (pKa =3.2) induces Donnan equilibrium-driven swelling in the CMC-B-containing hydrogel (Barbucci *et al*, 2000). It should be noted that the aldehyde content of the two polymers is essentially equivalent (32% for CMC and 37% for dextran, see Table 4.1.1 and 4.2.1), such that this difference in swelling cannot be attributed to different cross-link densities in the two

hydrogels. Thus, although the average pore size in CMC-A1/CMC-B hydrogels is significantly higher than that of CMC-A1/Dextran B hydrogels, the bulk hydrogel prepared with CMC-B releases drug more slowly. This is in contradiction to the result shown in Figure 6.3.1, in which higher bulk hydrogel swelling facilitated faster release.

Electrostatic interactions between bupivacaine and the ionized carboxylic acid groups in the CMC-B polymer, which are maintained during the oxidation process used to convert CMC to CMC-B, can be used to rationalize this apparent contradiction. While diffusion-based release will occur significantly faster in CMC-A1/CMC-B hydrogel systems, the presence of $-COO^-$ groups provides an electrostatic partitioning effect that restricts the diffusion of bupivacaine through the highly swollen bulk gel matrix. As a result, despite the significantly larger average pore size in CMC-A1/CMC-B hydrogels, slightly slower drug release is observed. This result is consistent with our observations regarding the effect of the total charge density in the microgel phase on bupivacaine release (Figure 6.1.1) and suggests that release kinetics from composite hydrogels can be sensitively tuned by altering both the cross-link density of the microgel (i.e. average pore size) as well as the affinity of either phase for the drug to be released.

Hydrophobic partitioning can also play a role. The log P of a NIPAM monomer sub-unit is approximately 0.06. For cationic bupivacaine (the predominant form at physiological pH), the log P value is 0.18 (Sudoh *et al*, 2004). As a result, bupivacaine has a similar hydrophobicity to the microgel and would thus prefer to partition within the microgel phase at physiological conditions rather than the water-based solvent (PBS).

Thus, even in the absence of charged groups, drug release should be slowed by the presence of the NIPAM-based microgel phase.

It should be noted that gel degradation via hydrolysis occurs rapidly with the very swollen CMC-B based composites (7-10 days), owing to the large water fraction present in these hydrogels. In comparison, the CMC-dextran hydrogels maintain their structure in excess of 30 days depending on cross-link density.

6.5 Hydrazide Functionalized Microgels

To investigate the effect of the microgel phase transition on the drug release achieved in hydrogel-microgel composites, cross-linkable microgels functionalized with hydrazide groups were synthesized and incorporated into the CMC-dextran bulk hydrogels. In this case, the hydrazide-modified microgels were mixed with CMC-A1 in the double barrel syringe and co-extruded with Dextran B to generate composite hydrogels in which the microgel phase is covalently cross-linked to the bulk hydrogel, not just physically entrapped. Drug release results for composite hydrogels of the same composition prepared with cross-linkable (hydrazide-functionalized) microgels and non-crosslinkable (acid-functionalized) microgels are shown in Figure 6.5.1.

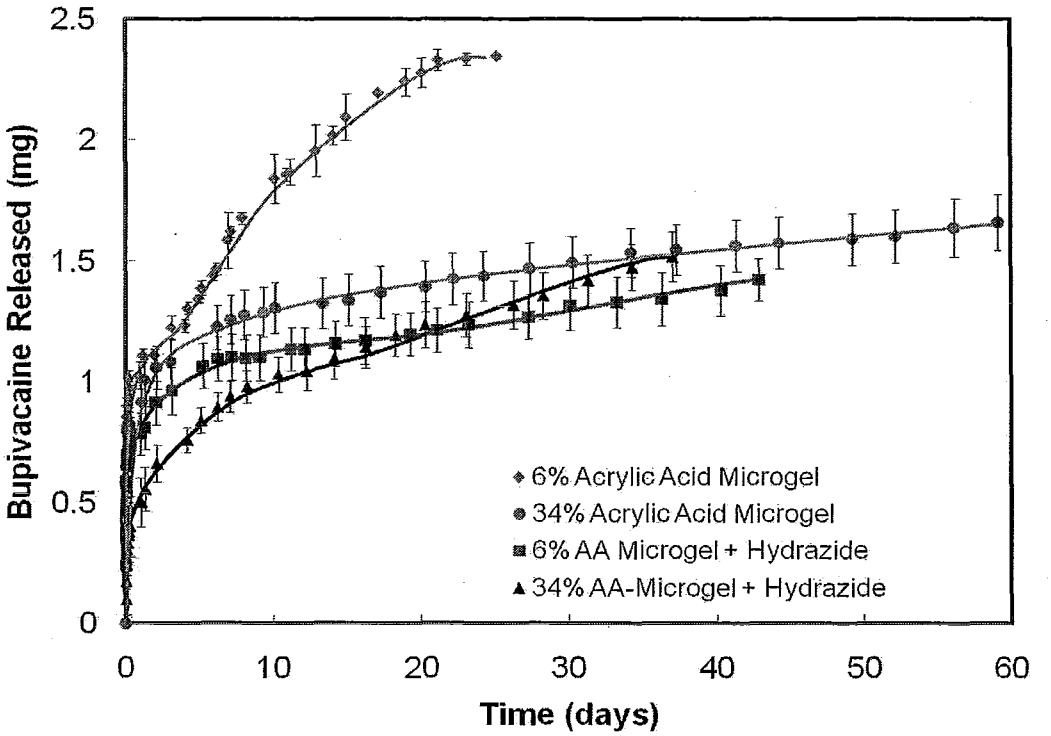

Figure 6.5.1: Bupivacaine Release from Hydrazide-Functionalized AA-P(NIPAM) Microgels

In both cases, when microgels are cross-linked to the bulk hydrogel matrix, the drug release rate from the hydrogel is slowed relative to hydrogels in which the microgels are only physically entrapped. This observation can be rationalized by two factors. First, cross-linking between the microgel and hydrogel phase physically restricts the deswelling of the microgels typically observed in the high salt environment at physiological temperature. This avoids the potential formation of a macroporous hydrogel, in which deswelling of the entrapped microgel within the swelling bulk hydrogel phase creates large free volumes around the embedded microgel phase, resulting in faster drug release. Second, cross-linking the microgel to the bulk hydrogel increases the total cross-link

density in the network, reducing the average pore size and thus the overall diffusion coefficient of drug through the polymer network.

However, the increased cross-link density (increasing diffusive resistances to drug release) is offset in part by the consumption of ionic $-COO^-$ groups via adipic acid dihydrazide functionalization, reducing the number of available ionic binding sites for bupivacaine. These competing effects are evidenced by the change in release kinetics observed upon microgel crosslinking between the 6mol% and 34mol%-functionalized microgels. In the 6mol% functionalized microgel, few carboxylic acid groups are present in the microgel in either the hydrazide-functionalized microgel or the unmodified microgel; as a result, relatively few electrostatic drug-polymer interactions are present even in the non-cross-linked microgel and consuming –COOH groups via reaction with adipic acid dihydrazide does not significantly change the electrostatic partitioning of drug into the microgel. Correspondingly, a large decrease in drug release rate is observed when the microgel is cross-linked to the hydrogel matrix due to the increase in overall cross-link density and mechanical prevention of a microgel phase transition. In comparison, adipic acid dihydrazide functionalization of the 34mol% functionalized microgels results in the consumption of a large number of –COOH groups, reducing the –COOH content of the microgel from 34mol% to 20 mol%. This can be seen from the titration of the microgels, shown in Figure 6.5.2.

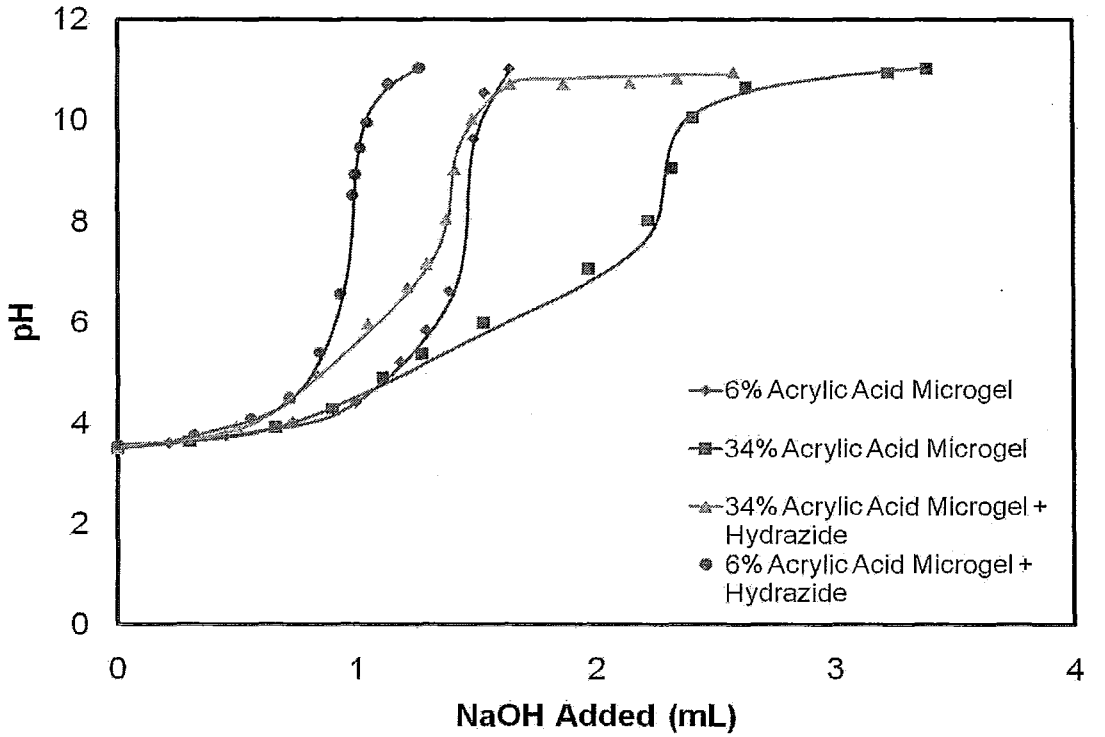

Figure 6.5.2: Titration of Hydrazide-Functionalized AA-P(NIPAM) Microgels

As a result, a significant number of electrostatic binding sites for bupivacaine are consumed by the cross-linking reaction, promoting faster drug release and partially offsetting the decreased diffusion coefficient resulting from microgel-hydrogel cross-linking. As a result, the difference in release kinetics between the entrapped and cross-linked microgels is significantly lower for the 34mol% AA microgel relative to the 6mol% AA microgel.

The different degrees of microgel deswelling observed at physiological temperature may also influence the release profiles observed. For 6mol% acrylic acid microgels, the microgel in the unconstrained (non-cross-linked) state undergoes

significant deswelling at physiological temperature (-70% volume change, Table 4.3.1). As a result, when the microgel is simply entrapped in the bulk hydrogel phase, convective mass transfer occurs to release bupivacaine from the microgel, resulting in the fast, burst release observed. In addition, larger free volumes are generated within the gel phase at physiological temperature due to the collapse of the embedded microgel phase, increasing the average diffusion coefficient of drug from the composite. In comparison, when the microgel is cross-linked to the bulk hydrogel, the phase transition is suppressed due to the elastic constraints imposed by the covalent crosslinks, preventing the same degree of burst release, minimizing or eliminating the formation of a macroporous hydrogel structure, and significantly reducing the rate of diffusion-driven drug release. For the 34mol% acrylic acid functionalized microgels, the higher charge content of the microgel restricts deswelling at physiological temperature, resulting in significantly less deswelling (-34% volume change, Table 4.3.1). Consequently, less deswelling is avoided by cross-linking the microgel to the hydrogel phase, less convective mass transfer occurs, and smaller macropores are generated in the microgel network at physiological temperature. As a result, and less difference is observed between the release profiles of hydrogels prepared using cross-linked or entrapped microgels.

While microgel deswelling is significantly affected by whether the microgel is physically entrapped or covalently cross-linked to the bulk hydrogel matrix, the overall swelling of the composite material is not affected by the presence of a cross-linked microgel phase, as shown in Figure 6.5.3. Thus, any differences in drug release are attributable exclusively to changes in the microgel phase. This result demonstrates the

power of using composite hydrogel systems for engineering drug delivery systems, since properties of both phases can be independently engineered to achieve new types of release behaviours.

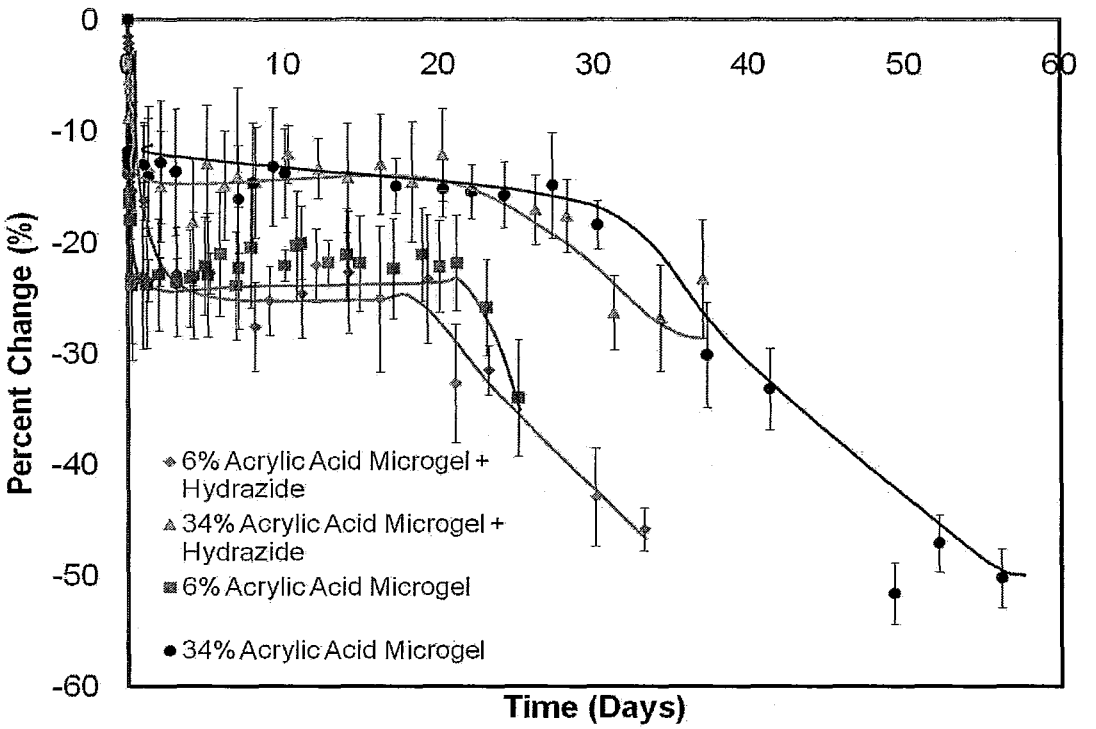

Figure 6.5.3: Swelling Characteristics of Hydrazide-Functionalized AA-P(NIPAM) in comparison to Non-Functionalized (Entrapped) AA-P(NIPAM)

Chapter 7: Discussion

The objective of this research project was to create a delivery vehicle for cationic, hydrophobic drugs utilizing the benefits of two distinct types of gels. The macroscopic hydrogel and the microscopic microgels have been shown to both be capable of independently tuning the release mechanisms of the hydrogel-microgel composites. This allows for the individual engineering of each component to optimize the release profiles of drug from the system. The biocompatible hydrogels can dictate release rates of bupivacaine depending on the degree of functionalization within the matrix, with release being governed by a combination of diffusion and phase partitioning. The hydrogels have also shown adequate mechanical strength to withhold the rigours of being in the body.

The composite hydrogels can control the release of bupivacaine via a combination of three mechanisms: electrostatic binding, diffusion, and hydrophobic partitioning. Electrostatic binding between cationic bupivacaine to the acrylic acid groups of the AA-P(NIPAM) microgels appears to be the primary driving force for bupivacaine uptake into the composite hydrogel and regulates the initial distribution of bupivacaine between the bulk and microgel phases, controlling the magnitude of the initial burst release achieved. In addition, increased densities of anionic functional groups in either the bulk hydrogel phase or the microgel phase (i.e. increases in the affinity of hydrogel or microgel phase for the drug) reduce the rate of drug release achieved. These ionic interactions appear to be the most critical factor for predicting release kinetics. Diffusion is determined by the cross-link density and thus the degree of swelling of the composite hydrogel as a function

of time. Composite hydrogels that swell more release drug faster due to the higher average diffusion coefficient of bupivacaine within a more swollen network. Hydrophobic partitioning of bupivacaine into the moderately hydrophobic domains of the NIPAM residues also contributes to release control, although this effect appears to be significantly less important than the ionic binding and cross-link effects.

By cross-liking the microgel to the bulk hydrogel the release profile of bupivacaine can be further tuned. The cross-linking of the microgel will result in a mechanical constriction on the phase transition of the microgel, reducing convective mass transport out of the microgel at short times via microgel deswelling (thus reducing burst drug release) and eliminating the potential for making macropores in the free volume around the collapsed microgels. Increased overall cross-linking density within the composite also contributes to slower drug release, although this effect is in part counteracted by the consumption of microgel charges upon crosslink formation.

The results of this work have significant relevance to the clinical challenge of pain management. Bupivacaine is a local anaesthetic that is used short term for pain relief, mainly post-surgery. Durations of release on the order of 8-10 hours are currently the state-of-the-art technology for bupivacaine release, effective for relieving surgical complications but ineffective for chronic pain relief. While controlled bupivacaine release over a long period would effectively relieve pain, it would also impair local motor function, a potential issue in the long-term use of the drug release systems studied depending on the location of drug administration in the body. In such cases, structurally similar drugs such as lidocaine-Q, an anaesthetic mainly used in chronic control of

posttherpetic neuralgia since it has no impact on motor functions, may be more relevant toward achieving the goal of chronic pain relief. (Lexi-Comp).

From the observations collected in this research, it can be determined that the creation of microgel-hydrogel composites will result in drug release that can be tuned by altering the crosslink density, chemistry, and charge density of different phases within the soft composite. The ~60-day release observed for 20% acrylic acid microgel-embedded composite hydrogels studied in this thesis, with a composition optimized for binding the target drug bupivacaine, is significantly longer than release durations previously reported from hydrogel-based materials. This duration of release is notable for a small molecule through a hydrogel matrix and suggests the potential for using soft nanocomposite hydrogels for long-term controlled local drug release. Similarly, we expect that the partitioning and electrostatic properties of the microgel can be tuned to design customizable *in situ* gellable drug delivery systems with potential for achieving long-term release of high doses of drugs from hydrogel-based materials. In theory, it should be possible to independently tune the compositions of the bulk hydrogel and microgel phases to optimize the affinity of those phases to any target drug and thus achieve the dual partitioning-diffusion-based control over drug release kinetics demonstrated in this study. The injectable nature of the hydrogels developed also contributes strongly to their potential applicability in the clinic, as drugs could be administered via traditional, minimally-invasive injection techniques rather than requiring minor surgical procedures as with most bulk hydrogel systems with similar elastic properties.

Chapter 8: Conclusions and Recommendations:

8.1 Conclusions

As a result of the work performed in this thesis, the following conclusions can be made.

The charge content and particle size of acrylic acid-functionalized P(NIPAM) microgels can be tuned by varying the amount of acrylic acid co-polymerized with the NIPAM. The charge content of the microgel primarily determined the amount of cationic bupivacaine that could be entrapped within the anionic-functionalized microgels, although hydrophobic partitioning also enhanced drug uptake.

The creation of a hydrogel based on hydrazone crosslinking is a suitable method for creating an *in situ* gelling hydrogels. The functionalization of polymers (CMC and dextran) with hydrazides and aldehydes produces polymers that facilitate easy flow in the syringe and through the needle. Upon contact, gelation occurs within seconds for the creation of a hydrogel matrix, creating a predominantly elastic hydrogel matrix even at very high microgel loadings (up to 50 dry weight percent) which is highly suitable for many *in vivo* applications. Degradation times and swelling responses can both be altered by changing the degree of cross-linking within the hydrogel. Degradation occurs primarily via hydrolytic cleavage of the hydrazone cross-links.

The cytotoxicity of both the composite precursor materials and the composite hydrogels was minimal at the concentrations at which the materials would be bioavailable inside the body.

Drug release from the hydrogel-microgel composites consisted of two distinct release regimes: fast burst or first-order release over the first 2-3 days (corresponding to diffusion of drug through the bulk hydrogel matrix) and slow, near zero-order release over the remainder of the release period (corresponding to drug partitioning from the microgel phase to the bulk hydrogel phase). The combining of the bulk hydrogel and the microgel significantly slowed drug release versus either component used alone. Release durations of up to 60 days were achieved for the small molecule drug bupivacaine, significantly longer than previously reported in other hydrogel drug delivery studies

The release of bupivacaine can be altered by changing the degree of cross-linking of the hydrogel. The higher the cross-link density, the slower the release of bupivacaine from the composite. However, significantly more control could be made via the modification of the microgels. The electrostatic interactions between bupivacaine and the acrylic acid groups and the hydrophobic partitioning behavior between bupivacaine and NIPAM residues were the two most important rate-governing parameters. By increasing the amount of acrylic groups in the microgels, the rate of release can be slowed.

Cross-linking the microgels directly to the bulk hydrogel matrix significantly changes the release kinetics achieved in composite hydrogel-microgel drug delivery systems since the phase transition of the thermoresponsive microgel is mechanically inhibited by the interphase cross-links. In general, release from composite hydrogels prepared with cross-linkable microgels is slower, attributable both to the lack of convective drug transport upon microgel deswelling as well as the decreased average pore size at the microgel-

hydrogel interface. However, the consumption of $-COO^-$ groups in the microgel via the hydrazide functionalization reaction limits the effectiveness of this approach in terms of further reducing the drug delivery rate achievable from composite hydrogels

8.2 Recommendations

More studies need to be conducted on how the degree of hydrogel cross-linking can be controlled by varying the degree of aldehyde functionalization. This could be used to further tune the rate of release of bupivacaine from the composite system.

The addition of a higher microgel fraction should be studied to determine how an increased fraction of microgels alters release kinetics. Specifically, a maximum microgel loading can be identified at which a stable composite hydrogel can be fabricated. Composite hydrogels with higher microgel fractions should result in slower release as there will be more acrylic acid locations for bupivacaine to interact.

Additional studies pertaining to the development of the hydrazide-functionalized AA-P(NIPAM) microgels should be conducted to determine a more complete mechanism for drug release from these type of systems.

To prevent aldehyde degradation after long periods of storage, the synthesis of aldehyde-functionalized dextran should instead be pursued by synthesizing acetal-functionalized dextran and subsequently hydrolyzing the acetal group as the polymer is

required (Chen *et al*, 2002). This method has been observed to create much more stable aldehyde-functionalized dextran polymers.

Additional bupivacaine detection tests should be conducted to determine the exact concentration of drug being eluted without the need for blank (polymer-only) control samples. It is suggested that HPLC be used in conjunction with UV spectrophotometer readings in any future drug release studies.

Different types of drugs should be studied to see how the magnitude of drug-gel interactions influence release kinetics. Examples of model drugs to be used are dopamine (cationic), acetaminophen (neutral charge), or naproxen (anionic) (Hoare, 2008).

In vivo studies should be conducted with the hydrogel-microgel composites. This should be done to determine cytotoxicity of the device in the body as well as to determine if and/or where bioaccumulation occurs. In addition, drug release testing can be completed in vivo to determine if localized drug delivery can be achieved with the hydrogel-microgel devices.

References

Alsberg, E., Anderson, K., Albeiruti, A., Franceschi, R., & Mooney, D. (2001). Cell interactive alginate hydrogels for bone tissue engineering. *Journal of Dental Research*, 80(11).

Anbergen, U., & Oppermann, W. (1990). Elasticity and swelling behaviour of chemically crosslinked cellulose ethers in aqueous systems. *Polymer,* 31(10), 1854-1858.

Bajpai, A. K., & Mishra, A. (2004). Ionizable interpenetrating polymer networks of carboxymethyl cellulose and polyacrylic acid: Evaluation of water uptake. *Journal of Applied Polymer Science*, 93(5), 2054-2065

Barbucci, R., Magnani, A., & Consumi, M. (2000). Swelling behavior of carboxymethylcellulose hydrogels in relation to cross-linking, pH, and charge density. *Macromolecules*, 33(20), 7475-7480.

Bazile, D., Prud'homme, C., Bassoullet, M., Marlard, M., Spenlehauer, G., & Veillard, M. (1995). Stealth me.PEG-PLA nanoparticles avoid uptake by the mononuclear phagocytes system. *J. Pharm. Sci*, 84, 493.

Berger, J., Reist, M., Mayer, J. M., Felt, O., Peppas, N. A., & Gurny, R. (2004). Structure and interactions in covalently and ionically crosslinked chitosan hydrogels for biomedical applications. *European Journal of Pharmaceutics and Biopharmaceutics*, 57(1), 19-34.

Bokias, G., Hourdet, D., & Iliopoulos, I. (2000). Positively charged amphiphilic polymers based on poly(N-isopropylacrylamide): Phase behavior and shear-induced thickening in aqueous solution. *Macromolecules*, 33(8), 2929-2935.

Bouhadir, K. H., Hausman, D. S., & Mooney, D. J. (1999). Synthesis of cross-linked poly(aldehyde guluronate) hydrogels. *Polymer*, 40(12), 3575-3584.

Bulpitt, P., & Aeschlimann, D. (1999). New strategy for chemical modification of hyaluronic acid: Preparation of functionalized derivatives and their use in the formation of novel biocompatible hydrogels. *Journal of Biomedical Materials Research*, 47(2), 152-169.

Cadée, J., Van Luyn, M., Brouwer, L., Plantinga, J., van Wachem, P., de Groot, C., et al. (2000). In vivo biocompatibility of dextran-based hydrogels. *Journal of Biomedical Materials Research*, 50(3), 397.

Chen, N., Hu, S., Pelton, R..(2002). Mechanisms of aldehyde-containing paper wet-strength resins. *Journal of Industrial and Engineering Chemistry Research.* 41, 5366-5371

Chiu, H., Lin, Y., & Hsu, Y. (2002). Effects of acrylic acid on preparation and swelling properties of pH-sensitive dextran hydrogels. *Biomaterials*, 23(4), 1103-1112.

Cleary, J., Bromberg, L. E., & Magner, E. (2003). Diffusion and release of solutes in pluronic-g-poly(acrylic acid) hydrogels. *Langmuir*, 19(22), 9162-9172.

Dai, C., Wang, B., & Zhao, H. (2005). Microencapsulation peptide and protein drugs delivery system. *Colloids and Surfaces B: Biointerfaces*, 41(2-3), 117-120.

Das, M., Zhang, H., & Kumacheva, E. (2006). Microgels: Old materials with new applications. *Annual Review of Materials Research*, 36, 117.

Deneer, J. W., Seinen, W., & Hermens, J. L. M. (1988). The acute toxicity of aldehydes to the guppy. *Aquatic Toxicology*, 12(2), 185-192.

Desai, M. P., Labhasetwar, V., Amidon, G. L., & Levy, R. J. (1996). Gastrointestinal uptake of biodegradable microparticles: Effect of particle size. *Pharmaceutical Research*, 13(12), 1838.

Doherty, M., Hughes, P., Korszniak, N., & Charman, W. (1995). Prolongation of lidocaine-induced epidural anesthesia by medium molecular weight hyaluronic acid formulations: Pharmacodynamic and pharmacokinetic studies in the rabbit. *Anesthesia & Analgesia*, 80(4), 740.

Edlund, U., & Albertsson, A. (2002). Degradable polymer microspheres for controlled drug delivery. Degradable aliphatic polyesters. *Advances in Polymer Science*,157, 67-112

Ghannam, M. T., & Esmail, M. N. (1997). Rheological properties of carboxymethyl cellulose. *Journal of Applied Polymer Science*, 64(2), 289.

Hiemstra, C., van, d. A., Zhong, Z., Dijkstra, P. J., & Feijen, J. (2007). Novel in situ forming, degradable dextran hydrogels by michael addition chemistry: synthesis, rheology, and degradation. *Macromolecules*, 40(4), 1165-1173.

Hoare, T. R., & Kohane, D. S. (2008). Hydrogels in drug delivery: Progress and challenges. *Polymer*, 49(8), 1993-2007.

Hoare, T., Bellas, E., Zurakowski, D., & Kohane DS. (2010). Rheological blends for drug delivery. II. prolongation of nerve blockade, biocompatibility, and in vitro-in vivo correlations. *Journal of Biomedical Materials Research A,* 92(2), 586.

Hoare, T., & McLean, D. (2006). Kinetic prediction of functional group distributions in thermosensitive microgels. *The Journal of Physical Chemistry B*, 110(41), 20327-20336.

Hoare, T., & Pelton, R. (2004). Functional group distributions in carboxylic acid containing poly(N-isopropylacrylamide) microgels. *Langmuir*, 20(6), 2123-2133.

Hoare, T., & Pelton, R. (2004). Highly pH and temperature responsive microgels functionalized with vinylacetic acid. *Macromolecules*, 37(7), 2544-2550.

Hoare, T., & Pelton, R. (2008). Impact of microgel morphology on functionalized Microgel-Drug interactions. *Langmuir,* 24(3), 1005-1012.

Hoare, T., Zurakowski, D., & Kohane, D. S. (2010). Rheological blends for drug delivery. I. characterization in vitro. *Journal of Biomedical Materials Research Part A*, 92A(2), 575.

Hoffman, A. S. (2002). Hydrogels for biomedical applications. *Advanced Drug Delivery Reviews*, 54(1), 3-12.

Huang, G., Gao, J., Hu, Z., St. John, J. V., Ponder, B. C., & Moro, D. (2004). Controlled drug release from hydrogel nanoparticle networks. *Journal of Controlled Release*, 94(2-3), 303-311.

Hudson, S. P., Langer, R., Fink, G. R., & Kohane, D. S. (2010). Injectable in situ cross-linking hydrogels for local antifungal therapy. *Biomaterials*, 31(6), 1444-1452.

Ikechukwu Ugwoke, M., Kaufmann, G., Verbeke, N., & Kinget, R. (2000). Intranasal bioavailability of apomorphine from carboxymethylcellulose-based drug delivery systems. *International Journal of Pharmaceutics*, 202(1-2), 125-131.

Ito, T., Yeo, Y., Highley, C. B., Bellas, E., & Kohane, D. S. (2007). Dextran-based in situ cross-linked injectable hydrogels to prevent peritoneal adhesions. *Biomaterials*, 28(23), 3418-3426.

Jeong, B., Bae, Y. H., & Kim, S. W. (2000). Drug release from biodegradable injectable thermosensitive hydrogel of PEG–PLGA–PEG triblock copolymers. *Journal of Controlled Release*, 63(1-2), 155-163.

Jia, X., Burdick, J. A., Kobler, J., Clifton, R. J., Rosowski, J. J., Zeitels, S. M., et al. (2004). Synthesis and characterization of in situ cross-linkable hyaluronic acid-based hydrogels with potential application for vocal fold regeneration. *Macromolecules*, 37(9), 3239-3248.

Jin, R., Hiemstra, C., Zhong, Z., & Feijen, J. (2007). Enzyme-mediated fast in situ formation of hydrogels from dextran–tyramine conjugates. *Biomaterials*, 28(18), 2791-2800.

Kang, G. D., Cheon, S. H., & Song, S. (2006). Controlled release of doxorubicin from thermosensitive poly(organophosphazene) hydrogels. *International Journal of Pharmaceutics*, 319(1-2), 29-36.

Kikuchi, A., & Okano, T. (2002). Pulsatile drug release control using hydrogels. *Advanced Drug Delivery Reviews*, 54(1), 53-77.

Kiser, P. F., Wilson, G., & Needham, D. (2000). Lipid-coated microgels for the triggered release of doxorubicin. *Journal of Controlled Release,* 68(1), 9-22.

Kulkarni, R. V., & Sa, B. (2008). Evaluation of pH-sensitivity and drug release characteristics of (polyacrylamide-grafted-xanthan)–Carboxymethyl cellulose-based pH-sensitive interpenetrating network hydrogel beads. *Drug Development and Industrial Pharmacy*, 34(12), 1406-1414.

Langer, R. (1990). New methods of drug delivery. *Science.* 249, 1527-33

Lapasin, R., & Pricl, S. (1995). Rheology of industrial polysaccharides: Theory and applications. New York: Aspen Publishers Inc.

Le Corre, P., Le Guevello, P., Gajan, V., Chevanne, F., Le Verge, R..(1994), Preparation and characterization of bupivacaine-loaded polylactide and polylactide-co-glycolide microspheres, *International Journal of Pharmaceutics*, 207, 41-49

Lee, K. Y., Bouhadir, K. H., & Mooney, D. J. (2000). Degradation behavior of covalently cross-linked poly(aldehyde guluronate) hydrogels. *Macromolecules*, 33(1), 97-101.

Lexi-Comp, I., & American Pharmaceutical Association. (1994). Drug information handbook (North American ed.). Washington, D.C.: American Pharmaceutical Association.

Li, J., Lewis, R. B., & Dahn, J. R. (2007). Sodium carboxymethyl cellulose. *Electrochemical and Solid-State Letters*, 10(2), A17-A20.

Lopez, V. C., Hadgraft, J., & Snowden, M. J. (2005). The use of colloidal microgels as a (trans)dermal drug delivery system. *International Journal of Pharmaceutics*, 292(1-2), 137-147.

Lynch, I., de Gregorio, P., & Dawson, K. A. (2005). Simultaneous release of hydrophobic and cationic solutes from thin-film plum-pudding gels: A multifunctional platform for surface drug delivery? *The Journal of Physical Chemistry B*, 109(13), 6257-6261.

McGillicuddy, F. C., Lynch, I., Rochev, Y. A., Burke, M., Dawson, K. A., Gallagher, W. M., et al. (2006). Novel ''plum pudding'' gels as potential drug-eluting stent coatings: Controlled release of fluvastatin. *Journal of Biomedical Materials Research Part A*, 79A(4), 923.

Mohanraj, V. J., & Chen, Y. (June, 2006). Nanoparticles - A review. *Tropical Journal of Pharmaceutical Research*, 5(1), 561.

Motlagh, G. H., Hrymak, A. N., & Thompson, M. R. (2007). Properties of a carbon filled cyclic olefin copolymer. *Journal of Polymer Science Part B: Polymer Physics*, 45(14), 1808-1820.

Nadagouda, M. N., & Varma, R. S. (2007). Synthesis of thermally stable carboxymethyl Cellulose/Metal biodegradable nanocomposites for potential biological applications. *Biomacromolecules*, 8(9), 2762-2767.

Naessens, M., Cerdobbel, A., Soetaert, & Vandamme, E. J. (2005). Leuconostoc dextransucrase and dextran: Production, properties and applications. *Journal of Chemical Technology & Biotechnology*, 80(8), 845.

Nathan, A., Zalipsky, S., & Kohn, J. (1996). PEG modified anticancer drugs: Synthesis and biological activity. *Journal of Bioactive and Compatible Polymers*, 11, 122.

Nguyen, K. T., & West, J. L. (2002). Photopolymerizable hydrogels for tissue engineering applications. *Biomaterials*, 23(22), 4307-4314.

Olivier, J. (2005). Drug transport to brain with targeted nanoparticles. *The Journal of the American Society for Experimental NeuroTherapeutic*s, 2(108)

Padula, C., Colombo, G., Nicoli, S., Catellani, P. L., Massimo, G., & Santi, P. (2003). Bioadhesive film for the transdermal delivery of lidocaine: In vitro and in vivo behavior. *Journal of Controlled Release*, 88(2), 277-285.

Park, H., Temenoff, J. S., Holland, T. A., Tabata, Y., & Mikos, A. G. (2005). Delivery of TGF-β1 and chondrocytes via injectable, biodegradable hydrogels for cartilage tissue engineering applications. *Biomaterials*, 26(34), 7095-7103.

Pawlikowska, P., Gajkowska, B., & Orzechowski, A. (2007). Mitofusin 2 (Mfn2): A key player in insulin-dependent myogenesis in vitro. *Cell and Tissue Research*, 327(3), 571-581.

Pelton, R. H., & Chibante, P. (1986). Preparation of aqueous latices with N-isopropylacrylamide. *Colloids and Surfaces*, 20(3), 247-256.

Pelton, R. (2000). Temperature-sensitive aqueous microgels. *Advances in Colloid and Interface Scienc*e, 85(1), 1-33.

Poole, S. K., & Poole, C. F. (2003). Separation methods for estimating octanol–water partition coefficients. *Journal of Chromatography B,* 797(1-2), 3-19.

Puttipipatkhachorn, S., Nunthanid, J., Yamamoto, K., & Peck, G. E. (2001). Drug physical state and drug–polymer interaction on drug release from chitosan matrix films. *Journal of Controlled Release*, 75(1-2), 143-153

Qiu, Y., & Park, K. (2001). Environment-sensitive hydrogels for drug delivery. *Advanced Drug Delivery Reviews*, 53(3), 321-339.

Rodríguez, R., Alvarez-Lorenzo, C., & Concheiro, A. (2003). Interactions of ibuprofen with cationic polysaccharides in aqueous dispersions and hydrogels: Rheological and diffusional implications. *European Journal of Pharmaceutical Sciences*, 20(4-5), 429-438.

Rosen, H., & Abribat, T. (2005). The rise and rise of drug delivery. *Nat Rev Drug Discovery*, 4(5), 381-385.

Roy, I., & Gupta, M. N. (2003). Smart polymeric materials: Emerging biochemical applications. *Chemistry & Biology*, 10(12), 1161-1171.

Saunders, B. R., & Vincent, B. (1999). Microgel particles as model colloids: Theory, properties and applications. *Advances in Colloid and Interface Science*, 80(1), 1-25.

Schild, H. G. (1992). Poly(N-isopropylacrylamide): Experiment, theory and application. *Progress in Polymer Science*, 17(2), 163-249.

Schild, H. G., & Tirrell, D. A. (1991). Microheterogeneous solutions of amphiphilic copolymers of N-isopropylacrylamide: An investigation via fluorescence methods. *Langmuir*, 7(7), 1319-1324.

Shah, J. C., & Maniar, M. (1993). pH-dependent solubility and dissolution of bupivacaine and its relevance to the formulation of a controlled release system. *Journal of Controlled Release,* 23(3), 261-270.

Shamala, T. R., & Prasad, M. S. (1995). Preliminary studies on the production of high and low viscosity dextran by leuconostoc spp. Process Biochemistry, 30(3), 237-241.

Shi, C., Morse, L., Ing, C., White, P. F., Rawal, S., Latham, P., et al. (2003). Use of a continuous local anesthetic infusion for pain management after median sternotomy. *Anesthesiology*, 99(4), 918.

Shibayama, M., & Tanaka, T. (1993). Volume phase transition and related phenomena of polymer gels, *Advances in Polymer Science*,109, 1-62

Sinha, V. R., & Trehan, A. (2003). Biodegradable microspheres for protein delivery. *Journal of Controlled Release*, 90(3), 261-280.

Snowden, M. J. (1992). The use of poly(N-isopropylacrylamide) latices as novel release systems. *J. Chem. Soc., Chem. Commun*, (11), 803.

Sudoh, Y., Cahoon, E. E., De Girolami, U., & Wang, G. K. (2004). Local anesthetic properties of a novel derivative, N-methyl doxepin, versus doxepin and bupivacaine. *Anesthesia & Analgesia*, 98(3), 672-676.

Sutton, C. (2005). Adhesions and their prevention. *The Obstetrician & Gynaecologist*, 7(3), 168-176.

Van Dijk-Wolthuis, WNE., Hoogeboom, JAM., van Steentergen, MJ., Tsang, SKY., Hennink, WE.. (1997) Degredation and Release Behaviour of Dextran-Based Hydrogels. *Macromolocules*, 30, 4639-4645.

Vihola, H., Laukkanen, A., Valtola, L., Tenhu, H., & Hirvonen, J. (2005). Cytotoxicity of thermosensitive polymers poly(N-isopropylacrylamide), poly(N-vinylcaprolactam) and amphiphilically modified poly(N-vinylcaprolactam). *Biomaterials,* 26(16), 3055-3064.

Yeo, Y., Ito, T., Bellas, E., Highley, C. B., Marini, R., & Kohane, D. S. (2007). In situ cross-linkable hyaluronan hydrogels containing polymeric nanoparticles for preventing postsurgical adhesions. *Annals of Surgery*, 245(5), 819.

Zhang, R., Tang, M., Bowyer, A., Eisenthal, R., & Hubble, J. (2005). A novel pH- and ionic-strength-sensitive carboxymethyl dextran hydrogel. *Biomaterials*, 26(22), 4677-4683.

Appendices

Appendix A: Material Information

Appendix A1 Reagents

Chemical	Abbreviation	Supplier	Product ID
Acrylic Acid, 99%	AA	Sigma Aldrich, Oakville, ON	147230
Adipic dihydrazide. 98%	ADH	Sigma Aldrich, Oakville, ON	A0638
Ammonium Persulfate	APS	Sigma Aldrich, Oakville, ON	215589
Bupivicaine Hydrochloride		Sigma Aldrich, Oakville, ON	B5274
Dextran from *Leuconstoc spp.*		Sigma Aldrich, Oakville, ON	31392
Dimethyl Sulphoxide	DMSO	Caledon Laboratory Chemicals, Georgetown, ON	4100-1
Ethylene Glycol	EG	Sigma Aldrich, Oakville, ON	324558
N'-ethyl-N-(3-dimethylaminopropyl)-carbodiimide, commercial grade	EDC	Sigma Aldrich, Oakville, ON	E7750
N-hydroxysuccinimide, 97%	NHS	Sigma Aldrich, Oakville, ON	130672
N-isopropylacrylamide, 97%	NIPAM	Sigma Aldrich, Oakville, ON	415324
N'N'-Methylene Bisacrylamide, 99%	MBA	Sigma Aldrich, Oakville, ON	146072
Sodium Dodecyl Sulfate (electrophoresis grade)	SDS	Bioshop Canada, Burlington, ON	SDS001
Sodium Periodate, ACS Reagent $\geq$ 99.8%		Sigma Aldrich, Oakville, ON	311448

Appendix A2 Cell Culture Supplies

Product	Abbreviation	Supplier	Product ID
3T3-Swiss albino *Mus musculus*	3T3	ATCC: Cedarlane Laboratories Ltd., Burlington, ON	CCL-92
C1C12 Mouse Muscle Myoblast	C1C12	ATCC: Cedarlane Laboratories Ltd., Burlington, ON	CRL-1772
Dulbecco's Modified Eagle Medium (high glucose)	DMEM	Invitrogen Canada, Burlington, ON	11965
Fetal Bovine Serum	FBS	Invitrogen Canada, Burlington, ON	10437
Horse Serum	HS	Invitrogen Canada, Burlington, ON	16050
Penicillin Streptomycin	Penn Strep	Invitrogen Canada, Burlington, ON	15140
Recovery Cell Culture Freezing		Invitrogen Canada, Burlington, ON	12648
Thiazolyl Blue Tetrazolium Bromide	MTT	Sigma Aldrich, Oakville, ON	M5655
Trypsin-EDTA, 0.25%		Invitrogen Canada, Burlington, ON	25200

Bright-Line Hemocytometer, Hausser Scientific, Horsham, PA, USA

Appendix B Cell Culture Procedures

Information from manufacturer procedures (ATCC)

Cell Thawing:

1. Thaw cryovial with gentle agitation in 37°C water bath for approximately 2 minutes.
2. Transfer vial contents into 15mL centrifuge tube and add 10mL proliferation (FBS) media.
3. Centrifuge at 1000rpm for 5 minutes
4. Aspirate off media and add 15mL freshly warmed FBS containing media.
5. Pipette gently to disperse cells.
6. Add mixtures to $75cm^3$ (T75) flask.
7. Incubate at 37°C with 5% CO_2.
8. Passage every 2-4 days.

Changing Media:

1. Aspirate old media
2. Add 15mL freshly warmed FBS containing media.
3. Place back in incubator.

Passaging Cells:

1. Aspirate off old media.
2. Add 5mL trypsin-EDTA into flask and gently tilt back and forth to detach cells. (5-10 minutes)
3. Add 6mL of media into flask and move contents to 15mL centrifuge tube.
4. Centrifuge at 1000rpm for 5 minutes.
5. Aspirate off media and add 15mL freshly warmed FBS containing media.
6. Pipette gently to disperse cells.
7. Add 100µL mixtures to $75cm^3$ (T75) flask with 15mL fresh FBS containing media.
8. Incubate at 37°C with 5% CO_2.
9. Passage every 2-4 days.

Counting Cells:

1. Aspirate off old media.
2. Add 5mL trypsin-EDTA into flask and gently tilt back and forth to detach cells. (5-10 minutes)
3. Add 6mL of FBS containing media into flask and move contents to 15mL centrifuge tube.
4. Centrifuge at 1000rpm for 5 minutes.
5. Aspirate off media and add 15mL freshly warmed HS containing media.
6. Remove 100µL of mixture and place in hemocytometer.

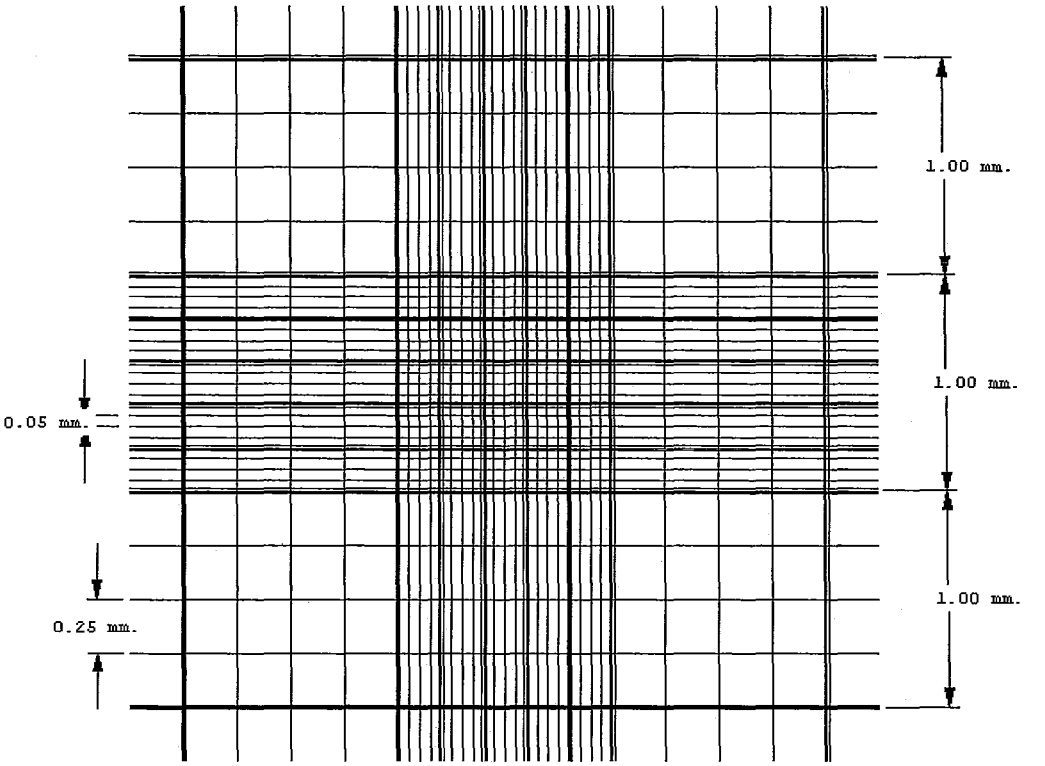

Figure B1.1: Hemocytometer Grid

7. Count number of cells in outer quadrants (single quadrant area = 0.1mm3) and calculate cells per quadrant. (See Figure A1.1)
8. Number of cells is calculated as follows:

$$Number\ of\ Cells = Cell\ Count\ (cells/0.1mm^3) \times 10000\ (0.1mm^3/mL) \times 15mL$$

Appendix C Calibration Curves

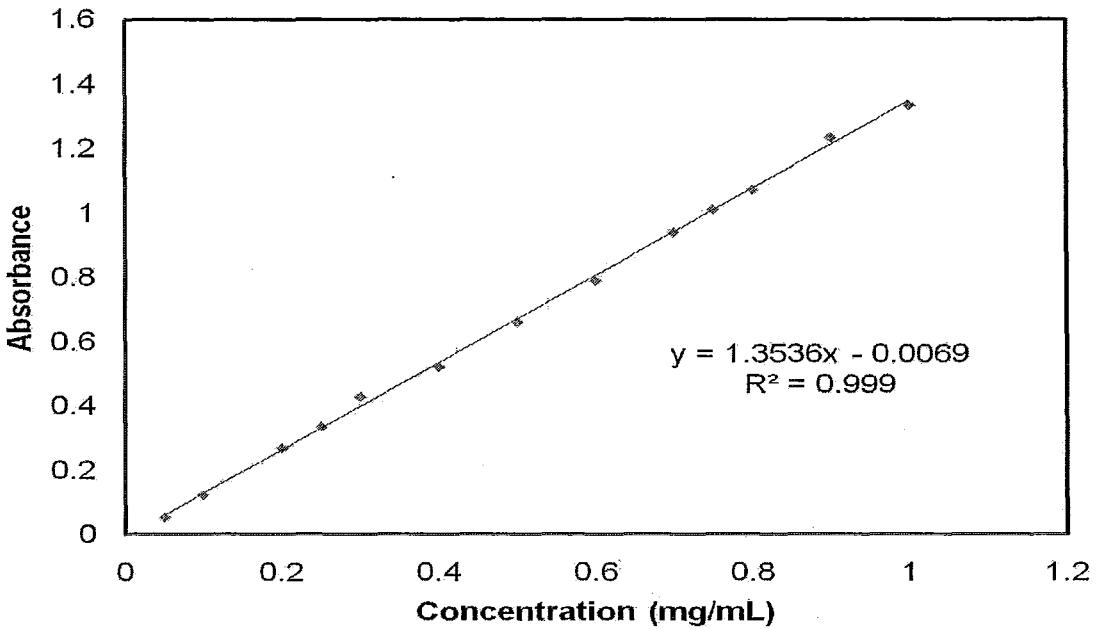

Figure C1: Absorbance – Bupivacaine Calibration Curve

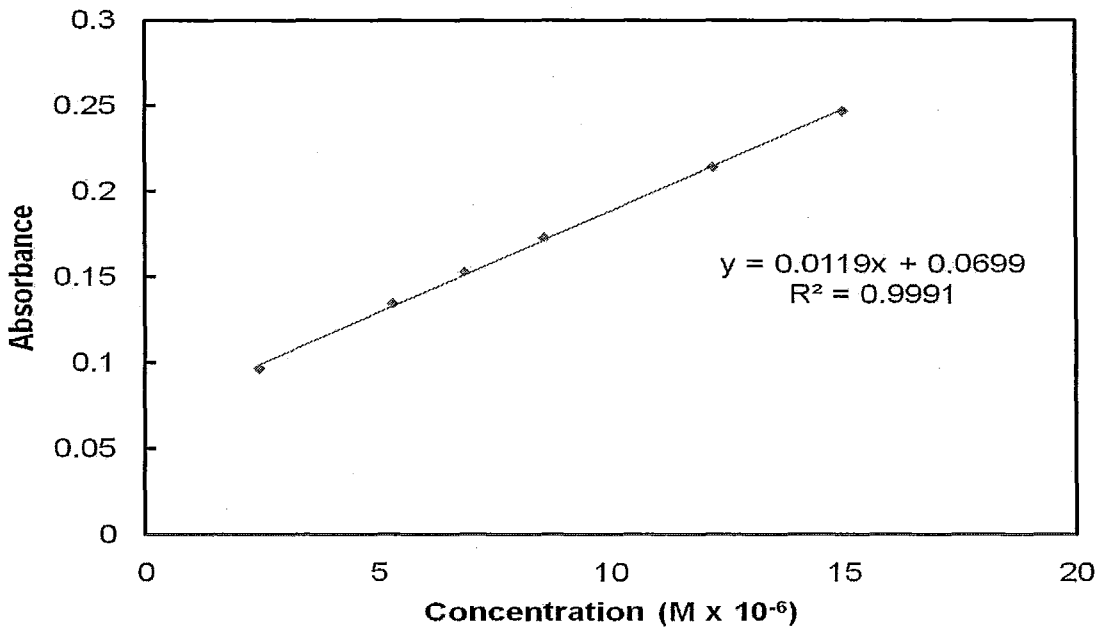

Figure C2: Absorbance –Carbazate-TNBS Calibration Curve

Appendix D Additional Data

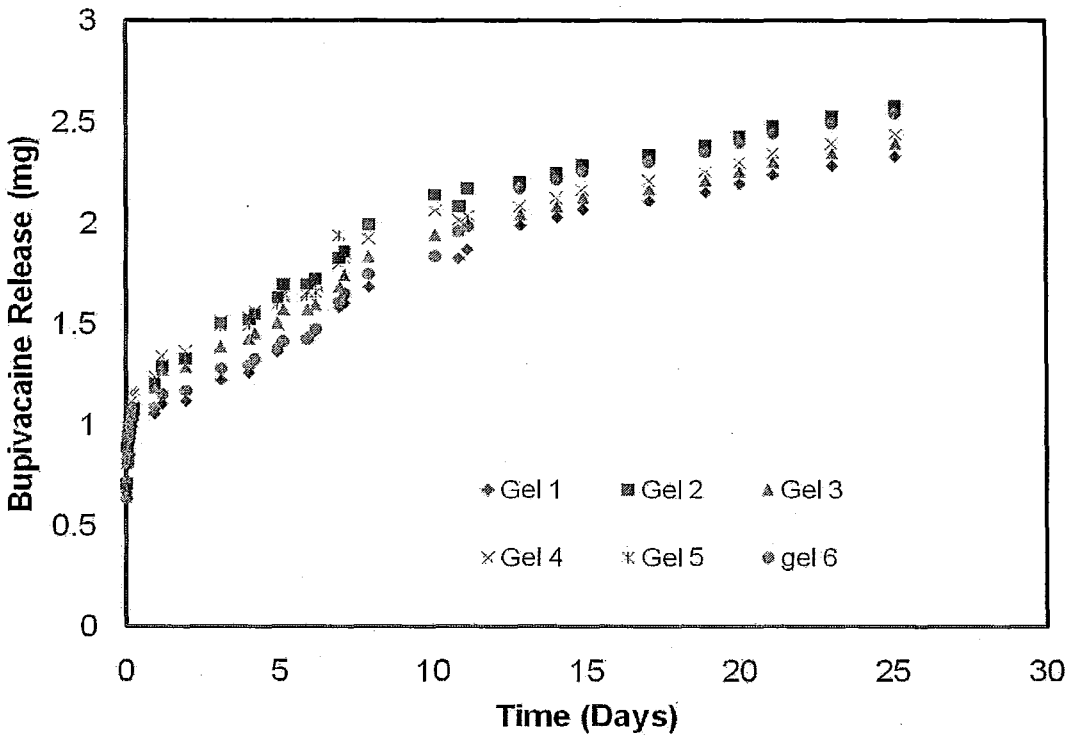

Figure D1: Reproducibility of Drug Release

Table D1: Acrylic Acid Functionalization of P(NIPAM) Microgel

Polymer	Mol COOH per gram of microgel
6mol% Acrylic Acid Microgel	7.0×10^{-4}
20mol% Acrylic Acid Microgel	1.3×10^{-3}
34mol% Acrylic Acid Microgel	2.4×10^{-3}

Table D2: Charge Density of AA-P(NIPAM) Microgels

Polymer	Mol COOH per cm^3 of AA-P(NIPAM) Microgel
6mol% Acrylic Acid Microgel	5.6×10^{-4}
20mol% Acrylic Acid Microgel	1.0×10^{-3}
34mol% Acrylic Acid Microgel	1.8×10^{-3}

Table D3: Charge Density of Hydrogels based on Hydrazide-Carboxymethyl Cellulose/Aldehyde-Dextan

Polymer	Mol COOH per cm^3 Hydrogel
CMC-A0.5	2.2×10^{-5}
CMC-A1.0	1.8×10^{-5}
CMC-A1.5	1.66×10^{-6}

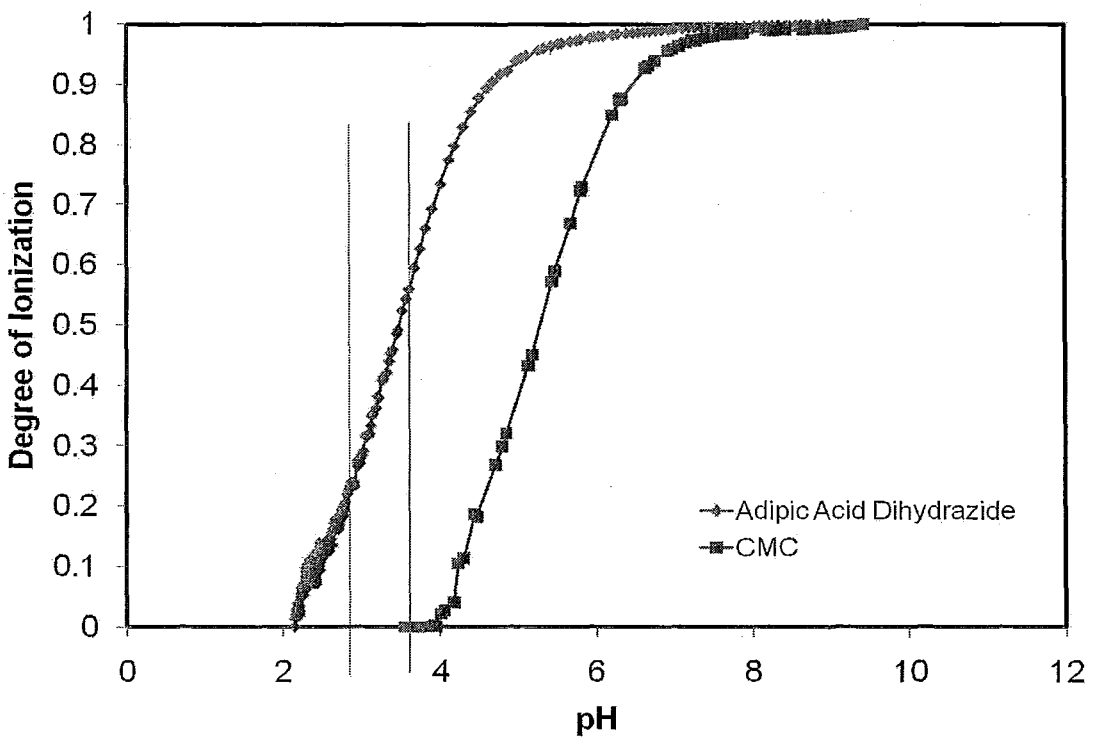

Figure D2: Degree of Ionization of Adipic Acid Dihydrazide and CMC

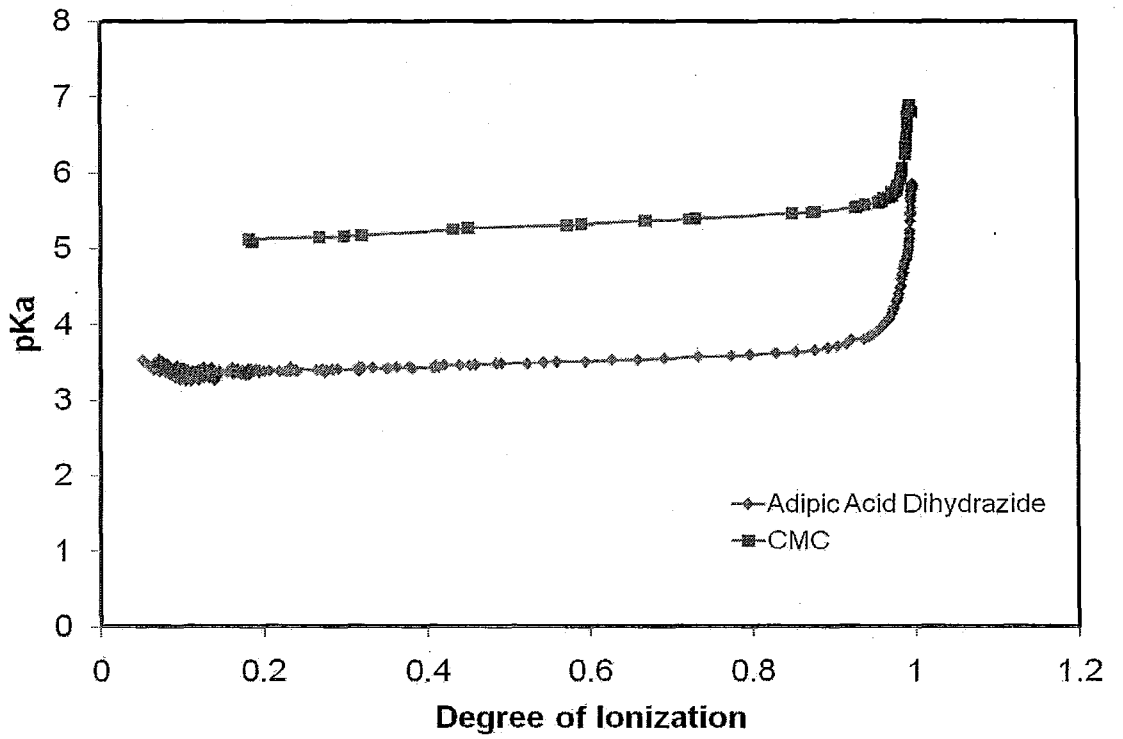

Figure D3: pKa of Adipic Acid Dihydrazide and CMC